



HAL
open science

Strut-and-Tie models for the design of non-flexural elements : computational aided approach

Gustavo Mendoza Chavez

► **To cite this version:**

Gustavo Mendoza Chavez. Strut-and-Tie models for the design of non-flexural elements: computational aided approach. Civil Engineering. Université Paris-Est, 2018. English. NNT: 2018PESC1030 . tel-02132474

HAL Id: tel-02132474

<https://theses.hal.science/tel-02132474>

Submitted on 17 May 2019

HAL is a multi-disciplinary open access archive for the deposit and dissemination of scientific research documents, whether they are published or not. The documents may come from teaching and research institutions in France or abroad, or from public or private research centers.

L'archive ouverte pluridisciplinaire **HAL**, est destinée au dépôt et à la diffusion de documents scientifiques de niveau recherche, publiés ou non, émanant des établissements d'enseignement et de recherche français ou étrangers, des laboratoires publics ou privés.

Thèse présentée pour obtenir le grade de
Docteur de l'Université Paris-Est

Spécialité: Génie Civil

par

Gustavo Mendoza Chávez

Ecole Doctorale : SCIENCES, INGÉNIERIE ET ENVIRONNEMENT

*Strut-and-Tie models for the design of
non-flexural elements: computational
aided approach*

Thèse soutenue le 10 juillet devant le jury composé de:

Patrick de Buhan	<i>Directeur de thèse</i>
Guillaume Hervé-Secourgeon	<i>Co-encadrant</i>
Christophe Rouzaud	<i>Co-encadrant</i>
Pierre-Alain Nazé	<i>Co-encadrant</i>
Fabrice Gatuingt	<i>Rapporteur</i>
Delphine Brancherie	<i>Rapporteur</i>
Panagiotis Kotronis	<i>Examineur</i>
Francis Barré	<i>Invité</i>

Acknowledgements

I would like to express my deep gratitude to my research supervisors, for their patient guidance, enthusiastic encouragement and useful critiques of this research work.

I wish to acknowledge the support and also the guidance received from personal of Géodynamique & Structure. Thanks for your trust in the project. Worth to mention the support received by the "Consejo Nacional de Ciencia y Tecnología (CONACYT)" and the "Consejo Mexiquense de Ciencia y Tecnología (COMECyT)". In particular, I am grateful for the opportunity they gave me to share my project and experiences in my country.

I would also like to extend my thanks to the technicians, the interns, the students and the staff of the ESTP: thank you for the time we shared.

I wish to thank those who were always there; my friends, my girlfriend, my family, and specially *quiero agradecer a mis padres*.

Contents

Acknowledgements	ii
Contents	vi
Introduction	2
Background	3
Summary of research contributions	7
Thesis structure	8
Related work	9
1 Design of reinforcement for non-flexural elements: a review.	11
1.1 Reinforced concrete elements	13
1.1.1 Flexure theory for reinforced concrete	13
1.1.2 Elements in compression	15
1.1.3 Elements resisting to diagonal tension and shear	16
1.2 Finite element models for RC structures	18
1.2.1 Membranes	19
1.2.2 Slabs and shells	21
1.2.3 3D solid modelling	33
1.2.4 Structural analysis and design using non-linear modelling	34
1.3 Strut-and-Tie models	35
1.3.1 Discontinuity regions	36
1.3.2 Fundamentals	36
1.3.3 Design procedure	37
1.3.4 Recommendations and thumb rules to be taken into account	43
1.3.5 Remarks	44
1.4 Non-Linear strut-and-tie model approach	44
1.5 Summary	44
2 Automatic strut-and-tie models	46
2.1 Structural optimisation	48
2.1.1 General problem definition	48
2.1.2 Solution procedure	51
2.1.3 Exact solution tools	53
2.1.4 Optimality Criteria (OC) based methods	54

2.1.5	Methods based on mathematical programming	57
2.1.6	Simultaneous analysis and design	60
2.1.7	Convergence	60
2.2	Continuum optimisation	62
2.3	Discrete optimisation	63
2.3.1	Special cases of the ground structure approach	68
2.4	Summary	69
3	Computational aided approach through locally weighted regressions	71
3.1	Basis and description of the algorithm	72
3.1.1	Input	73
3.1.2	Linear-elastic FE analysis	74
3.1.3	Ground structure	74
3.1.4	Optimisation procedure	80
3.1.5	Termination	85
3.1.6	Acquiring the strut-and-tie model and reinforcement	85
3.1.7	Outputs	87
3.2	Illustrative example	88
3.2.1	Input	88
3.2.2	Ground structure	89
3.2.3	Truss optimisation	90
3.2.4	Mesh sensibility analysis	92
3.2.5	Literature results	94
3.2.6	Different load cases	95
3.3	Behaviour of the algorithm	96
3.3.1	Linear-elastic FE analysis	96
3.3.2	Ground structure	96
3.3.3	Truss optimisation	96
3.4	Summary	97
4	Comparative example	98
4.1	Example selection	100
4.2	2D planar model	100
4.3	Surface model representation	109
4.4	Remarks	112
4.5	3D brick model	114
4.6	Results	118
4.7	Discussion	118
4.7.1	Capabilities of the algorithm	118
4.7.2	Quantity of reinforcement	120
	Concluding remarks	121
	Bibliography	133
	List of Figures	136

List of Tables	137
A Other examples	138
A.1 Trimmed deep wall	138
A.2 Trimmed square	140
B Anchorage: different load cases	142
B.1 Load eccentricity of 0.75 meters	142
B.1.1 Input	142
B.1.2 Ground structure	143
B.1.3 Truss optimisation	145
B.1.4 Literature results	146
C 3D strut-and-tie model corbel	147

Introduction

Within the field of Reinforced Concrete (RC) structures and more specifically, at the design of non-flexural elements such as corbels, nibs, and deep beams, the rational procedure of conception and justification referred as Strut-and-Tie Method (STM) has shown some advantages over classical algorithms of reinforcement computation based on FE analysis (eg. Wood-Armer or Capra-Maury).

The STM remains a suitable alternative for the design of concrete structures presenting either elastic or plastic behaviour whose application framework is well defined in concrete structures' design codes like the EuroCodes and the AASHTO-LRFD Bridge Design Specifications. Nevertheless, this method has the main inconvenient of requiring a high amount of resources investment in terms of highly experienced personal or in terms of computational capacity for, respectively, its manual application or an automatic approach through topology optimisation.

The document proposes a light alternative, in terms of required iterations, to the automation of the STM, which starts from the statement that the resultant struts and ties of a suitable ST model can be distributed according to the direction of the principal stresses, σ_{III} and σ_I , obtained from a planar or a three-dimensional FE model.

Résumé

Dans le domaine des structures en Béton Armé (BA) et plus spécifiquement, lors de la conception d'éléments non-flexibles tels que les corbeaux, les poutres bayonnetts et les poutres profondes, la Méthode Bielle-Tirant (MBT) présente des avantages par rapport aux algorithmes classiques de calcul de ferrailage basé sur l'analyse FE (par exemple Wood-Armer ou Capra-Maury).

La Méthode Bielle-Tirant reste une alternative adaptée pour la conception de structures en béton présentant un comportement élastique ou plastique dont le cadre d'application est bien défini dans les codes de conception des structures en béton comme les EuroCodes et les spécifications de conception des ponts AASHTO-LRFD. Néanmoins, cette méthode présente l'inconvénient majeur de nécessiter un investissement important en ressources humaines ou en capacité de calcul pour, respectivement, son application manuelle ou une approche automatique par optimisation de topologie.

Le document propose une alternative légère, en termes d'itérations requises, à l'automatisation de la MBT, qui part de l'affirmation que les entretoises résultantes et les attaches d'un modèle ST approprié peuvent être distribuées selon la direction des contraintes principales, σ_{III} et σ_I , obtenus à partir d'un modèle préliminaire aux EF.

Background

In the industrial context of engineering, most of the structural elements in reinforced concrete structures are conceived under the Bernoulli and Navier's hypotheses. Nevertheless, these solutions face problems when treating local non-flexural regions of the structure where the strain distribution is significantly nonlinear (corbels, openings, gussets or near the surroundings of concentrated loads). Sharp discontinuities can occur in the direction of internal forces and it is imperative to provide a proper reinforcement able resist the tension while being consistent with the pertinent codes in terms of the quantity, distribution, anchorage length, etc. In many cases, standard guides found in the construction manuals like the ACI detailing recommendations or in the EuroCodes fulfil the design but it is up to the structural engineer to decide whether special considerations are or are not needed.

For the exceptional cases, the structural engineer should isolate specific regions, analyse them and provide the required reinforcement computed through a convenient methodology.

The work of Schlaich [Schlaich et al., 1987] describes in detail the use of ST models as a reliable solution to treat the denominated D-regions (where D stands for discontinuity, disturbance or detail). Discontinuity (which is associated with high shear stresses) is either static (as a result of concentrated loads) or geometric (as a result of abrupt change of geometry) or both [El-Metwally and Chen, 2017]. In brief, this procedure proposes that the real structure should be replaced by a fictitious skeletal structure whose geometry allows keeping the boundary conditions and load case, of the real structure, in such a way that it complies with the Bernoulli hypothesis. This can be achieved by imposing an idealised truss-like distribution of inner forces, where the compressive forces are taken by inner concrete bar-type elements (struts) and the tensile forces are taken by the steel reinforcement (ties); a third type of elements, the nodes, connect the struts and ties at their extremities to assure the interaction between different elements. One of the shortcomings of the applications of ST models is that, in most of the cases the model should be carried out through a manual procedure by a highly experienced engineer.

However, the models can also be established through an elastic FE analysis of the whole structure by considering the direction of the principal stresses along the geometry or, in recent years, by powerful structural optimisation procedures.

Due to the interest that the STM has taken during the last decades, an effort to automatise its application has been done by different research groups all around the world. Computer aided approaches such as CAST [Kuchma and Tjhin, 2001], or the one established in "Computer graphics in detailing of ST models" [Alshegeir and Ramirez, 1992], propose tools that overlaps images of the direction fields of principal stresses over an interactive CAD-like interface. The interface allows the user to manually propose a suitable ST model whose distribution of elements follows the trajectory of the linear elastic stresses. This procedure simplifies the selection and evaluation of feasible ST systems requiring, however, the intervention of a skilled structural engineer at the earliest stage of the method.

On the other hand, structural optimisation procedures have been also applied to find truss-like structural configurations out of plain concrete structures. Most commonly applied for aeronautics, optimisation problems can be stated for a large variety of elements and structures found in the civil engineering field. Current approaches of structural optimisation are based on iterative Finite Element Analysis (FEA) where, according to its representation, two approaches can be distinguished:

- Continuum optimisation.
- Discrete optimisation.

In the application of continuum optimisation, the structure is discretised into continuum finite elements such as plates, shells or bricks. The process is focused on determining the optimal layout through the placement of a given isotropic material within the limits of a material domain Ω^{mat} .

Even if some authors believe that optimal ST models can be found starting from continuum-type optimal topology, [Bendsøe et al., 1994, Almeida et al., 2013], the characteristics of the discrete and continuum structures are very different, and there is no unified criteria for constructing truss topologies from the results of optimal finite element solutions [Starčev-Čurčin et al., 2013, Baldock and Shea, 2006]: this step relies on empirical selection and experience. Most of the ST models product of this type of optimisation do not provide mechanism free structures when replaced by their associated truss topology. This can be seen as major drawback with respect of the current constructive guidelines and codes. In addition, due to the characteristics presented by the interaction concrete-reinforcement and according to some studies, [Swan et al., 1999], a more adequate ST model would be found through a discrete optimisation.

Another type of applied optimisation is referred as discrete structural optimisation. In this approach, the structure is represented by skeletal systems. Most of the available literature establishes the problem of truss optimisation as a ground structure approach, [Bendsøe and Sigmund, 2003], where a group of n joints is proposed and a set, or the totality, of all the m possible elements connecting the joints are considered to form the initial truss system. Then, the optimisation process can be established inside an iterative algorithm where the chosen structure gradually evolves according to predefined criteria and active constraints at each step. At each iteration, the cross sections can vary and take a value from a given list (discrete variables) or take any possible value between a range (continuous variables) .

As it can be inferred, this type of structural optimisation has been developed for skeletal structures such as steel trusses but, in recent years, its application has been extended to solid RC structures through the STM [Muttoni et al., 2015].

Even though the ground structure approach has been proved a powerful tool for computing ST models allowing the optimisation to be seen as a relatively simple sizing problem, it arises many difficulties principally related to: 1) the singularity of the stiffness matrix, K , 2) the stability of the optimised structure, and 3) the optimality of the structure *per se*.

The first complication derives from the fact that, during the optimisation process, the element cross section, a_i , could approach or even reach a zero value, which has obvious repercussion on the diagonal of the stiffness matrix. To solve it, the possibility of zero cross sections is not permitted and in most cases, an inferior limit, a_{min} , is imposed for a_i ($a_i > 0$ or $a_i \geq a_{min}$).

A non-zero lower bound will generally produce "secondary" elements whose only purpose is often only to guaranty the non-singularity condition on the global stiffness matrix and to avoid inner mechanisms on the structure. Such elements are often erased or simply ignored at the last stage of the optimisation, [Ohsaki and Swan, 2002]. This decision im-

plies that most optimal designs have a singular matrix and present potential mechanisms when described as a part of the ground structure leading to the second listed complication.

The third complication is related to the choice of the ground structure itself. The ground structure approach may or may not lead to the optimal structure according to the group of nodes proposed (quantity and position) and the set of allowed elements; the optimal structure appears to be limited by the original geometrical restrictions and possible connections. An alternative to overcome this difficulty is to treat the coordinates of the structural nodes as a variable within the optimisation procedure.

Taking also the nodal coordinates as variables allows to adapt the geometry to the boundary may induce improvements in terms of performance or weight reductions. Nevertheless, the structure is still strongly dependant on the initial layout: number of elements and connectivity.

To summarise, regardless the fact that existent procedures are suitable for computing ST models, the obtained trusses are still highly dependant on the selected initial truss and, consequently, on the experience of the structural engineer. Even though the selection of a "good" initial truss could be an easy task for "classic" or well referenced examples, complication arises when dealing with complex load cases (in plane and out of plane loads, multiple loads, displacements, etc.), whimsical geometries or three-dimensional models.

Ideally, a tool intended to find ST models should propose and evaluate truss-like structures keeping the experienced based decisions as minimum as possible. The results must be feasible, not only from the point of view of mechanics but also from the point of view of the construction codes. Additionally to these needs, the results shall be economically viable which is an evidence that a sort of optimisation procedure must be involved.

In the context of nuclear civil works, the conception of non-flexural elements (e.g. deep beam, joints, trimmed walls) has become such a common task that most of the times they do not receive the detailing that they deserve during their modelling. The design and justification of these elements is frequently based on force equilibrium along FE models based on shell elements that must be checked for transitions between different thicknesses, gradient in the mesh size, verification of sides-thickness ratios, etc; aspects that could produce a diminution in the model accuracy if an exhausting detailing is not executed.

The development of a light computational tool able to threat a large variety of structural problems and, also, able to automatically propose optimised reinforcement of concrete structures based on the STM, could represent a huge improvement in the industrial context. The main advantages are listed below:

- **Decision support in the design process.** Most of the times, decisions in the earlier stages of design are not made based on rigorous justified structural aspects but, they are made based on previous experience or intuition of the engineer. Computer-aided tools can provide non-experienced engineers with a justified insight of complex problems.
- **Automatic analysis and justification of local zones.** This is desirable in the early stages of a project, permitting a wider and more thorough exploration of the design space than could be achieved manually.
- **Time saving through computer-aided design tools.** Within the detailing phase, computer-aided design has the potential to save engineer time by avoiding the need

of a layout search through a manually iterative process. During the post-treatment phase, the saves in time can be achieved by avoiding manual smoothing of the results commonly carried out when using FE based algorithms such as C&M.

- **More realistic representations of 3D structures.** Compared to models based on shell and plate elements, ST models (specially 3D ones) represent a more accurate representation of the stress distribution and may lead to a better steel reinforcement distribution.
- **Marketability.** The use of optimisation may produce a substantial interest in the market.

All previously listed advantages may lead to a reduction in engineer-time consumption, computational time and even to a more adequate steel reinforcement distribution.

Whether the advantages may seem quite straightforward, the algorithmic development and implementation of a computational tool still must overcome several issues:

- **Consistency between rational approaches and optimisation techniques.** Whether at first sight the idea of rational approach seems to be incompatible with automatised iterative procedures, the amalgam between this two ideas should be established in order to present an effective STM tool.
- **Ill-conditioned results.** As mentioned, some design optimisation processes throw results full of mechanisms when expressed as ST model. However, as it will be discussed in Chapter 3, discrete optimisation methods are capable of handling such complications if special considerations are made.
- **Engineer's lack of experience and knowledge required to implement optimisation methods.** Most of the available structural optimisation programmes or complementary modules require technical and theoretical expertise. This need makes of them a difficult or even an inaccessible tool to structural designers who do not use them on a regular basis.
- **Prohibitive time consumption.** Since design time is never unlimited, the optimisation procedure cannot be allowed to become critical and the amounts of time devoted to building up a model and parameter adjusting should be small.
- **Prohibitive computational cost.** The developed algorithm should not require prohibiting computational efforts.
- **Accordance to practical reinforcement layout.** Considering that in practice, steel reinforcement is preferred to be placed along principal directions, the results must be easily projected into those reinforcement axis.
- **Consistency with current codes of construction and recommendations.** Maybe the most important gap to be close, or at least to be reduced, is the disparity between the characteristics of the results product of optimisation procedures and the recommendations and thumb rules found in construction codes.

This document presents a consistent and rational approach for the generation of Strut-and-Tie models for D -regions in accordance to practical reinforcement layout. The presented approach intends to present a practical alternative for the design of non-flexural regions.

The research presented in this thesis is motivated by two principal aspects of the current engineering practice:

1. The concerns regarding the justification of non-flexural elements through FE based procedures conceived fundamentally for flexural phenomena.
2. The disparity between the vast volume of academic literature in the field of structural optimisation and the low practical application in RC structures.

The core research objective is therefore to contribute towards reducing the evident gap between the rational approach known as Strut-and-Tie and automatic applied methodologies based on finite element analysis industrially applied. The accompanying central hypothesis is that based on the direction fields of principal stresses, plausible ground structures can be automatically proposed and optimised to create suitable Strut-an-Tie models respecting consideration of industrial specific issues.

The research objective is achieved through the proposal of ground structure construction technique and an investigation of optimisation methods and techniques focusing on discrete Fully Stressed Design (FSD) for simultaneous size, topology, and geometric optimisation.

Additionally, the approach proposed within this document is coded in Matlab environment; the developed algorithm is applied and compared to studied cases of elements whose ST models are found in the literature.

Summary of research contributions

A thorough discussion of the research contributions of this thesis, in the context of previous work, is presented within the concluding chapter. A brief summary is presented in this section.

- The methods proposed in this work, discussed in chapters 3 and 4, contribute to the development of an open computational-aided tool addressed to the building industry.
- A straightforward algorithm has been developed to automatically generate feasible initial ground structures out of common FE analysis results.
- Examples of application are presented and directly compared to results found in the literature. Additionally, an example has been performed in order to compare results with those expected from an industrial design.
- An efficient discrete optimisation technique, able to point out a suitable ST model, has been adapted to the rational process of layout selection.
- Following the recommendations found in the building codes (specially the Euro Codes), an exhaustive revision of the elements has been performed not only in terms of material resistance but also regarding spacial and size constraints.

Thesis structure

This work consists of 5 chapters intended to explore the optimisation of Strut-and-Tie models in the structural design of non-flexural zones. Major themes are developed in this work and an original contribution is proposed. To guide the reader, before tackling the main subject, a brief introduction is presented at the beginning of each chapter. In the same spirit, each chapter ends with a discussion of the content. The structure of the thesis is then presented with an overview of each subsequent chapter.

Chapter 1 presents a review and comparison of the state-of-the-art in academic research and building engineering practice, to explore the analysis and design of non-flexural elements. For this purpose, a list of methods was chosen to be discussed. The selection of methods and engineering practices to be discussed was made regarding its appearance in recent scientific bibliography and its reference or mention in current building codes. This chapter highlights the main advantages and disadvantages of the selected methods topics.

Chapter 2 explores the vast domain of structural optimisation. This chapter summarise the optimisation techniques and procedures applied to the optimisation of structures within the civil works domain. The text is principally focused on the use of discrete optimisation in the building industry, choice that is justified within the chapter. This area of application is not intended to be exclusive, since generality is desirable in any method, but rather to provide a unifying theme to the distinct elements of this thesis.

Chapter 3 describes and introduces the application of the developed algorithm. The computational aided procedure is dismembered and each step and sub-algorithm is presented. In order to compare the performance of the proposed algorithm, this chapter presents the results of its application on an example extracted from the literature. At this stage, the comparison focuses in aesthetic aspects such as quantity of resultant elements, distribution and inclination, geometrical aspects directly related with the optimisation process and the automatic selection of the initial truss. A parametric study is carried out to display the advantages and disadvantages of the application of the proposed methodology.

Chapter 4 presents a case that directly compares the results of the proposed algorithm to those obtained through a model that follows a common engineering practice.

The document concludes by summarising the results of the preceding research and discussing future work required in developing these methods.

Related work

The computational power of common desktop computers increases every year. This has been one of the main aspects that have brought the use of advanced analysis programs of research institutes closer to the designer in engineering practice. At the same time, this has impulse the research institutes to develop new techniques and software to better suit the needs of current practice engineers.

Listed here below are some research programs or research topics that have been developed by different research groups The list, not aiming to be exhaustive, contains notable work that is considered to be related with the main topic of this thesis.

CAD interfaces. The CAST (Computer Aided Strut-and-Tie) program is a graphically interactive design tool developed in the University of Illinois. The program , designed to serve as an instructional device for students and practitioners, guides the user to the stages of the Strut-and-Tie Method. To help the user in the selection of a truss, an elastic finite element analysis feature is being developed to generate stress contours and principal stress trajectories. The designer manually defines the truss by first selecting the location of the centre of the nodes and then forming truss members by interconnecting these nodes [Kuchma and Tjhin, 2001]. Similar tools have been developed by different authors [Alshegeir and Ramirez, 1992].

SPanCAD is a software for interactive design of shear walls and deep beams of irregular geometry developed by the Technische Universiteit Delft.

The program SPanCAD is implemented on a finite element program containing only two types of elements: a stringer element (straight bar) and a panel element (rectangle or quadrilateral). According to [Blaauwendraad and Hoogenboom, 2002] SPanCAD is developed to apply the coarsest mesh for a given geometry.

Based on a three design step process that allows to obtain the need of reinforcement for shear walls, deep beams and cellular structures.

The first step is the construction of the model. Using its experience and rules of thumb, the user builds up the model by placing the stringers and panels within the structure. The software proceeds to perform the linear-elastic analysis for all load combinations.

In the second step, the user selects the reinforcement based on force flow computed in the precedent stage. For elements in tension the cross-section area depends on the position and diameter of the bars. With all input quantities being determined and entered into the program, the software performs a nonlinear analysis. The model used accounts for concrete cracking in the tensioned stringers and panels. A revision of the steel is performed at this point: the reinforcement of the stringers is must remain within the linear-elastic domain while the panel reinforcement can yield.

For the third and final step, the user improves the reinforcement using the just computed force flow and crack widths.

A strut-tie2017 <http://astruttie.road.co.kr/index.php/advisor/>

Stress tubes is an approach developed at the Asian Institute of Technology, Bangkok

The described methodology intends to construct suitable Strut-and-Tie models based on linear-elastic Finite Element models. The "extraction" of the models is based on a direct comparison of every principal direction and pointing out groups of elements presenting similar stress trajectories. The following steep deal with the selection of the cross section. Having identified those groups of elements belonging the same trajectory, all the stress vectors are directed in to vertical direction and scattered along the vertical axis. Then plan area of those scattered points is divided in to grid introducing sufficient grid spacing in which each cell in the grid represent the cross section area of the strut or tie [Dammika and Anwar, 2013].

Stress field topology The stress field method has traditionally been based on the assumption of a rigid-plastic stress-strain law without tensile strength for the concrete. Neglecting the tensile strength of concrete requires placing a minimal amount of reinforcement for crack control to ensure a satisfactory behaviour of the structure. This reinforcement ensures that no brittle failure occurs at cracking and that the cracks are suitably smeared over the element at the serviceability limit state. The development of stress fields with the previous assumptions allows a great freedom in the choice of the load-carrying mechanism of a structure.

Continuum structural optimisation techniques. Since early research by Bendsøe and Kikuchi [Bendsøe and Kikuchi, 1988], topology optimisation has been recognized as an important technique to figure out the optimal structure layout within the given design domain. Recently, this technique has been introduced as a most efficient method in searching for optimum structure and Strut-and-Tie optimal patterns.

Micro trusses. Nowadays, several authors intend to implement this method to the RC field (e.g. [Zhong et al., 2016, Nagarajan et al., 2010]). The micro truss is based on the framework method proposed by [Hrennikoff, 1941], in which the structure is replaced by an equivalent pattern of truss elements. Then, each element is given physical characteristics according to geometrical parameters or through an optimisation procedure with the aim to erase or "deactivate" low stress elements from the structure.

Chapter 1

Design of reinforcement for non-flexural elements: a review.

In the Civil Engineering field, most of the conventional reinforced concrete structures are designed as frame systems. Ascribable to their structural configuration, the geometry of the resistant members, and their predominant flexural performance, the global behaviour of a structure can be accurately represented through analytic or numerical models based on flexural beam theory. For this type of elements, the need of reinforcement can be easily computed by determining the internal equilibrium of the resistant forces (given by the steel and concrete) and the resulting system of local forces. On the other hand, at a local scale, zones where the stresses due to shear are predominant over those generated by bending, tend to develop non-flexural elements; in general, these elements are out of the range of validity of beam theory and require a different approach to be implemented.

According to reference [Devadas, 2003], most of the cracks and failures of the structures occur due to an inadequate attention to detailing. Often, these problems are located at geometrical discontinuities such as joints, trims or elements presenting an abrupt change in their thickness but also, in the zones under the effect of exceptional concentrated forces, case of corbels and nibs. In such situations, complex stress states arise and must be taken into account while designing the reinforcement.

As in all other zones of a structure, the main requirements are that all the existing forces from the surroundings could be safely transmitted to the supporting members and/or foundations. Sharp discontinuities can occur in the direction of internal forces and it is imperative to provide a proper reinforcement able resist the tension while being consistent with the pertinent codes in terms of the quantity, distribution, anchorage length, etc.

In many cases, standard guides found in the construction manuals like the ACI detailing recommendations or in the EuroCodes fulfil the design but it is up to the structural engineer to decide whether special considerations are or are not needed.

For the exceptional cases, the structural engineer should isolate specific regions, analyse them and provide the required reinforcement computed through a convenient methodology.

In this chapter are discussed some of the most widely used methodologies for the design of the reinforcement at non-flexural elements and, more generally, applied at disturbed regions. The first section briefly treats the theory applied to the design of common elements and behaviour hypothesis. The second section addresses to the use of the FEM for the structural design. Finally, the Strut-and-Tie method is presented in the third section.

Dimensionnement des armatures pour des éléments non-soumis aux effets de flexion.

Dans le domaine du génie civil, la plupart des structures conventionnelles en béton armé sont conçues comme des systèmes de portiques. Compte tenu de leur configuration structurale, de la géométrie des éléments résistants et de leur performance prédominante en flexion, le comportement global d'une structure peut être représenté avec précision à l'aide de modèles analytiques ou numériques basés sur la théorie de la flexion. Pour ce type d'éléments, le besoin de renforcement par armatures noyées peut être facilement calculé en déterminant l'équilibre interne des sections résistantes (acier et béton) et le système résultant des forces locales. D'autre part, à l'échelle locale, les zones où les contraintes dues au cisaillement sont prédominantes par rapport à celles générées par la flexion ont tendance à développer des éléments non flexibles ; en général, la théorie des poutres ne s'appliquant pas à ces éléments, leur traitement nécessite de mettre en oeuvre une approche différente.

Selon [Devadas, 2003], la plupart des fissures et des défaillances des structures se produisent en raison d'une attention insuffisante aux détails. Souvent, ces problèmes sont localisés dans des discontinuités géométriques telles que des joints, des remplissages ou des éléments présentant un changement brusque de leur épaisseur mais aussi sous l'effet de forces concentrées exceptionnelles dans les zones de liaisons comme les corbeaux et les baïonnettes. Des états de contraintes complexes apparaissent et doivent être pris en compte lors de la conception du ferrailage.

Comme dans toutes autres zones d'une structure, les forces existantes doivent être transmises aux éléments de support et/ou aux fondations en limitant la concentration de contraintes. De fortes discontinuités peuvent ainsi se produire suivant la direction des efforts internes. Il est alors impératif de prévoir un ferrailage approprié capable de résister à la traction tout en étant cohérent avec les codes pertinents en termes de quantité, de distribution, d'ancrage, etc.

Dans la plupart des cas, les guides trouvés dans les manuels de construction comme les recommandations de l'ACI ou dans les EuroCodes répondent à la conception, mais il est de la responsabilité de l'ingénieur structure de décider si des considérations spéciales sont ou non nécessaires.

Pour les cas exceptionnels et suivant les recommandations faites dans la littérature telle que [Schlaich et al., 1987] et [Hsu, 1992], l'ingénieur structure devrait isoler des régions spécifiques, les analyser et dimensionner le ferrailage au moyen d'une méthodologie appropriée.

Dans ce travail de recherche sont discutées certaines des méthodologies les plus largement utilisées pour la conception du ferrailage de renforcement des éléments non travaillant en flexion et, plus généralement, les approches mises en oeuvre dans les régions dites perturbées. La première section traite brièvement de la théorie appliquée à la conception d'éléments communs et des hypothèses de comportement. La deuxième section porte sur l'utilisation de la méthode des Éléments Finis pour la conception structurale. Pour finir, la méthode bielle-tirant est présentée.

1.1 Reinforced concrete elements

A structure can be defined as a well-organised load-bearing system composed by a set of properly connected elements intended to withstand forces. On the other hand, Reinforced Concrete (RC) is a composite material in which concrete's relatively low tensile strength is counteracted by the inclusion of reinforcement (commonly steel bars). Thus, a reinforced concrete structure can be seen as an organised system formed of individual composite elements made up of concrete and steel that, properly connected, display an adequate load-bearing capacity, stiffness, deformability and energy-dissipating capacity.

Most reinforced concrete structures can be subdivided into beams, slabs, and columns; beams and slabs are elements subjected primarily to flexure (bending) while columns are generally subjected to axial compression and bending. In addition to this subdivision, the non-flexural elements can be pointed out as elements whose behaviour does not correspond to neither flexion nor compression.

The combination of the bending and shear loads produces maximum normal and shearing stresses in a specific plane inclined with respect to the global axis of the structure. In a 3 point bending test, the principal stress in tension acts at an approximately along a 45° plane to the normal at sections close to the supports. Due to the low tensile strength of concrete material, diagonal cracking develops along planes perpendicular to the plane of principal tensile stress. These are zones where shear failure, or strictly speaking diagonal tension failure, governs over flexural or compressive ones; hence special considerations must take place while designing.

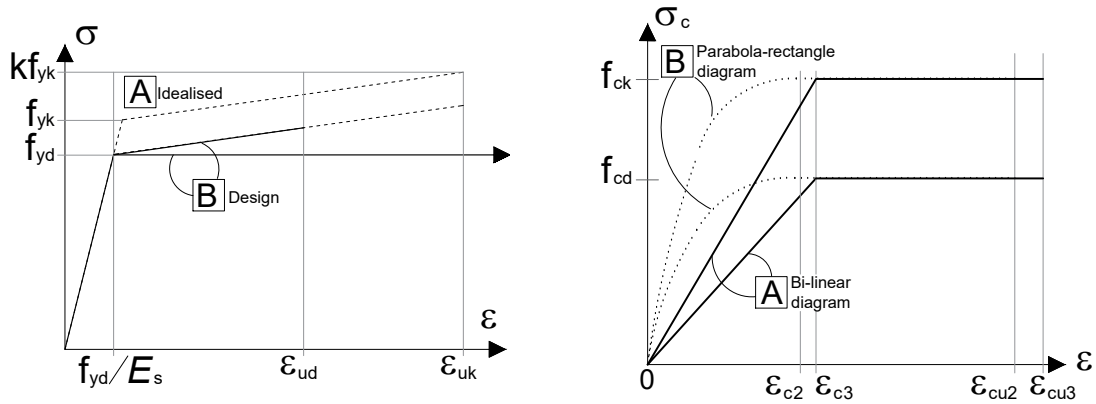
1.1.1 Flexure theory for reinforced concrete

Among all the phenomena concerning RC structures, the flexural behaviour (moment versus curvature relationship) is one of the most well studied. The theory of flexure that allows the analyse of the resistance of a reinforced concrete beam, is based in three basic assumptions:

- Plane sections, perpendicular to the axis of bending, remain plane.
- The strain in the concrete is equal to the strain in the reinforcement at the same level.
- The stresses along the element can be computed from the strains by using stress-strain curves for each individual material (concrete and steel).

Few words must be said about the above assumptions. The first one is the traditional “plane sections remain plane” assumption made in Euler-Bernoulli theory for beams made of any material. The second assumption implies a perfect bonding condition between the concrete and the steel

The third assumption needs to be attached to reference stress-strain relationships like the ones depicted in figure 1.1. Concrete model generally consists of a parabola (equations 1.1) from zero stress to the compressive strength of the concrete. The strain that corresponds to the peak compressive stress, ϵ_0 , is often assumed to be 0.002 for normal strength concrete.



(a) Assumed steel reinforcement stress-strain (b) Assumed concrete stress-strain for the design of cross-sections

Figure 1.1: Assumed material stress-strain relationships according to Eurocode2.

$$f_c = f'_c \left[2 \left(\frac{\epsilon_c}{\epsilon_0} \right) - \left(\frac{\epsilon_c}{\epsilon_0} \right)^2 \right] \quad (\text{ACI}) \quad (1.1a)$$

$$\sigma_c = f_{cd} \left[1 - \left(1 - \frac{\epsilon_c}{\epsilon_{c2}} \right)^n \right] \quad \text{for } 0 \leq \epsilon_c \leq \epsilon_{c2} \quad [\text{Eq. (3.17) of EC2}] \quad (1.2a)$$

$$\sigma_c = f_{cd} \quad \text{for } \epsilon_{c2} \leq \epsilon_c \leq \epsilon_{cu2} \quad [\text{Eq. (3.18) of EC2}] \quad (1.2b)$$

where n is an exponent depending on the class of concrete (commonly 2), ϵ_{c2} is the strain at reaching the maximum strength and ϵ_{cu2} is the ultimate allowed strain.

For explanatory purposes, in the last expressions f_{cd} corresponds to the value of the design compressive strength of the concrete defined as $f_{cd} = \alpha_{cc} f_{ck} / \gamma_c$ (Eq. (3.15) of EC2). Being γ_c the partial safety factor for concrete (1.5 recommended for persistent design situations), α_{cc} the coefficient taking account of long term effects on the compressive strength and of unfavourable effects resulting from the way the load is applied (taken as 1), and .

Beyond ϵ_0 , the stresses developed by the concrete are assumed to be inversely proportional to strain. In tension the concrete can be assumed to present a simplified linear stress-strain relationship up to the value of the design tensile strength, f_{ctd} , defined as:

$$f_{ctd} = \alpha_{ct} \frac{f_{ckt,0.05}}{\gamma_C} \quad [\text{Eq. (3.16) of EC2}] \quad (1.3)$$

For steel reinforcement, the considered model is much more simple. As depicted in figure 1.1a, a elastic-perfectly plastic model will be assumed for the steel acting in tension or in compression.

Even if these three assumptions allow the calculation of the behaviour of flexural RC elements, for design purposes, additional assumptions can be made.

- The tensile strength of concrete is neglected

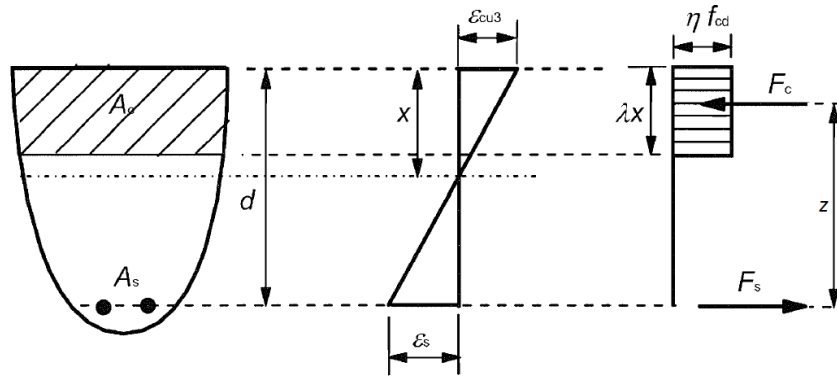


Figure 1.2: Simplified strain and stress distribution in a plane section [EC2].

- The material stress–strain curves may be assumed to be rectangular, trapezoidal, parabolic, or any other shape that results in a good prediction in agreement with the results of comprehensive tests
- The nominal flexural strength is assumed to correspond to the attain maximum allowed compression strain in the extreme concrete compression fiber

The beam flexure formula, $\sigma = \frac{M}{I}y$, allows to find the maximum bending stress on an homogeneous, isotropic, and linearly elastic beam element. When resisting pure bending, flexural stresses are developed in the element; tension stresses are developed in the external fiber of the element while compression stresses are developed in the internal fiber. Due to its high resistance to compressive forces but its poor resistance to tensile ones, in practice, the concrete section subjected to tension stresses is neglected and only the zone in compression is considered to provide a resistance force to the element. To satisfy the equilibrium of the resultant horizontal forces, the tensile force F_s in the steel should balance the compressive force in the concrete F_c (see figure 1.2).

Experimental results have shown that the strength of concrete in tension is roughly one-tenth of the compressive strength [Cuevas and Villegas, 2006], [Foster et al., 2003]. As a consequence, the tensile force developed in the concrete below the zero strain axis, is small compared with the tensile force in the steel. Hence, the contribution of the tensile stresses in the concrete to the element flexural capacity is small and can be neglected. Additionally, rather than using a closely representative stress–strain curve, simplified diagrams are commonly used in computations (see figures 1.1).

It should be noted that these assumptions are made primarily to simplify the calculations and they may slightly influence the final results [MacGregor, 1992].

1.1.2 Elements in compression

When a symmetrical element is subjected to a concentric axial load, P , longitudinal strains develop uniformly across the section. As in the case of flexion, perfect bounding is assumed which assures that the strains in the concrete and steel are equal. For any given strain, it is possible to compute the stresses and, given that the forces and in the concrete and steel are equal to the stresses multiplied by the corresponding areas, the total load on the column is the sum of the force developed in the concrete plus the force developed in the steel.

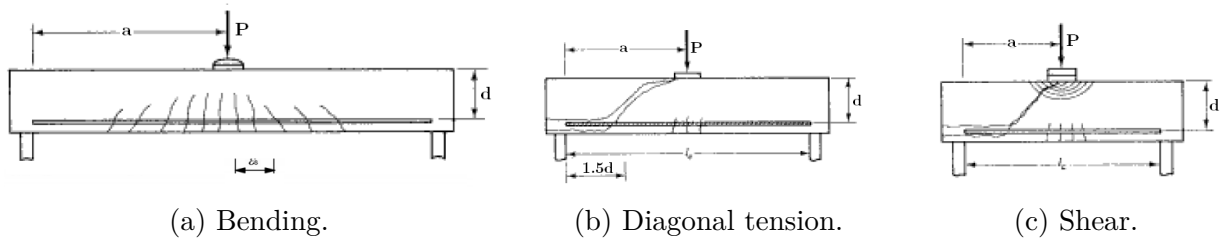


Figure 1.3: Failure patterns as a function of beam slenderness [Nawy, 2000].

This additional contribution of the resistance can be approached as the product of the steel transverse, a_s , area multiplied by the yielding stress, σ_y . Hence, the maximum resisting load, P_0 , that a prismatic concrete section reinforced with longitudinal steel can develop is given by:

$$P_0 = \phi \sigma_c a_c + a_s \sigma_y \quad (1.4)$$

where a_c represents the concrete's cross section and ϕ is reduction factor that takes into account geometric imperfections.

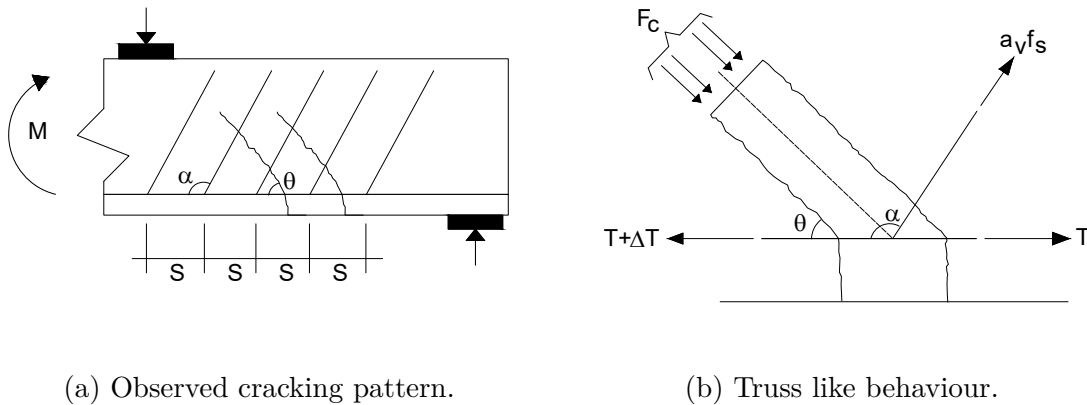
In real structures is not common to find elements working under pure compressive actions. Due to accidental eccentricity in addition to the fact that almost every structure is continuous, the axial loading and bending moments are considered together. Most design codes recommend to take into consideration the effects of elements subjected to flexo-compression even if the structural analysis points out zero bending forces.

1.1.3 Elements resisting to diagonal tension and shear

As depicted in the last paragraphs, the behaviour of a simply supported reinforced concrete beam under bending effects produce compressive stresses above the neutral axis and tension stresses under it. The maximum bending moment is found under the centroid of the loading. Its intensity decreases toward the supports and the shear stress increases. The major principal stress acts along a plane tilted approximately 45° to the normal at sections close to the support. Due to the concrete's low tensile resistance, diagonal cracking is formed perpendicular to the tension stresses. To prevent this cracks, diagonal tension reinforcement has to be provided.

Diagonal tension failure, figure 1.3b, occurs in elements where the shear span/depth ratio is of an intermediate "magnitude" (a/d between 2.5 and 5.5). For smaller shear span/depth ratios (a/d between 1 to 2.5) the failure is mainly attributed to shear (figure 1.3c).

Considering the true nature of the concrete as a non-elastic and a non-homogeneous material, the intricacy of the problem increases and consequently, the behaviour of RC elements become more complex than previously explained. The stress distribution is modified once the concrete's tensile capacity is reached and cracking starts. Some characteristics such as position and length of the fissures cannot be accurately predicted due to local resistance variations within the matrix of the concrete. Due to this difficulty, it must be added the fact that the concrete is not an elastic material and, in consequence, the stress distribution changes for different level of loading.



(a) Observed cracking pattern.

(b) Truss like behaviour.

Figure 1.4: Ritter's truss analogy.

Owing to the complexity of the problem, the current methods used for designing RC elements undergoing shear are based on the results of experimental campaigns (e.g [Mattock et al., 1976] and [Aguilar et al., 2002]). Those campaigns are principally focused on determining the concrete resistance against diagonal cracking and the contribution of the transverse reinforcement to the global resistance

In an attempt to predict the behaviour of elements governed by shear, Ritter [Ritter, 1899] proposed that reinforced beam presenting inclined fissures can be idealised as a truss where the longitudinal reinforcement acts as a tensile chord, the transverse reinforcement acts as webs withstanding traction and, finally, the segments of concrete between the principal cracks idealised as the webs in compression. This idealisation is depicted in figure 1.4.

The premises considered are the following:

- The element's compressed zone develops only normal compressive stresses
- All transverse traction is resisted by the transverse reinforcement
- The fissures extend from the lowest fiber to the centroid of the compressed zone
- The self weight is neglected and distributed loads acting between cracks. In other words, the increment in the shear, ΔV , of two sections is given by V_s where V is the shear force in the zone between the two considered sections and s is the distance separating them.

The analogy considers an angle θ measured between the crack pattern and the element axis, and an angle α that corresponds to inclination of the transverse reinforcement also compared to the element axis. In accordance to figure 1.4, the horizontal spacing between inclined cracks and the stirrups is denoted by s . The compression force at the concrete diagonal is F_c and the traction acting at the diagonal reinforcement is given by $a_v f_s$ (being a_v the cross section of the transverse reinforcement and f_s the force acting on it)

As result of the increment in the bending moment, ΔM , an increment in the longitudinal tension, ΔT is also produced. From the equilibrium over the vertical and horizontal forces it is found that the maximum shear force, V_{max} , is given by:

$$V_{max} = \frac{a_v \sigma_y z}{s} \left[\cos \alpha + \frac{\sin \alpha}{\cos \theta} \right] \quad (1.5)$$

where a_v represents the available shear reinforcement presenting; an array of individual stirrups separated a distance s and tilted an angle α . σ_y represents the steel's yield limit, z lever arm (distance between the centroids of compressive and tensile chords), and T is the force of traction acting on the longitudinal steel.

From the latter expression, it can be deduced that, if the load capacity of an element is directly dependant on its resistance to inclined stresses, the maximum admissible load corresponds to the development of the yielding stress at the stirrups or the transverse reinforcement. This implies that both parts, the concrete forming the compression cords as well the reinforcement forming the tension ones, must be able to withstand the force increments originated by the crack evolution.

The truss analogy has been used to estimate the shear resistance of elements with transverse reinforcement. For practical purposes and with the aim of obtaining a good correlation between the calculated resistance and the experimental tests [Turmo et al., 2009] [Rao et al., 2007], the resulting admissible load has been expressed as the addition of the computed resistance plus the resistance of the element supposing no transverse reinforcement. As expressed, this resolution achieves good correlation but lacks of theoretical framework [Grandić et al., 2015].

Some authors have proposed modifications to the original truss model like taking into account important factors such as the angle of cracks, transverse deformations, fan-shaped-crack pattern, normal stress continuity along cracks to cite some of them but such modifications have not been included in the design codes [for Structural Concrete, 2008] and will not be detailed in this document.

Given that vertical shear force has been taken to be a good indicator of diagonal tension, diagonal tensile forces are not calculated for most of the structural elements. For flexural elements requiring design shear reinforcement, the EuroCodes bases its hypothesis on the truss model. Nevertheless, for beams with loads near to supports, corbels and any element where a non-linear strain distribution exist this codes suggest to apply strut-and-tie models.

1.2 Finite element models for RC structures

Computer-based analysis and design for RC structures, have seen tremendous advancement in the last half-century and its application has become a common step in most structural engineering companies. Nowadays, elastic based stress analysis using finite element method (FEM) is a reliable tool to model any conceivable structure with acceptable precision [Bathe, 2006] allowing various degrees of sophistication. Some of the advantages of the use of FEM for structural design are:

- Numerous FEM freeware and shareware software packages conceived for structural design and analysis are available.
- Linear FE modelling is well established and, nowadays, relatively easy to apply.

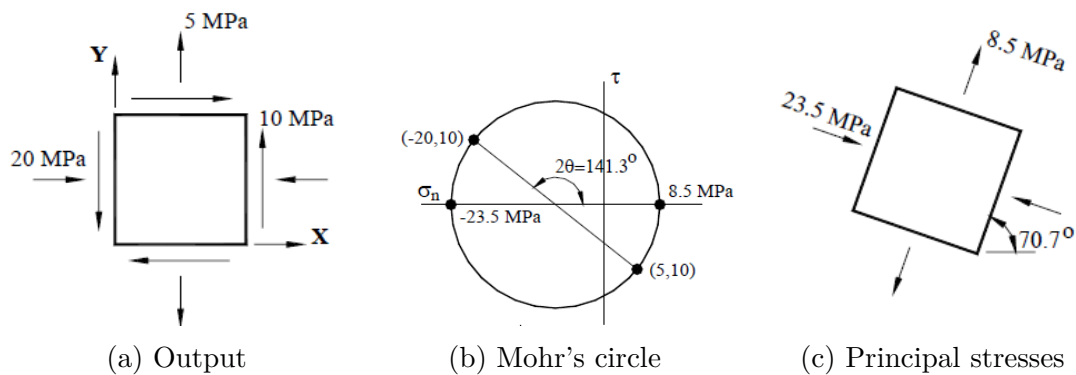


Figure 1.5: Example of output from a membrane's FE modelling

- Multiple load cases can be easily programmed and added one to another according to the principle of superposition.
- It indirectly helps to control crack propagation by placing the greatest quantity of reinforcement in the high-tension regions that is, in regions corresponding to the initial crack locations.

For each advantage we can find one, or more, disadvantages. Some of the main drawbacks in using the FEM are:

- No information is given about collapse load.
- Linear FEM does not explicitly take cracking into account.
- Careful detailing procedures must be established and followed in order to meet the serviceability and ductility demands.

1.2.1 Membranes

Usually, the output of linear elastic FE modelling of membranes is given in terms of stresses and strains in the Cartesian coordinate system, whose principal axes are generally chosen to be collinear with the envisaged preponderant reinforcement directions. The presented solution satisfies equilibrium but presents constructive difficulties. Whilst principal stresses are of interest as they give the elastic load path and from a simple resistance point of view, the best reinforcement trajectory, it is usually preferable to place the reinforcement along the axes of the structure or the structural element. For this case, the sum of the stress resultants of concrete and steel reinforcement must equilibrate the global stresses on the membrane. In most approaches [Collins and Mitchell, 1980], [Vecchio and Selby, 1991], [Vecchio and Collins, 1986], the concrete is assumed to be a no-tension material and, in the same manner, the steel reinforcement is idealised to carry no compression (unilateral stress-strain relationship).

For a general element, the concrete and reinforcement stress resultants must sum to the global stresses on the membrane (see figure 1.6). However, this approach does not

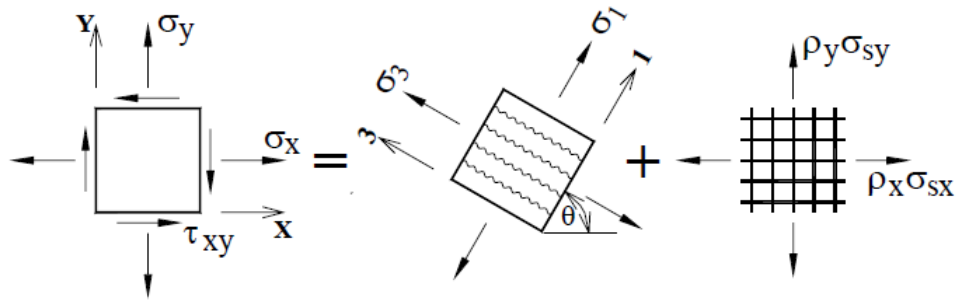


Figure 1.6: Concrete and steel reinforcement stress components

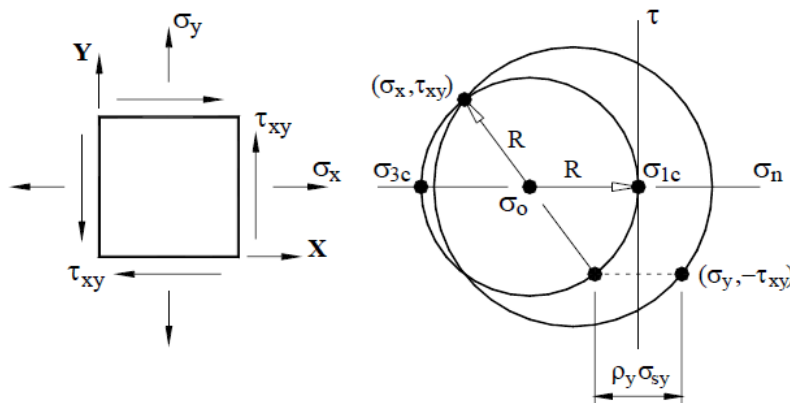


Figure 1.7: Mohr's circle for reinforcing steel placed solely in the Y-direction

necessarily conducts to a unique response due to the multiple values of $\rho_x \sigma_{xy}$ and $\rho_y \sigma_{yx}$ that combined can assure equilibrium .

A practical solution is to place the reinforcement along just one principal direction [Park and Gamble, 2000]. If, for example, the designer chooses to reinforce only along the Y direction, the prescribed solution would automatically implies that $\rho_x = 0$. Since no stress in traction acts on the concrete ($\sigma_{1c} = 0$), the minor stress acting on the concrete can be obtained from $\sigma_{3c} = 2\sigma_0$; the Mohr's circle of concrete stress state calculated from two points on the circle (see figure 1.7) where σ_0 is the normal stress at the centre of the Mohr's circle of concrete stresses and σ_x and τ_{xy} are the X -normal and shear stresses, respectively.

From the geometry of the circles it can also be appreciated that the required stress in the reinforcement direction (Y -direction) is given by $\rho_y \sigma_{sy} = \sigma_x + \sigma_y - 2\sigma_0$.

In figure 1.8, the Mohr's circle for an isotropically reinforced concrete panel is presented. It can be appreciated that the circle representing the concrete stress state is a mere translation of the global stresses represented before (1.6) and that the quantities $\rho_x \sigma_{sx}$ and $\rho_y \sigma_{sy}$ equal the major principal stress σ_I . It should be pointed out that the area of reinforcement acting at each of the global axis, X and Y , is equal to the area needed for the case where the steel is placed along the direction corresponding to the major principal stress.

The most general case of reinforcement, is given by the denominated plasticity criterion [Johansen, 1962], [Nielsen, 1964] where a series of formulae (equations 1.6a to 1.6g)

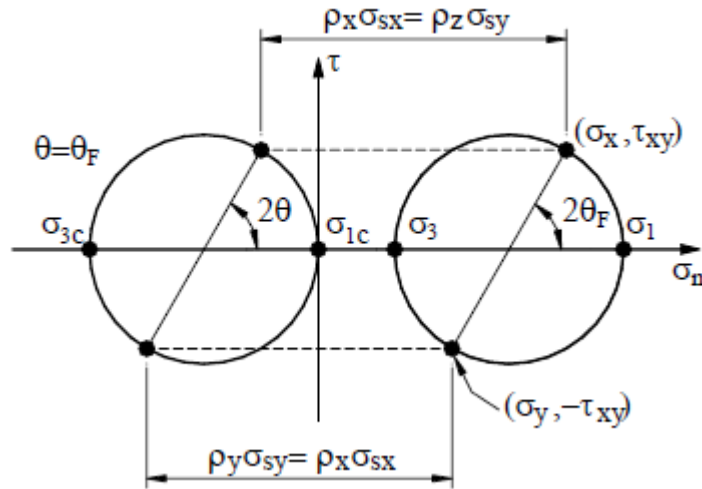


Figure 1.8: Mohr's circles for isotropically reinforced panels

approach a failure surface.

$$Y_1 = \tau_{xy}^2 - (\rho_x \frac{\partial f_{yt}}{\partial x} - \sigma_x)(\rho_y \frac{\partial f_{yt}}{\partial y} - \sigma_y) = 0 \quad (1.6a)$$

$$Y_2 = \tau_{xy}^2 - (f_{cd} - \rho_x \frac{\partial f_{yt}}{\partial x} + \sigma_x)(\rho_x \frac{\partial f_{yt}}{\partial x} - \sigma_x) = 0 \quad (1.6b)$$

$$Y_3 = \tau_{xy}^2 - (f_{cd} - \rho_y \frac{\partial f_{yt}}{\partial y} + \sigma_y)(\rho_y \frac{\partial f_{yt}}{\partial y} - \sigma_y) = 0 \quad (1.6c)$$

$$Y_4 = \tau_{xy}^2 - f_{cd}/4 = 0 \quad (1.6d)$$

$$Y_5 = \tau_{xy}^2 + (f_{cd} + \rho_x \frac{\partial f_{yc}}{\partial x} + \sigma_x)(\rho_x \frac{\partial f_{yc}}{\partial x} + \sigma_x) = 0 \quad (1.6e)$$

$$Y_6 = \tau_{xy}^2 + (f_{cd} + \rho_y \frac{\partial f_{yc}}{\partial y} + \sigma_y)(\rho_y \frac{\partial f_{yc}}{\partial y} + \sigma_y) = 0 \quad (1.6f)$$

$$Y_7 = \tau_{xy}^2 + (f_{cd} + \rho_x \frac{\partial f_{yc}}{\partial x} + \sigma_x)(\rho_x \frac{\partial f_{yc}}{\partial x} + \sigma_x) = 0 \quad (1.6g)$$

where f_{cd} is the design value of the concrete's compression strength variations, $\frac{\partial f_{yt}}{\partial x}$ and $\frac{\partial f_{yt}}{\partial y}$ are the design strength variations of the steel reinforcement in tension in the global directions, and $\frac{\partial f_{yc}}{\partial x}$ and $\frac{\partial f_{yc}}{\partial y}$ are the design strengths of the steel reinforcement in compression.

In spite of its relatively straightforward application, its applicability may not be easy due to the difficulties related to a 3-dimensional stress space plotting and as alternative graphic solution remains the use of Mohr's circles of stress [for Structural Concrete, 2008].

1.2.2 Slabs and shells

Similar to that for membranes, the dimensioning of shell elements is typically based on yield conditions derived from plasticity theory according to their stress state. While a meticulous analysis, taking into account limited ductility of concrete, is important for membrane

elements design, there is much less concern with shells since such structures are typically under-reinforced [for Structural Concrete, 2008]. In other words, the failure of this kind of elements is governed by yielding of the reinforcement bars and not by crushing at the concrete section. An important exception can be mentioned about concentrated transverse forces, that may result in brittle punching failures without transverse reinforcement [Unnikrishna and Devdas, 2003].

As expressed before, placing the steel bars aligned with the principal (major) stress direction could minimise the quantity of required reinforcement for shell elements. The so-called “trajectory reinforcement” has been applied to several slab and shell structures in the past [?]. However, if several different load-cases must be considered, the principal stress directions may vary from one case to another thus, making impossible to align the reinforcement. For these and other constructibility reasons mentioned before, orthogonal reinforcement is provided in almost all slabs and shell structures.

The output of a shell element consists in eight independent stress resultants: bending and twisting moments (M_{xx} , M_{yy} , M_{xy} , and M_{yx}), transverse shear forces (T_{xz} and T_{yz}) and membrane forces (N_{xx} , N_{yy} , and N_{xy}) 1.10a. By applying equilibrium equations over the body, it can be stated that:

$$\frac{\partial T_{xz}}{\partial x} + \frac{\partial T_{yz}}{\partial y} + q = 0 \quad (1.7a)$$

$$\frac{\partial M_{xx}}{\partial x} + \frac{\partial M_{xy}}{\partial y} - T_{xz} = 0 \quad (1.7b)$$

$$\frac{\partial M_{yy}}{\partial y} + \frac{\partial M_{yx}}{\partial x} - T_{yz} = 0 \quad (1.7c)$$

Moment equilibrium equations yields to:

$$M_n = M_{xx} \cos^2 \phi + M_{yy} \sin^2 \phi + M_{xy} \sin 2\phi \quad (1.8a)$$

$$M_t = M_{xx} \sin^2 \phi + M_{yy} \cos^2 \phi - M_{xy} \sin 2\phi \quad (1.8b)$$

$$M_{nt} = (M_{yy} - M_{xx}) \sin \phi \cos \phi + M_{xy} \cos 2\phi \quad (1.8c)$$

This last group equations can be interpreted as the transformation of bending and twisting moments acting on any boundary perpendicular to the direction n , where the orientation is determined by the angle ϕ . Analogously, the equations for the equilibrium of the forces acting on the slab elements yields to the transformation of transverse shear forces perpendicular to n are given by equations 1.9.

$$V_n = T_{xz} \cos \phi + T_{yz} \sin \phi \quad (1.9a)$$

$$V_t = -T_{xz} \sin \phi + T_{yz} \cos \phi \quad (1.9b)$$

1.2.2.1 Normal moment yield criterion

For a given simply supported concrete slab, subjected to a distributed service load, the response is expected to remain within the elastic domain with the maximum level of stresses

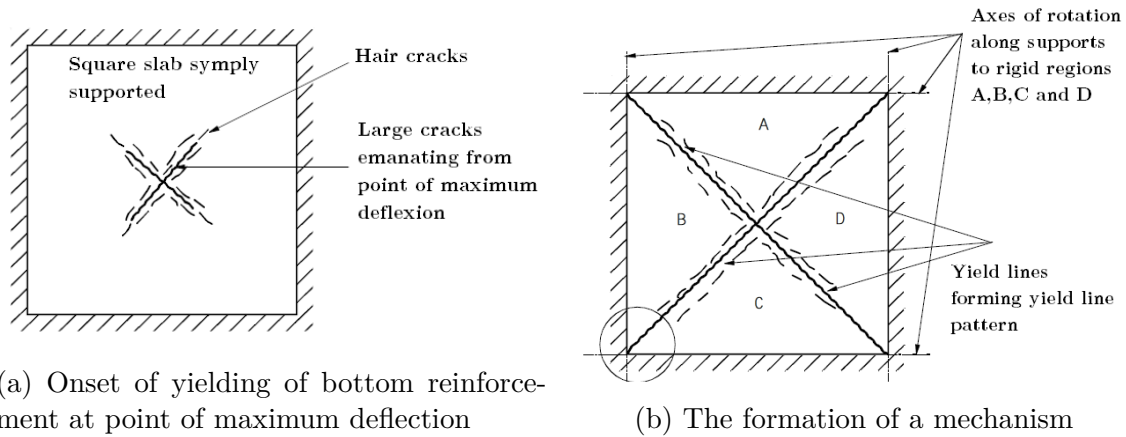


Figure 1.9: Simply supported two-way slab with the bottom steel having yielded along the yield lines

at steel reinforcement and maximum deflection occurring at the centre of the element. At this stage, negligible cracking may occur at the lower layer, zone where the concrete's tensile capacity will be exceeded due to the forces carried out by flexural behaviour (figure A.6c). Increasing the load beyond the service limit, will increase the size and depth of the cracks and may induce the yielding of the reinforcement. Increasing the load still further, will propagate the cracks to the free edges of the element generating the yielding lines to cross all reinforcing bars. At this ultimate state, the yield lines form boundaries and allow rotation between the rigid or "intact" parts, thus creating mechanisms and the instability of the element (figure 1.9b).

The ultimate load of concrete slabs and shells has been investigated by considering local stresses and strains within the element and their corresponding yield conditions under the basis of plasticity theory and flow rules for concrete and for the inner reinforcement [Nilson, 1997]. This approach gives accurate results for almost any case but its application is rarely justified.

By superimposing the ultimate shell's moments M_{xu} and M_{yu} along the global reinforcement directions and setting M_{xy} , N_{xx} , and N_{yy} equal to zero, a simplified statically admissible state of stress is obtained. Now, for an arbitrary direction n , and based on equations 1.8, it can be stated that $N_n = N_{tn} = 0$, $M_n = M_{xu} \cos^2 \phi + M_{yu} \sin^2 \phi$ and $M_{tn} = (M_{yu} - M_{xu}) \sin \phi \cos \phi$. For most cases, the resultant depths of the compression zone in the concrete section do not coincide for the two orthogonal directions, $c_x \neq c_y$. As a result, there is no development of compatible mechanism (figure 1.10c). The difference between the value obtained for M_n and the value of M_{nu} for $c_x \neq c_y$ have been found of a negligible order leading to:

$$M_{nu} = M_{xu} \cos^2 \phi + M_{yu} \sin^2 \phi \quad (1.10)$$

$$M'_{nu} = M'_{xu} \cos^2 \phi + M'_{yu} \sin^2 \phi \quad (1.11)$$

From equations 1.8, a state of stress in terms of M_{xx} , M_{yy} , and M_{xy} corresponds to bending and twisting moments in direction n is given by $M_n = M_{xx} \cos^2 \phi + M_{yy} \sin^2 \phi + M_{xy} \sin(2\phi)$. From combining these previous expressions with the inequality condition, $-M_{yu} \leq M_n \leq M_{yu}$, the yield conditions for orthogonally reinforced shell elements can be

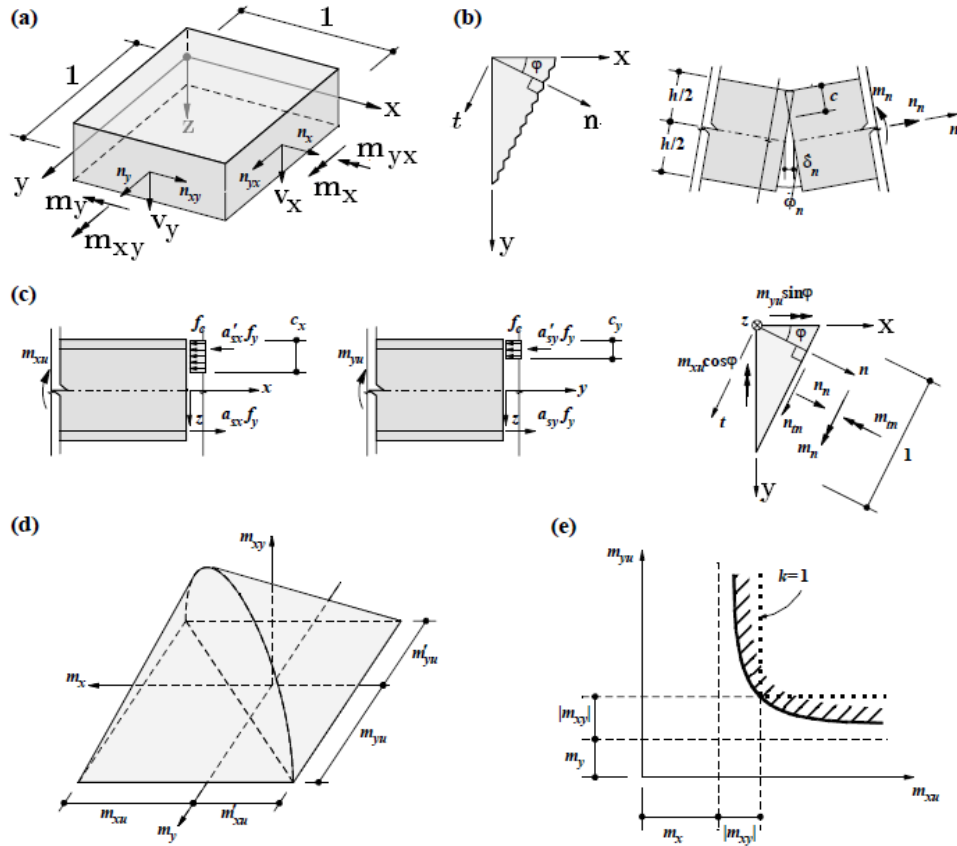


Figure 1.10: Normal yield criterion: a) shell element, b) Yield line, c) superimposition of ultimate moment in directions X and Y d) Yield condition e) dimensioning.

obtained (see equations 1.12).

$$Y = M_{xy}^2 - (M_{xu} - M_{xx})(M_{yu} - M_{yy}) = 0 \quad (1.12a)$$

$$Y' = M_{xy}^2 - (M'_{xu} - M_{xx})(M'_{yu} - M_{yy}) = 0 \quad (1.12b)$$

where some restrictions are applied; $(M_{xu} - M_{xx} \geq 0, M_{yu} - M_{yy} \geq 0, M'_{xu} + M_{xx} \geq 0,$ and $M'_{yu} + M_{yy} \geq 0$. In figure 1.10, the conditions Y'_0 and $Y = 0$ are represented.

Finally, the yielding reinforcement layers are generally substituted by an equivalent orthogonal reinforcement. Hence, fictitious resistances, N_{xs} , N_{ys} and N_{xys} , are computed in order to take into account the effect of the reinforcement distributed into several layers oriented in directions differing by angles Θ_i measured from the X -axis and with individual resistances equivalent to its cross section, $N_{is} = (a_s f_{sy})_i$ per unit width.

$$N_{xs} = \sum_i N_{is} \cos^2 \Theta_i \quad (1.13a)$$

$$N_{ys} = \sum_i N_{is} \sin^2 \Theta_i \quad (1.13b)$$

$$N_{xys} = \sum_i N_{is} \cos \Theta_i \sin \Theta_i \quad (1.13c)$$

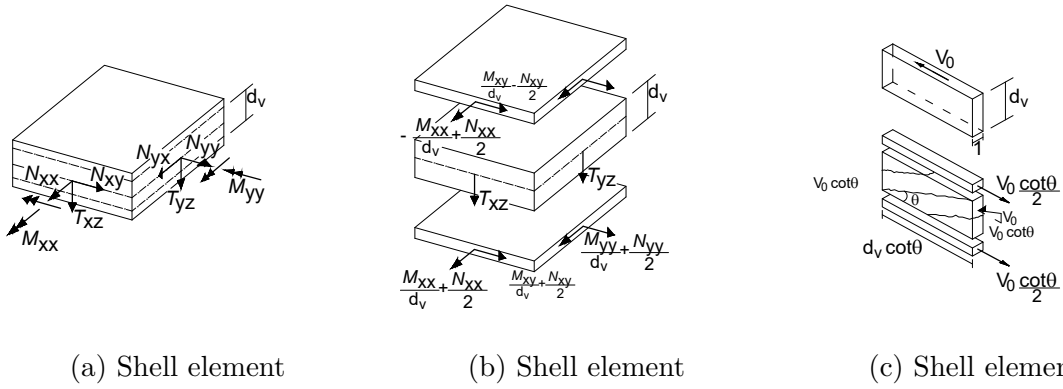


Figure 1.11: Sandwich model.

Due to its simplicity, the normal yield criterion is widely used for the design of concrete slabs in current practice [Kennedy and Goodchild, 2004]. Nevertheless, this method is not conceived for elements presenting excessive reinforcement ratios [Marti, 1978].

1.2.2.2 Sandwich model for shell elements

This model idealises the behaviour of a slab, or a shell, section as the interaction of three complementary elements [Marti, 1990]. The covers withstand the bending and twisting moments (M_{xx} , M_{yy} , M_{xy}) as well as the in-plane forces (N_{xx} , N_{yy} , N_{xy}) while the transverse shear forces (T_{xz} , T_{yz}) are resisted by the core as depicted in figure 1.11.

The middle planes of the covers are taken to coincide with the middle planes of the reinforcing meshes close to the element surfaces. Assuming equal cover thickness, c , at both sides of the element, the resultant lever arm of the developed inplane forces at the covers, d , is equal to the effective shear depth of the core, d_v .

In general, the model considers the principal transverse shear force to be transferred only by core, $V_0 = \sqrt{T_{xz}^2 + T_{yz}^2}$ along direction $\phi_0 = \tan^{-1}(T_{xz}/T_{yz})$. If the nominal shear stress, V_0/d_v is below the nominal concrete's shear cracking, $\tau_{C,red}$, the core is considered to be uncracked and the forces at the covers are given by:

$$N_x \text{ inf,sup} = \pm \frac{M_{xx}}{d_v} + \frac{N_{xx}}{2} \quad (1.14a)$$

$$N_y \text{ inf,sup} = \pm \frac{M_{yy}}{d_v} + \frac{N_{yy}}{2} \quad (1.14b)$$

$$N_{xy} \text{ inf,sup} = \pm \frac{M_{xy}}{d_v} + \frac{N_{xy}}{2} \quad (1.14c)$$

On the contrary, if the shear stress exceeds the nominal concrete's shear cracking resistance, the core fissures and is treated as the web of a girder of flanged cross-section along direction ϕ_0 (figure 1.11). The inclination produces tensile forces that must be resisted by the covers modifying equations 1.14 as follows:

$$N_x \text{ inf,sup} = \pm \frac{M_{xx}}{d_v} + \frac{N_{xx}}{2} + \frac{T_{xz}}{2V_0 \tan \theta} \quad (1.15a)$$

$$N_y \text{ inf,sup} = \pm \frac{M_{yy}}{d_v} + \frac{N_{yy}}{2} + \frac{T_{yz}}{2V_0 \tan \theta} \quad (1.15b)$$

$$N_{xy} \text{ inf,sup} = \pm \frac{M_{xy}}{d_v} + \frac{N_{xy}}{2} + \frac{T_{xz}T_{yz}}{2V_0 \tan \theta} \quad (1.15c)$$

For cases where the concrete remains elastic and the failure is governed by yielding of the reinforcement, the force per unit width acting at the reinforcement in the X and Y directions can be determined by:

$$a_{SX}\sigma_y \geq \frac{M_{xx}}{d_v} + \frac{N_{xx}}{2} + \frac{T_{xz}}{2V_0 \tan \theta} + k \left| \frac{M_{xy}}{d_v} + \frac{N_{xy}}{2} + \frac{T_{xz}T_{yz}}{2V_0 \tan \theta} \right| \quad (1.16a)$$

$$a_{SY}\sigma_y \geq \frac{M_{yy}}{d_v} + \frac{N_{yy}}{2} + \frac{T_{yz}}{2V_0 \tan \theta} + k^{-1} \left| \frac{M_{xy}}{d_v} + \frac{N_{xy}}{2} + \frac{T_{xz}T_{yz}}{2V_0 \tan \theta} \right| \quad (1.16b)$$

$$a'_{SX}\sigma_y \geq \frac{-M_{xx}}{d_v} + \frac{N_{xx}}{2} + \frac{T_{xz}}{2V_0 \tan \theta} + k' \left| \frac{-M_{xy}}{d_v} + \frac{N_{xy}}{2} + \frac{T_{xz}T_{yz}}{2V_0 \tan \theta} \right| \quad (1.16c)$$

$$a'_{SY}\sigma_y \geq \frac{-M_{yy}}{d_v} + \frac{N_{yy}}{2} + \frac{T_{yz}}{2V_0 \tan \theta} + k'^{-1} \left| \frac{-M_{xy}}{d_v} + \frac{N_{xy}}{2} + \frac{T_{xz}T_{yz}}{2V_0 \tan \theta} \right| \quad (1.16d)$$

where a k and k' are arbitrary positive factors (normally taken equal to 1), θ is the inclination of the diagonal compression, a_s and a'_s are the bottom and top reinforcement areas per unit width.

For the case where the core is cracked, the need of transverse reinforcement ratio is computed by $\rho = \frac{V_0 \tan \theta}{d_v \sigma_y}$. For the opposite case, the terms containing T_{xz} or T_{yz} can be ignored from equations 1.16 and it is assumed that no transverse shear reinforcement is needed.

1.2.2.3 Industrial practice

Nowadays, the tasks of structural modelling and designing are principally carried out via specialised software based mainly on the finite element method and the design of non-flexural elements is not an exception. The EuroCodes and the ACI design recommendations give their approval to the use of simplified design methods for determining the need of reinforcement for in-plane stress fields, allowing to obtain the required reinforcement directly from the membrane and bending forces, assessed through finite element analysis, at each single element of the mesh. The amount of reinforcement is then determined by dividing the developed tensile stresses by the design strength of the adopted reinforcement.

Common post-processing option available in a great number of commercial programs include the, often called, Wood-Armer (W&A) and Capra-Maury (C&M) algorithms.

1.2.2.4 Wood-Armer algorithm

R.H. Wood and G.S.T. Armer [Wood, 1968, Armer et al., 1968] proposed one of the most popular design methods that explicitly incorporates twisting moments in the slab design.

Aiming to prevent yielding in all directions, this method considers the Johansen's yield criterion (normal moment yield criterion); at any point in the slab, the moment normal to any given direction, n , due to design moments M_x , M_y , and M_{xy} (figure 1.12), must not exceed the ultimate normal resisting moment in that same direction. The ultimate normal resisting moment is typically provided by ultimate resisting moments M_{ux} and $M_{u\Theta}$ related to the reinforcement in the X and Θ directions.

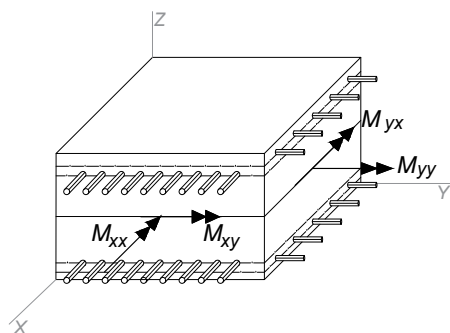


Figure 1.12: Reinforced plate moments

Based on the principles of the plate-type behaviour and the consideration of solid concrete elements reinforced with unidirectional layers of reinforcement oriented along the global axis, the W&A method considers a regular geometry element subjected to a moment field (M_x , M_y , M_{xy}). The reinforcement is considered to undergo only tensile forces developing a resistant stress σ_s while the compressive forces are taken by the concrete.

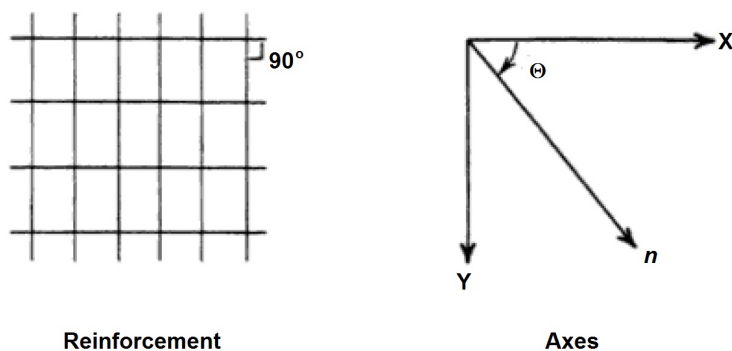


Figure 1.13: Orthogonal reinforcement

The procedure attempts to find a feasible solution to reinforce along the principal axis. For this purpose, a transformation of the moments over the principal axes is needed and then, the requirement is ensured by calculating the resisting moment M^* and the actuating moment as a function of the triad of acting moments according to equations 1.17 to 1.22 for the top and the bottom reinforcement [Wood, 1961]. Two types of design moments M^* are calculated then calculated. The lower (positive) and the upper (negative) moments (respectively causing mainly tension in the bottom parts and in the upper parts).

Based on these concepts, the reinforcement at the bottom of the slab in both directions must be designed to provide positive bending moment resistance in an X-Y system and

compared to the transformed moments acting in an $n-t$ system. When the external normal is at an angle Θ measured clockwise from the X-axis, the general transform is as follows:

For the lower reinforcement

$$M_x^* = M_{xx} + 2M_{xy} \cot \Theta + M_{yy} \cot^2 \Theta + \left| \frac{(M_{xy} + M_{yy} \cot \Theta)}{\sin \Theta} \right| \quad (1.17)$$

$$M_\Theta^* = \frac{M_{yy}}{\sin^2 \Theta} + \left| \frac{(M_{xy} + M_{yy} \cot \Theta)}{\sin \Theta} \right| \quad (1.18)$$

$$\text{If } M_{xx}^* < 0 : \quad (1.19a)$$

$$M_x^* = 0 \quad (1.19b)$$

$$M_\Theta^* = \frac{\left(M_{yy} + \left| \frac{(M_{xy} + M_{yy} \cot \Theta)^2}{M_{xx} + 2M_{xy} \cot \Theta + M_{yy} \cot^2 \Theta} \right| \right)}{\sin^2 \Theta} \quad (1.19c)$$

$$\text{If } M_\Theta^* < 0 : \quad (1.20a)$$

$$M_\Theta^* = 0 \quad (1.20b)$$

$$M_x^* = M_{xx} + 2M_{xy} \cot \Theta + M_{yy} \cot^2 \Theta + \left| \frac{(M_{xy} + M_{yy} \cot \Theta)^2}{M_{yy}} \right| \quad (1.20c)$$

As expected, while considering previous equations for the upper reinforcement, the sign of of the last term must be inverted [Clarke and Cope, 1984].

In a similar manner, the effects of the in-plane forces (membrane effect) are considered as follows:

$$N_x^* = N_{xx} + 2N_{xy} \cot \Theta + N_{yy} \cot^2 \Theta + \left| \frac{(N_{xy} + N_y \cot \Theta)}{\sin \Theta} \right| \quad (1.21)$$

$$N_\Theta^* = \frac{N_{yy}}{\sin^2 \Theta} + \left| \frac{(N_{xy} + N_{yy} \cot \Theta)}{\sin \Theta} \right| \quad (1.22)$$

$$\text{If } N_{xx}^* < 0 : \quad (1.23a)$$

$$N_x^* = 0 \quad (1.23b)$$

$$N_\Theta^* = \frac{\left(N_{yy} + \left| \frac{(N_{xy} + N_{yy} \cot \Theta)^2}{N_{xx} + 2N_{xy} \cot \Theta + N_{yy} \cot^2 \Theta} \right| \right)}{\sin^2 \Theta} \quad (1.23c)$$

$$\text{If } N_\Theta^* < 0 : \quad (1.24a)$$

$$N_\Theta^* = 0 \quad (1.24b)$$

$$N_x^* = N_{xx} + 2N_{xy} \cot \Theta + N_{yy} \cot^2 \Theta + \left| \frac{(N_{xy} + N_{yy} \cot \Theta)^2}{N_{yy}} \right| \quad (1.24c)$$

$$M_n = M_{xx} \cos^2 \Theta + M_{yy} \sin^2 \Theta - 2M_{xy} \sin \Theta \cos \Theta \quad (1.25)$$

M_{xx} , M_{yy} and M_{xy} are bending and twisting moments, usually obtained from a finite element analysis program. Θ is the angle corresponding to the disposition of the transverse steel, measured clockwise, from the M_x axis (see figure 1.13).

Following this procedure the required resisting moments M_{xx}^* , M_{yy}^* as well as the required resisting normal forces N_{xx}^* , N_{yy}^* can be computed and common flexure theory for RC can be applied.

1.2.2.5 Capra-Maury algorithm

A method used for the calculation of reinforcement in hull elements subjected to a system of axial forces and bending moments is based on the design presented by A. Capra and J. Maury [Capra and Maury, 1978]. This method has been implemented in some specialized structural calculation software such as *Code_Aster* [Delmas, 2011] and *AutoDesk Robot* [RoboBat, 2002].

Considering a reinforced concrete shell where the steel layers are disposed along two orthogonal directions X and Y , the state of forces is produced by the value of the three densities of moments M_{xx} , M_{yy} , M_{xy} and the three membrane tensions N_{xx} , N_{yy} , N_{xy} .

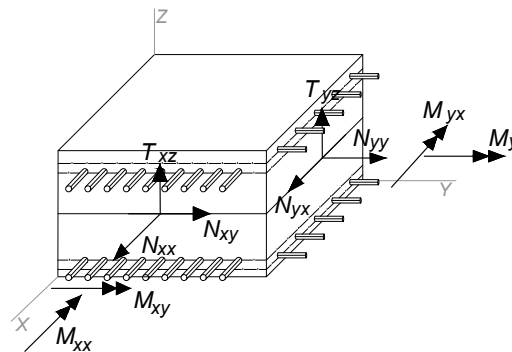


Figure 1.14: Reinforced shell element

This method acts as a post-processing step conducted over the state of generalised stresses previously obtained on a FE calculation. The problem is to determine the optimal economic values of the longitudinal reinforcement sections, a_s in the upper layer, U , and the lower one, L . In order to attain that result, the algorithm is based on the principle of the equilibrium of different facets centred at the point of calculation whose normal rotates in the plane tangent to the average sheet.

For each one of these facets, the bending moment ($\{M\}$) and the membrane tension ($\{N\}$) are applied according to the current stress state tensors and are evaluated using the following equations:

$$M = M_{xx} \cos^2 \theta + M_{yy} \sin^2 \theta - 2M_{xy} \sin \theta \cos \theta \quad (1.26)$$

$$N = N_{xx} \cos^2 \theta + N_{yy} \sin^2 \theta - 2N_{xy} \sin \theta \cos \theta \quad (1.27)$$

Taking into account the resultant bending moment and the membrane forces, the moment of service which steel must take can be evaluated. By a combined compression-and-bending calculation, it is now possible to determine the lower tensile forces $\Phi(\theta)$ and higher $\Phi'(\theta)$, perpendicular to the section, which must be balanced by the bottom and top layers of reinforcement.

The resisting forces, Φ'^* , in the direction θ of the two plies can be evaluated using the following expressions:

$$\Phi^*(\Theta) = (a_{XL} \cos^2 \theta + a_{YL} \sin^2 \theta) \sigma_y \quad (1.28)$$

for the lower layer

$$\Phi'^*(\Theta) = (a_{XU} \cos^2 \theta + a_{YU} \sin^2 \theta) \sigma_y \quad (1.29)$$

for the upper layer

where σ_y represents the maximal admissible stress in the steel (identical for both directions).

Considering that the resisting forces $\Phi^*(\Theta)$ and $\Phi'^*(\Theta)$ must be greater than the applied ones, $\Phi(\Theta)$ and $\Phi'(\Theta)$ respectively, the optimum of the reinforcement corresponds to the minimum quantities of:

$$(a_{XU} + a_{YU}) \text{ for the top layer}$$

$$(a_{XL} + a_{YL}) \text{ for the bottom layer}$$

Normally, the problem is solved numerically by checking the resistance of the section for a finite number n of values of Θ regularly spaced [Capra and Maury, 1978, Delmas, 2011, RoboBat, 2002]. The computed bending calculations are carried out in a typical manner and, for the calculation of the upper reinforcement, we must solve:

$$\text{minimise: } (a_{XL} + a_{YL}) \quad (1.30)$$

$$\text{subject to: } a_{XL} \cos \Theta + a_{YL} \sin \Theta \geq \frac{\Phi'(\Theta_i)}{\sigma} \quad (1.31a)$$

$$a_{XL} \geq 0 \quad (1.31b)$$

$$a_{YL} \geq 0 \quad (1.31c)$$

$$(1.31d)$$

A graphical representation of the previous inequalities (equation 1.31) gives a validity domain defined in figure 1.15. Considering an orthonormed plane defined by the required steel area along the X and Y directions (a_{XL} and a_{YL}), the inequalities given in equations 1.31 define a semi-space of the feasible design.

By exploring different values of Θ , a general domain of validity of the imposed conditions can be obtained (figure 1.16).

C&M assumes that the compression of the concrete is acceptable and that the reinforcements are strained to the limit constraint σ_y . A verification of these hypotheses, by going through a rigorous or simplified calculation in combined compression-and-bending, is then

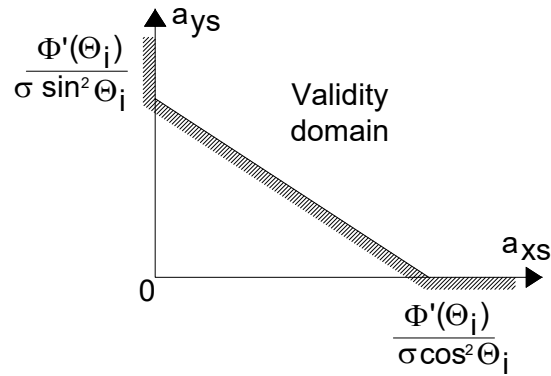


Figure 1.15: Validity domain (adapted from [Capra and Maury, 1978]).

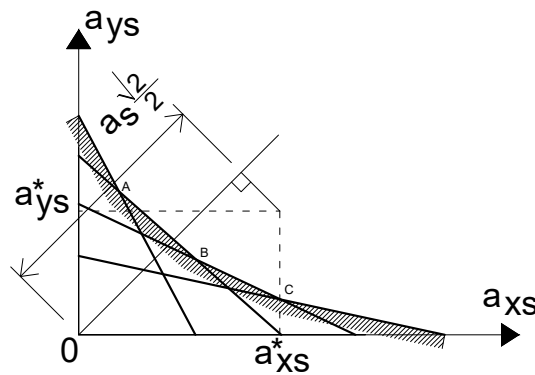


Figure 1.16: General validity domain for different values of Θ (adapted from [Capra and Maury, 1978]).

indispensable. The maximum constraint of compression in the concrete can be estimated as follows:

$$\sigma_{c,max} = \frac{|M|}{I}y - \frac{N}{A} \quad (1.32)$$

For transverse reinforcement, the proposed calculation starts from the equivalent shear stress expressed as:

$$\tau = \frac{1}{2}\sqrt{T_{xz}^2 + T_{yz}^2} \quad (1.33)$$

where z represent the arm of lever of the elastic couple of the section and T_{ZX} and T_{ZY} are the stresses cutting-edges. Thus, the section of transverse reinforcement is simply obtained by dividing this constraint by the acceptable ultimate stress of steel.

1.2.2.6 Remarks

Laboratory test campaigns carried out on slabs elements have shown that the use of yield line theory leads to conservative designs [Marti et al., 1987]. The same tests have been

numerically reproduced confirming previous results [May and Ganaba, 1988]. Normally, yield line analysis supposes mechanisms that ignores possible membrane effects. In other words, most mechanisms are not kinematically admissible for a section in which the neutral axis is not at the centre of the section. In addition, recent literature [May and Lodi, 2005] points out that conservatism carried out by the method decreases or even disappears as the area of reinforcement increases.

On the other hand, transverse shear forces obtained from a FE model will generally be less accurate than bending and twisting moments, since, transverse shear forces are calculated as derivatives of the bending and twisting moments (see equations 1.8). Thus, a relatively fine mesh would be required in zones potentially presenting important shear forces; however, in practice, mesh sizes and geometries are commonly dictated by the size of particularly large overall building models.

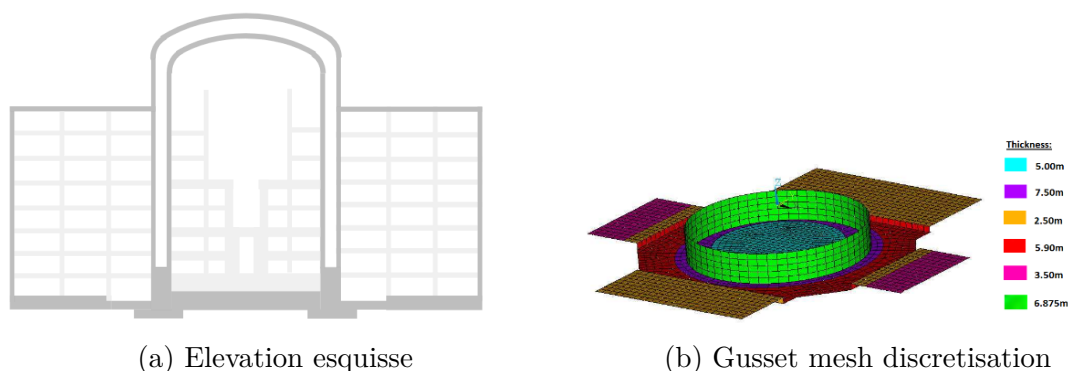


Figure 1.17: Typical nuclear island structural outline adapted from [Herve et al., 2014]

In the current industry of nuclear civil works, meshes presenting elements from 0.5 to 1 meter side are typically used to estimate reinforcement ratios [Herve et al., 2014]. Furthermore, the intensive use of surface elements may lead to poor representations of geometric discontinuities; e.g. abrupt thickness transitions, heterogeneous mid-plane positions and joints.

One of the ways to evaluate the quality of the mesh is to compare results to test data or to theoretical values. Unfortunately, test data and theoretical results are often not available. So, other means of evaluating mesh quality are needed. These include mesh refinement and interpretations of results discontinuities.

The most fundamental and accurate method for evaluating mesh quality is to refine the mesh until a critical result, such as the maximum stress in a specific location converges (i.e. it doesn't change significantly with each refinement). Another option is to evaluate the magnitude of stress discontinuity between adjacent elements in the critical region. In most cases, the finite element method computes stresses directly at interior locations of the element (Gauss points) and extrapolates them to the nodes on the element boundaries. While it is common to view these stresses as average values, the reality is that each element calculates different stresses at shared nodes.

Figure 1.17a exposes an overview of the thicknesses of the different structural parts.

Figure 1.17b indicates the relative thicknesses of the different shells that are used. Figure 1.17b delivers a typical modelling using only shell elements where the position of the mid-plane of the shell elements may present huge differences with the real structure.

Figures 1.18a and 1.18b, show a thermal load case the drawback only for the thermal gradient description even before considering the associated generalised forces or stresses that such a modelling generate compared to the brick modelling.

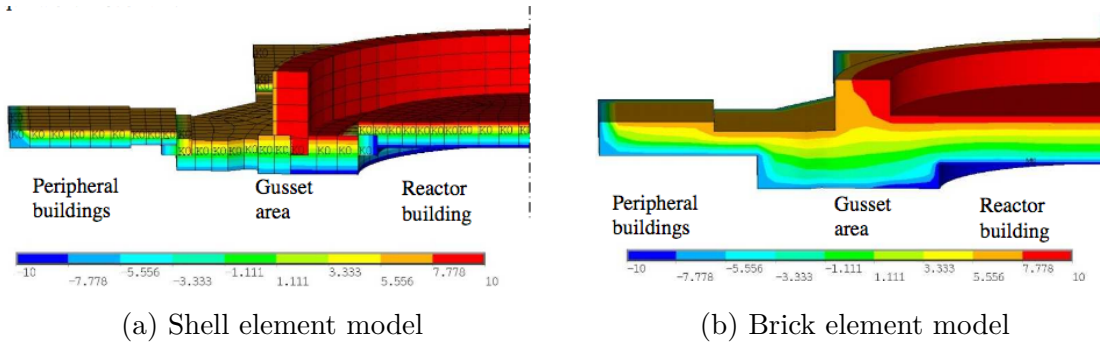


Figure 1.18: Thermal load case modelling of a thick raft with engineering practices [Herve et al., 2014]

1.2.3 3D solid modelling

Linear elastic stress analysis has been also employed as tool for the analysis and the design of 3-dimensional structures. The equivalent 3-dimensional frame [Lew and Narov, 1983] is a procedure where the vertical walls are modelled as continuous columns located at the centroid of the wall and rigid beam elements are rigidly connected to them and extend to the ends of the wall. This process avoids the direct use of solid elements reducing the complexity of the solid problem to a frame model with robust elements.

On the contrary, real three-dimensional solid modelling can bring better results but is less common. As one can suppose, its results are not always intuitive on how to dimension the reinforcing steel in three-dimensional space in order to meet the stress demands. Similar to 2-dimensional elements, one possible solution would be the trajectory reinforcement which present the same constructive drawbacks mentioned before.

In 2003, [Foster et al., 2003] proposed an approach allowing to compute the need of reinforcement on concrete solids using the stress tensor obtained from a linear stress analysis. Based on Mohr's circles, Foster retakes the idea that the RC elements behave as the sum of the reactions of the individual materials (see figure 1.19). As steel reinforcement cannot take shear stresses into account, the points relating compression and shear, σ_{ci} and S_n respectively, must fall within the major stress circle (plotted in figure 1.19). Hence, the tensor of stresses in the concrete is supposed to be the difference between the element stress tensor σ_{ij} and the orthogonal stresses taken by the reinforcement σ_{sij} .

$$\sigma_{cij} = \begin{bmatrix} (\sigma_x - \sigma_{sx}) & \tau_{xy} & \tau_{xz} \\ \tau_{xy} & (\sigma_y - \sigma_{sy}) & \tau_{yz} \\ \tau_{xz} & \tau_{yz} & (\sigma_z - \sigma_{sz}) \end{bmatrix} \quad (1.34)$$

The precedent tensor can be limited, according to the used materials and code design, by:

$$|\sigma_{sj}| \leq \Phi_t \rho_{sj} f_{yj} \quad (1.35)$$

and

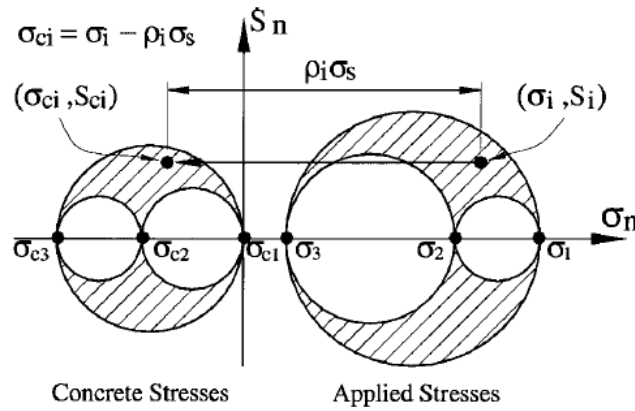


Figure 1.19: Compression field for 3-dimensional stresses

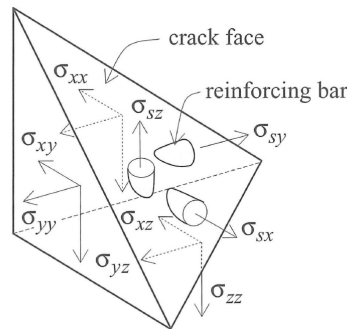


Figure 1.20: Idealised 3-dimensional reinforcement

$$-\sigma_{cIII} \leq \beta \Phi_c \rho_{sj} f_{cp} \quad (1.36)$$

where Φ_s and Φ_c are reduction factors associated with their respective materials, β is the factor to account the triaxial effect on concrete, and ρ_{sj} ($j = x, y, z$) are the reinforcement ratios along the global axis X , Y and Z .

Making an analogy between the tensor in equation 1.36 and figure 1.19, it can be observed that there are six unknowns: σ_{sx} , σ_{sy} , σ_{sz} , σ_{cI} , σ_{cII} , and σ_{cIII} but only three equations: $I_{c1} + I_{s1} = I_1$, $I_{c2} + I_{s2} = I_2$, $I_{c3} + I_{s3} = I_3$ which produce an infinity of solutions. Hence, the designer must choose to determine constraints over the variables in order to obtain a unique solution for the system of above equations [Hoogenboom and De Boer, 2010].

1.2.4 Structural analysis and design using non-linear modelling

The results provided by linear-elastic finite element analysis represent a practical way to safely dimension common structures for serviceability limit states. And have become the basis of the structural design.

For some design problems, however, a linear analysis may not be sufficient. Special cases can be mentioned when existent structures may need analysis that take into account cracking and ageing. Another example is for new structures may require a non-linear revision of the dimensioning using a plasticity-based design procedure. In addition, nonlinear

analysis can also be used for evaluating complex geometries or poorly detailed structures presenting effects of localised cracking.

One common application of non-linear analysis is the confirmation of safety for complex design details.

In the industrial practice, and due to the associated cost, this type of analyses are implemented in situations specific situations:

- large deformations are expected
- sensible materials are used
- coupled effects may occur

Specifically speaking for RC structures, the implementation of non-linear analysis corresponds to situations when

- verification of the pattern is needed
- the amount/distribution of the reinforcement may considerable modify the linear stress distribution.

1.3 Strut-and-Tie models

In the presence of structural members subjected to important punctual loads or possessing abrupt changes in their cross-section and geometry, conventional methods of plane section analysis seems to be no longer sufficient [Thompson, 2002]. Such locations are generally detailed using good practice rules based on experience or based on empirical guidelines. Strut-and-Tie Method (STM) arises as a rational in-between design procedure for complex structural detailing; the procedure has a basis in mechanics but it is simple enough to be readily applied in design.

First proposed by [Ritter, 1899], Strut-and-Tie models represent a simplification to visualise the path of internal forces in cracked elements. First models were the basis for the design of concrete beams [Mörsch, 1902]. Years later, the theory continued to be refined with the contributions of [Marti, 1985] who created the basis of the rational application of the STM. At the same time, [Collins and Mitchell, 1980] derived a rational criteria for shear and torsion. Meanwhile, [Schlaich et al., 1987] extended the beam truss models to all parts of structure in the form of generalised ST systems.

Generally speaking, STM involves the idealisation of a complex structural member into a simple truss able to represent the flow of stress paths within the member. The truss is composed of struts that model concrete compression fields, ties that model tensile steel reinforcement, and nodes which represent the localised zones where the elements interconnect one another or the zones where the tensile steel is anchored into the concrete. The struts and ties carry only uniaxial forces. This truss mechanism must be stable and properly balance the applied loads. Failure of the truss is dictated by yielding of one or more ties or also defined by excessive compressive stresses within the struts or nodes. Ideally, only the first failure mode should occur.

Even if the principle can be directly applied to elements resisting flexion with a linear distribution of stresses [Hsu, 1992], this document will focus only on its application for detailing discontinuity regions undergoing no-linear distribution of the stresses through the member depth.

1.3.1 Discontinuity regions

The primary tenets of beam theory imply that a linear distribution of strains occurs through the member depth: plane sections are assumed to remain plane. The element is therefore dominated by sectional behaviour, and the design can proceed on a section-by-section basis. For the design of elements in flexion, the compressive stresses are conventionally assumed to act over a rectangular stress block, while the tensile stresses are assumed to be carried by the longitudinal steel reinforcement.

On the other hand, D-regions ("D" standing for discontinuity or disturbed) occur in the vicinity of load or geometric discontinuities. The applied loads, support reactions and abrupt geometric changes are discontinuities that "disturb" the stress distribution within the member near the locations where they act. Corners, openings, and corbels are examples of geometric discontinuities that correspond to the existence of D-regions.

As a characteristic of D-regions, it is considered that the distribution of the strains through the member depth presents a non-linear profile, therefore, the assumptions that underlie the sectional design procedure are invalidated. According to Saint Venant's principle, an elastic stress analysis indicates that the stresses due to axial forces and bending, are approaching a linear distribution at a distance approximately equal to the depth of the member, h , away from the discontinuity. In other words, a nonlinear stress distribution exists within one member depth from the location where the discontinuity is introduced [Schlaich et al., 1987]. Following this, it can be stated that D-regions are therefore assumed to extend up to a distance h from the applied load and support reactions.

In general, a region of a structural member is assumed to be dominated by nonlinear behaviour, or a D-region, when the span/depth ratio, a/h , is less than 2 or 2.5. The shear span, a , is defined as the distance between the applied load and the closest support in simple members.

1.3.2 Fundamentals

A ST model design adheres to two principles: 1) the resultant truss model must be in equilibrium with the external force system and, 2) the concrete element has enough deformation capacity to accommodate the assumed distribution of forces [Schlaich et al., 1987]. Proper anchorage length of the reinforcement is an implicit requirement in order to assure the needed ductility. Complementary, the compressive stresses developed in the concrete must not exceed the factored concrete strengths, and the tensile stresses the factored steel capacities. If all of the mentioned above requirements are satisfied, the application of the STM should result in a conservative design [Williams et al., 2012].

As mentioned before, the STM consists of three principal components: struts, ties, and nodes. The compression members, referred as struts, are considered to be made out of concrete C_c ; the tension members, referred to as ties, may be made of concrete without reinforcement T_c (case not considered within this work) or reinforced by layers of mild steel

reinforcement or prestressing steel T_s . The struts and the ties intersect at regions referred to as nodes. Due to the concentration of stresses from intersecting truss members, the nodes are the most highly stressed regions of a structural member and their revision should be considered during the overall analysis.

1.3.3 Design procedure

ST modelling is suitable for use in a wide range of design problems and has been incorporated into several design codes. Among others, the method is referred in the EuroCode2 [Eurocode2, 2008], the Appendix A of ACI 318-02 [ACI-318, 2008] and, the International Federation for Structural Concrete [for Structural Concrete, 2008]. These account for design conditions using the same equations with exception of notation and minor differences in the value of safety factors.

Typically, the design procedure points out a sequence of steps as follows.

1.3.3.1 Region discrimination

The first step in the STM design process is to define whether the STM is a good alternative to solve the problem. Based on the Saint-Venant's principle, the structure can be divided into B- and D-regions. The STM design process should be used to design the sections that are found as D-regions while regions expected to be dominated by sectional behaviour can be designed using the sectional design approach. If the structure results in a combination of B- and D-regions, the designer may decide to treat the structure by sections, substructures, or to decide if using only one approach for the whole structure is reasonable and will result in a suitable design.

1.3.3.2 Defining load case

The second step is to determine the critical load cases that the structure shall withstand. If the structural component consists of both B- and D-regions, only the discontinuity parts of the component will be designed using strut-and-tie modelling. Each D-region found should be processed as an isolated element where the nodal boundary conditions originate from the interaction with the adjacent elements and global support reaction of the structure under the design system of loads (figures 1.22): the forces acting at the boundaries of the D-region become the boundary conditions for the further ST analysis.

The internal forces and moment at the interface of the B- and D-regions can be assumed linearly distributed and should be applied at the boundary of the isolated D-region (figure 1.22c). The definition of the boundary forces between D- and B-regions are applied to the STM in order to 1) determine the forces carried by the truss and 2) determine the geometry of the model by defining the position of some nodes. As it can be inferred, an overall elastic analysis of the structure should be performed in order to determine the support reactions and the interface loads for the different D-regions.

Considering that the truss elements are unable to withstand specific loads (eg. moment, distributed loads) some modifications may be necessary to produce an equivalent load system. The most current modification can be resumed as follows:

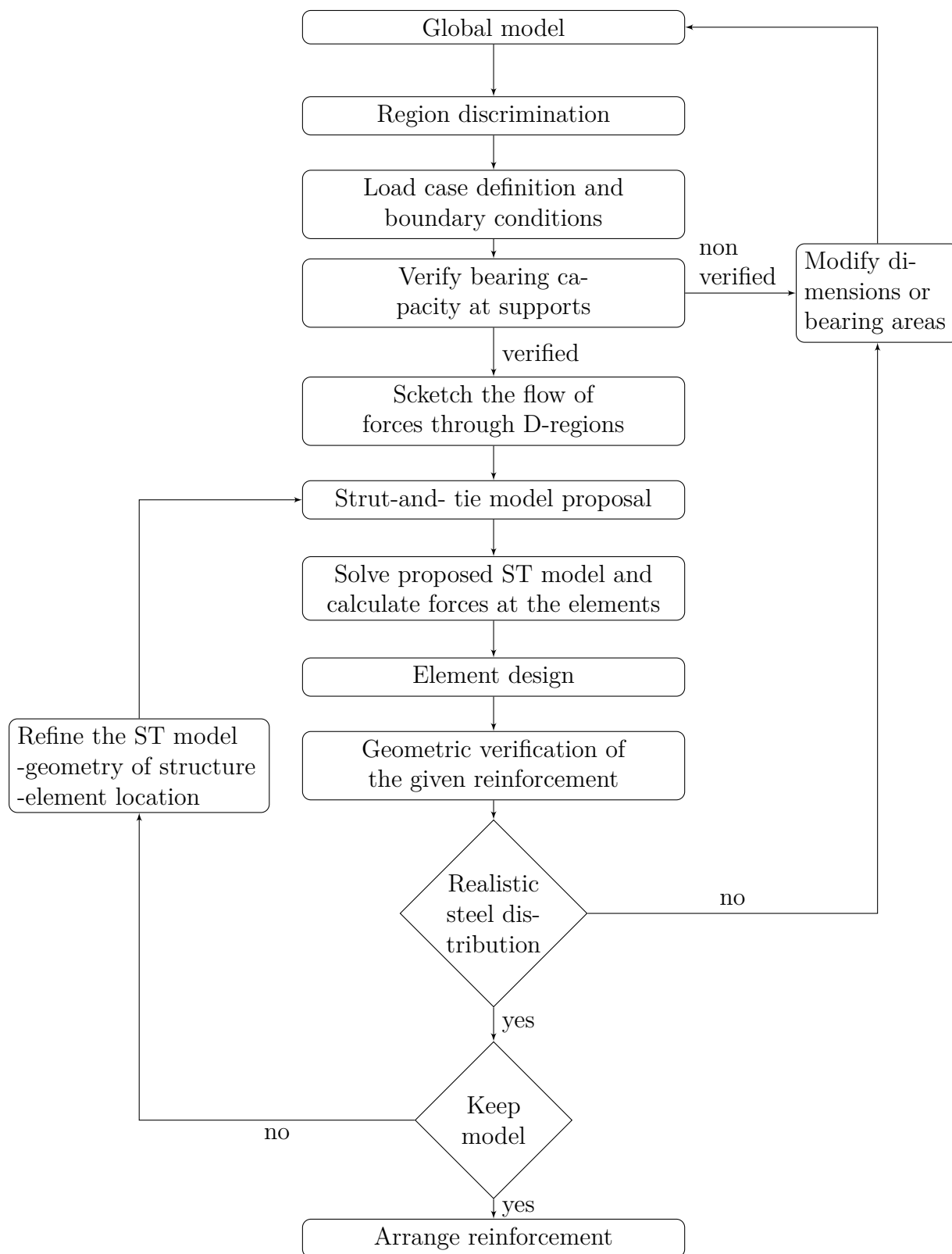


Figure 1.21: Flowchart design procedure using STM (inspired by [El-Metwally and Chen, 2017])

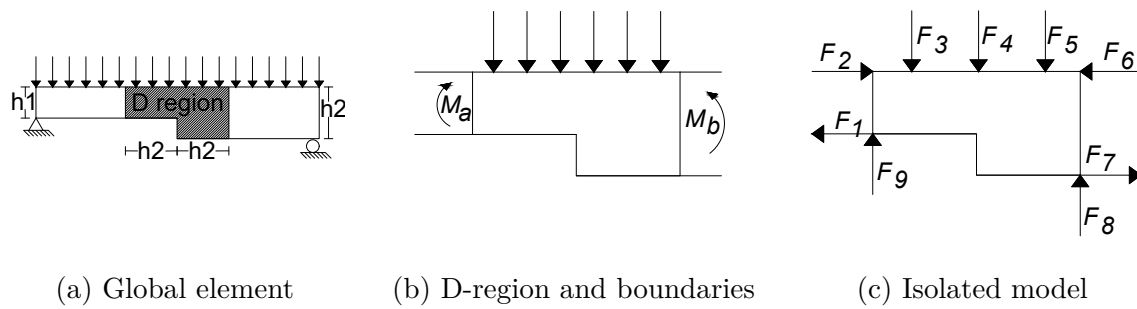


Figure 1.22: Local zone of a beam with sudden thickness change

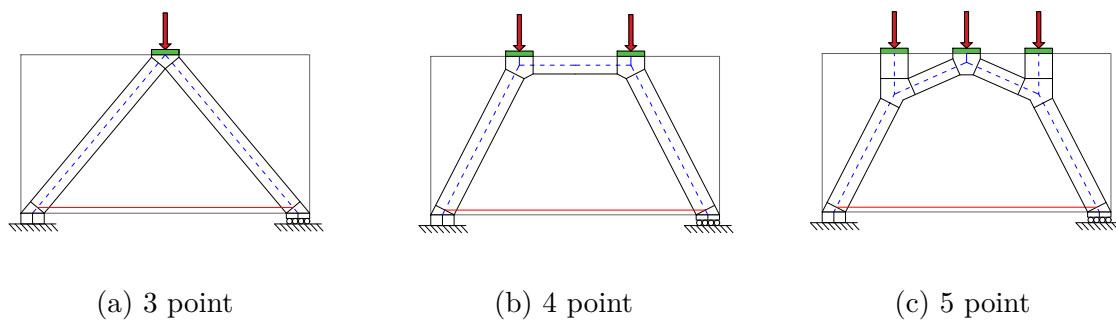


Figure 1.23: Different ST models developed under different loading systems.

- A moment acting on the structure must be replaced by an equivalent set of forces.
- Punctual loads acting on the structure at a very close proximity to each other may be resolved together to simplify the development of the strut-and-tie model. The decision whether or not to merge loads together is left to the designer.
- A distributed load must be divided into a set of punctual loads acting at the nodes of the truss system. The self-weight of the structure must be applied to the STM in the same manner.

In some occasions, each load case will create a unique set of forces causing the locations of the critical regions of the STM to change. Therefore, depending on the load cases, a ST analysis should be performed for each individual load case generating as many truss systems as load cases (see figure 1.23).

1.3.3.3 Strut and Tie proposal.

A two-step process is often performed while developing ST models. The first step consists in the proposal of the element distribution of a truss consistent with the previously generated load case and boundary conditions. The second step deals with the analysis of the so defined truss structure to determine the internal forces developed in the struts and the ties.

Geometry proposal. Based on the equivalent punctual loads derived from the previous step (initial nodes), the designer projects the struts and the ties as straight elements

from one node to another with the aim of developing a stable structure within the solid element. This process may or may not include the interaction of all the initial nodes and, in addition, it may include secondary nodes depending on the designer's criteria. For this step, a linear finite element model is commonly used in order to visualise the flow of forces within the member; and align the truss elements according to the stress trajectories [Schlaich et al., 1987].

Analyse ST models and member design. At this point, the ST model corresponds to a planar (or spatial) truss depicted by a nodal list, an element list and, an inter-connectivity table. Using these three items, a mathematical model can be then built and solved. The forces developed in the elements are determined by solving a model including the previously determined boundary conditions and factored system of loads. The area of material needed for each element in the STM should be sufficient to safely resist the computed force without surpassing the yield strength of the steel nor the limit resistance in the concrete. In a conventionally reinforced structure, the area of reinforcement needed for a tie, A_{st} , is determined from the following equation:

$$A_{st} = \frac{F_u}{\phi R} \quad (1.37)$$

where:

F_u corresponds to the largest force in the element for all load combinations considered, R the material's resistance (σ_y for steel, σ_c the resistance for concrete material) and, ϕ the safety factor (0.9 for traction [Eurocode2, 2008, ACI-318, 2008])

Additionally, the Eurocodes requires the diminution of the design strength for struts in cracked compression zones:

$$\sigma_c = 0.6(1 - f_c/250)f_{cd} \quad [\text{Eq. (6.56) and (6.57N) of EUC2}] \quad (1.38)$$

1.3.3.4 Nodal verification

Due to the level of stresses that must be equilibrated within a small volume of concrete, the nodes are the most highly stressed regions of a structural component. As a consequence, a logical step on the design process is the verification of the resistance of the zones generated by the intersection of different elements.

Briefly said, the nodes are a mere simplified idealisation of a more complex reality and the definition of their geometry lies also on the designer's criteria. Ideally, nodes may be conceived such that the stresses on all faces are equal. If the stresses are equal, the ratio of the area of the side face is proportional to the applied force. In this case, the node is referred as a hydrostatic node: principal stresses are equal on all sides and shear stresses disappear. In the other hand, if a node is conceived in a manner where unequal stresses exist on each face, then, the node is referred to non-hydrostatic 1.24.

Based on the nature of the elements that converges to a connection zone, another classification can be made. According to the sign of converging forces, the node may be

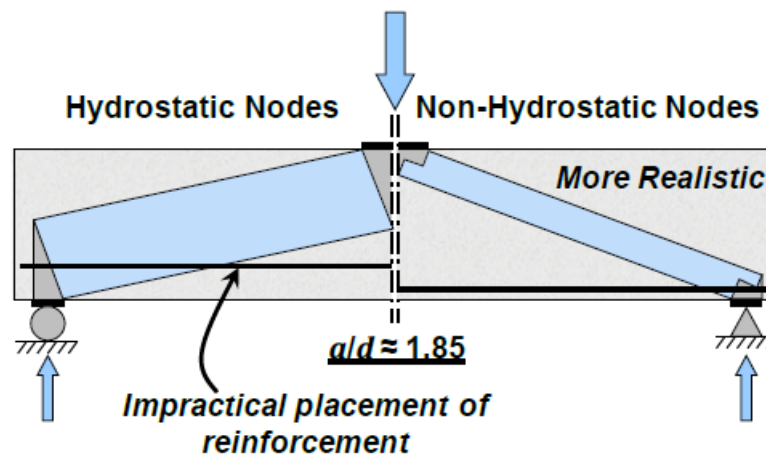


Figure 1.24: Nodal proportioning techniques - hydrostatic versus non-hydrostatic nodes [Birrcer et al., 2009]

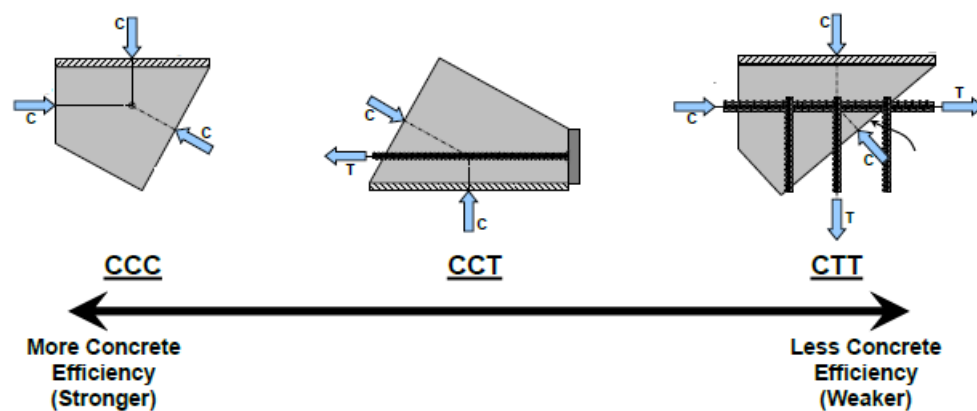


Figure 1.25: Representative node types [Birrcer et al., 2009]

referred as CCC, CCT, CTT or TTT (C standing for compression forces and T standing for tension ones). Due to geometric complications, it is highly recommended to merge groups of forces in order to reduce their number. If more than three elements intersect at one node. However, this is not always possible and often generates other possible type of nodal combinations as showed in figure 1.25.

For hydrostatic nodes, the faces are perpendicular to the attached elements and the length sides are proportional to the strut forces. In the presence of ties, position of the faces are proposed by assuming the tie forces act from behind the node to compress the nodal region.

Table 1.1: ACI and Eurocode values for nodal zones resistance

Nodal zones, $\sigma_{Rd,max}$	$\sigma_{Rd,max}$	
	ACI	Eurocodes
CCC type nodes	$0.85(1)\beta_s f'c$ (A.5.2.1)	$1\nu' f_{Ecd}$ (6.5.4)
Nodal zones anchoring a tie	$0.85(0.8)\beta_s f'c$ (A.5.2.2)	$0.85\nu' f_{Ecd}$ (6.5.4)
In nodal zones anchoring two or more ties.	$0.85(0.6)\beta_s f'c$ (A.5.2.3)	$0.75\nu' f_{Ecd}$ (6.5.4)

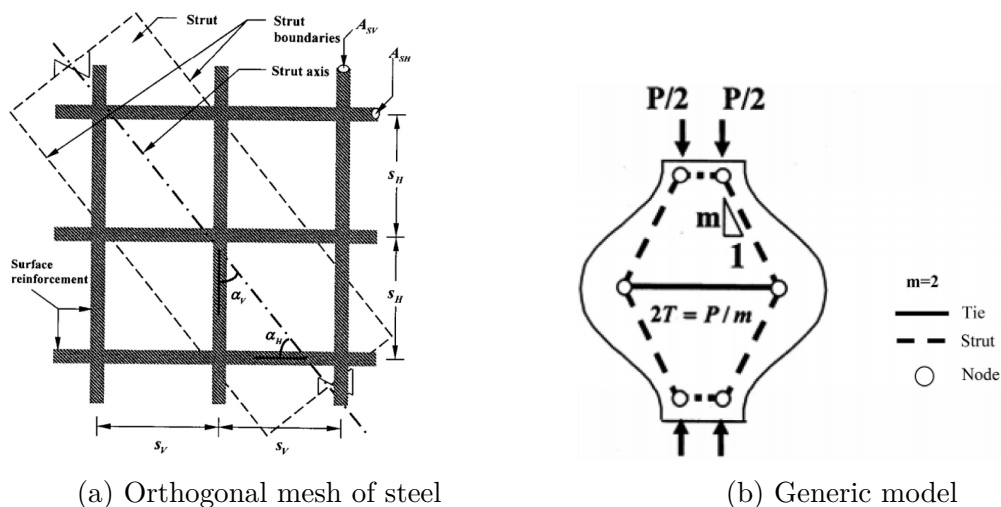


Figure 1.26: Bottle-shaped strut (adapted from [Singh et al., 2018]).

Non-hydrostatic nodes are proportioned based on the origin of the applied stress. In the case of CCC non-hydrostatic nodes, the approach is to set the back face dimension as the effective depth of the compression block. In the presence of a CCT, the back face dimension is taken as twice the distance from the centroid of the longitudinal reinforcement to the extreme tension fibre of the beam. Regarding the nodes located at the boundary conditions and supports, the dimension of the bearing face is determined by the dimensions of the bearing plate. This proportioning technique allows the geometry of the nodes to closely correspond to the actual stress concentrations at the nodal regions. In contrast, the use of hydrostatic nodes can sometimes result in unrealistic nodal geometries and impractical reinforcement layouts [Birrercher et al., 2009].

1.3.3.5 Transverse reinforcement

One of the most frequent assumptions is to idealise the struts as prismatic elements. However, according to Birrercher *et al* [Birrercher et al., 2009], this simplification does not eliminate the fact that most struts in two dimensions are bottle-shaped struts. The lateral spreading of bottle-shaped struts introduces tensile stresses transverse to the element, stresses that could cause longitudinal cracking along the length of the strut resulting in premature failure; hence, transverse reinforcement should be provided in order to control the cracking.

Ideally, reinforcement placed inside the strut and aligned with the transverse tension forces would be the best to resist the transverse tension and to control crack widths. However, in practice, the resistance to "splitting" may derive from the orthogonal mesh of steel typically detailed in such elements 1.13.

Even though reinforced bottle-shaped struts seem to represent a more realistic distribution of stress than prismatic elements, its real behaviour has been little studied and its application seem not to be standardised among different codes. While codes such as the AASHTO LRFD Bridge Design Specifications required to the bottle shaped struts to be detailed with reinforcement ratio of 0.003, the Eurocodes present the elements as regions of partial and full discontinuity (see figure 1.27) proposing two equations.

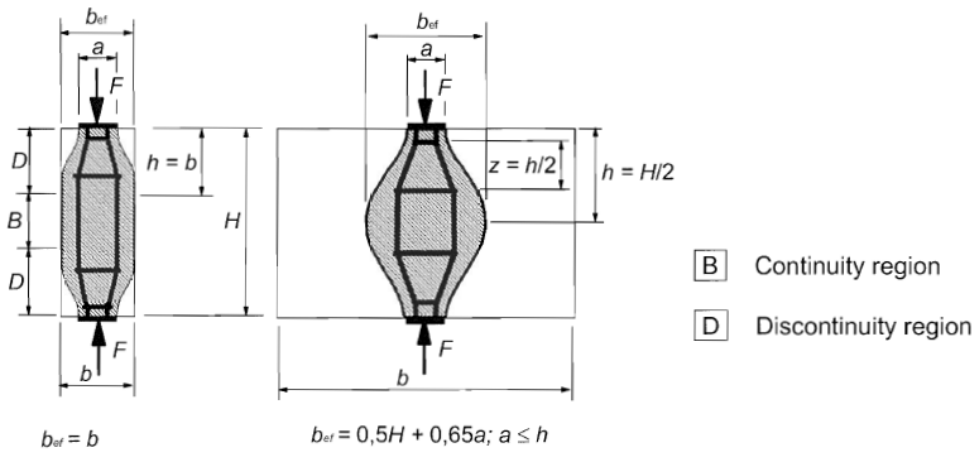


Figure 1.27: Parameters for the determination of transverse tensile forces in a compression field with smeared reinforcement [Eurocode2, 2008].

Table 1.2: ACI and Eurocode values for strut resistance

Struts	β_s	
	ACI	Eurocodes
Rectangular struts	$0.85(1)\beta_s f'c$ (A.3.2.1)	f_{cd} (6.5.2)
Bottle-shaped struts		
a) reinforced struts	$0.85(0.75)s f'c$ (A.3.2.2)	f_{cd} (6.5.2)
b) non reinforced struts	$0.85(0.6\lambda) f'c$ (A.3.2.2)	f_{cd} (6.5.2)
Struts in tension members	$0.85(0.4)_s f'c$ (A.3.2.3)	f_{cd} (6.5.2)
Other case	$0.85(0.6\lambda) f'c$ (A.3.2.4)	—
Strut in cracked zone	—	$0.6\nu' f_{cd}$ (6.5.2)

- for partial discontinuity regions ($b \leq \frac{H}{2}$):

$$T = \frac{1}{4} \left(1 - \frac{b-a}{b} \right) F \quad [\text{Eq. (6.58) of EUC2}] \quad (1.39)$$

- for full discontinuity regions ($b > \frac{H}{2}$):

$$T = \frac{1}{4} \left(1 - 0.7 \frac{a}{h} \right) F \quad [\text{Eq. (6.59) of EUC2}] \quad (1.40)$$

where, a is the width of the loaded area, b is the strut width at its mid-length, h is half the strut length and P is the axial load on the strut

1.3.4 Recommendations and thumb rules to be taken into account

Being a rational approach, the results obtained through the application of STM are highly dependent on the experience of the designer and may vary from one designer to another. In other, to achieve an economical solution through a conservative model, able to assure the resistance and the stability under the requirements, the designer is strongly advised to appeal to several good practice recommendations found in the literature;

- The distribution of the truss elements can be based on the stress distribution of a prior elastic FEM analysis [Schlaich et al., 1987], [Eurocode2, 2008].
- Align the struts with $\pm 15^\circ$ of the stress trajectories to represent the nature of the element [Ramirez and Breen, 1991].
- The most efficient ST models are typically those with the fewest and shortest ties [Williams et al., 2012].
- The ties should coincide in position and direction with the corresponding reinforcement [Eurocode2, 2008].
- According to [Eurocode2, 2008], all strut-and-tie models may be optimised by energy criteria .

1.3.5 Remarks

The most important benefit of ST modelling is its versatility. Almost any structure can be treated with this method in order to obtain a conservative design. In contrast, the flexibility of its application is granted by the lack of explicit guidance and consistency in the current codes [Barton et al., 1991].

1.4 Non-Linear strut-and-tie model approach

This approach proposes the development of a classic ST model and its further revision through a non-linear model [Yun and Lee, 2005].

The ST initial model can be formulated from experience, from a linear elastic FE model or from experimental information such as crack patterns and recorded strains and the process continues as depicted in figure 1.21.

To evaluate the behaviour and ultimate resistance of the selected ST model, a non-linear FE analysis is carried out of the model. This model needs to consider the final (real) dimensions of the proposed struts and ties as well as an accurate representation of their respective materials. The process allows to verify the resistance at the nodal zones by evaluating the developed stresses according to a failure failure. If the bearing capacities are not sufficient or the considered load produces failure or mechanisms, the original ST model is modified and the process is repeated.

1.5 Summary

In the field of engineering practice, the construction codes allow the analysis and design of non-flexural RC elements through 3 principal approaches: recommendations based on empirical relations, FEM based algorithms and also rational methods.

Even if several campaigns have been carried out with the aim of determine the behaviour and the resistance of elements such as ribs and deep beams, the results remain valid for a small range of cases where the geometry of analysed element as well of the load system and steel disposition resembles to those studied restricting its application for particular

cases. When a special case is confronted, a FE analysis is, probably, the first alternative to manual calculation.

As expressed before most structural designs are performed using FEM software and post-processed through automatic algorithms. Most of the applied methodologies were conceived to treat elements where the effects carried out by a flexural behaviour predominate over those produced by shear, limiting their range of validity if no special considerations are implemented. It is also worth to mention the fact that, in the most popular methods, W&A nor C&M, no explicit check of the assumed failure mode is made at the elements designed. These methodologies implicitly assume that the reinforcement ratios obtained are small enough to avoid concrete crushing. While this condition is usually satisfied in slabs, a check of the assumed failure mode should always be carried out for shells, particularly for elements subjected to significant axial compression or cases with high reinforcement ratios.

Despite the fact of the existence of some other FE-based methods such as the sandwich or a full three-dimensional solid design do indeed take into account a verification on the concrete, their application has not been included within the construction codes until this day.

Other alternative is the use of the rational methods that can be seen as an intermediate point between structural mechanics and the empirical methods. The main drawbacks of the use of such methods has been their lack of explicit guidance and consistency in the current codes, aspects that propitiate a strong dependency on the designer's expertise.

The guidance provided by the elastic stress field, result of a prior FE analysis, ensures a good behaviour at the serviceability limit state and can also be used to study its ultimate limit state response. The procedure seems to be straightforward for cases where the ties are aligned to the orthogonal reinforcement; for cases where this does not occur, the final reinforcement may not present the desired behaviour

The performance of a model developed through rational methods is totally dependent on the intuition and practice of the structural engineer as well as the expertise on the problem to solve. The modifications and decisions taken within the design process becomes a repetitive and logic task for common geometries and load cases but, it can also be a rather difficult task when facing unusual cases.

The modification of a model in order to adapt it to different requirements, or just in order to improve its response, requires a knowledge on the relation of the mechanical characteristics and the evolution on the structural behaviour. In a conventional process, any modification is dictated by preexisting codes and construction recommendations. For STM these rules can sometimes depend on the typology of the problem and even be subjective rules presenting guidance for a series of solved recurrent examples but needing a sort of extrapolations for different problems.

In recent years, the development of Computational Aided Design (CAD) tools allows to include rational techniques intended to guide the engineer through the design process. Different techniques adapting mathematical methods have been proposed in order to achieve optimal solutions for automatically computing the reinforcement of concrete structures through ST models. Next chapter intends to make an overall revision of the most common optimisation techniques and algorithms that have been applied to propose and to justify the trajectory of ST models.

Chapter 2

Automatic strut-and-tie models

The selection of the "best" Strut-and-Tie model has always been a concern. In addition, among the actual market demands are those aiming for lower costs, shorter time and higher quality standards that, have forced the designers to choose methodologies that allow the reduction of costs in the stages of conception and implementation.

Within the application of the STM, one of the principal difficulties have been to overcome the manual tasks and decisions based on thumb rules.

Some researchers, such [Alshegeir and Ramirez, 1992, Kuchma and Tjhin, 2001], are focused on developing tools and criteria to aid engineers to perform the manual tasks and to provide information to take decisions. Nevertheless these approaches allow the designer to provide satisfactory models with relative ease, the manual trial-and-error-method used to compare one model to another is still present. In contrast, other groups of research incline their studies to fully automatise the process based principally in structural optimisation methods.

In order to fulfil an appropriate Strut-and-Tie model, the design of a structural concrete member can be transformed into a structural design optimisation problem. The solution of such problem can be then solved by different methods or techniques depending on the desired objective and the imposed constraints.

This second chapter presents a review of academic literature, in the areas where the present work is contributing, namely structural optimisation and computer aided tools for Strut and Tie models.

The first part concerns the methodologies applied to the structural optimisation while the second and third parts deal with the practice of the structural optimisation to compute ST models.

Approches automatiques de calcul de modèles bielle tirant

La sélection du «meilleur» modèle Bielle-Tirant a toujours été une préoccupation. En outre, parmi les demandes réelles du marché figurent celles qui visent à réduire les coûts, à raccourcir les délais et à améliorer les normes de qualité, ce qui a forcé les concepteurs à choisir des méthodologies permettant de réduire les coûts de conception et de mise en oeuvre.

Dans l'application de la méthode BT, l'une des principales difficultés a été de surmonter les tâches manuelles et les décisions basées sur les règles du pouce.

Certains chercheurs, tels que [Alshegeir and Ramirez, 1992, Kuchma and Tjhin, 2001], se concentrent sur le développement d'outils et de critères pour aider les ingénieurs à effectuer les tâches manuelles et à fournir des informations pour prendre des décisions. Néanmoins, ces approches permettent au concepteur de fournir des modèles satisfaisants relativement facilement, la méthode manuelle d'essai et d'erreur utilisée pour comparer un modèle à un autre est toujours présente. En revanche, d'autres groupes de recherche orientent leurs études pour automatiser entièrement le processus basé principalement sur des méthodes d'optimisation structurelle.

Afin de réaliser un modèle BT approprié, la conception d'un élément en béton armé peut être transformée en un problème d'optimisation structurelle. La solution d'un tel problème peut alors être résolue par différentes méthodes ou techniques en fonction de l'objectif recherché et des contraintes imposées.

Ce deuxième chapitre présente une revue de la littérature académique, structurée pour considérer les domaines auxquels cette thèse contribue: l'optimisation structurelle et les outils assistés par ordinateur pour les modèles BT.

La première partie présente les méthodologies appliquées à l'optimisation structurelle tandis que les deuxième et troisième parties traitent de la pratique de l'optimisation structurelle pour calculer les modèles BT.

2.1 Structural optimisation

In mechanics, a structure is defined by J.E. Gordon [Gordon, 2009] as "any assemblage of materials which is intended to sustain loads". Optimisation is a process concerned with achieving the best possible outcome of a given system satisfying certain restrictions. Thus *structural optimisation* can be understood as the subject dealing with obtaining the best outcome from an assemble of materials and elements that shall respect pre-established restrictions. From the early years of the structural optimisation, the outcome of a structure has been commonly measured trough the volume and/or the mass of the element itself, while the restrictions are generally, but not limited, expressed in terms of the displacements and the stresses [Haftka and Gürdal, 2012].

2.1.1 General problem definition

As any other optimisation problem, the standard form of a structural optimisation (see equations 2.1 and 2.2) consists in the minimisation (or maximisation) of an objective function, $F(X)$, in terms of design variables, X_i and restricted by one or more constraints functions, $g_j(X)$. The objective function can be interpreted as the mathematical representation of characteristics that are meant to be minimised or maximised.

The notion of improving the objective function implies a freedom of change. This change is commonly expressed in terms of ranges of permissible modifications of one single parameter or a group of them. Such parameters are referred to design variables and can represent geometric aspects of a structure such as cross-section or length of some elements or material parameters like resistance or Young's modulus. Design variables can take continuous or discrete values according to realistic constraints. Continuous variables can take any value within a range while discrete variables are subjected to a permissible list. In practice, the discrete nature of design variables is commonly disregarded while the optimisation process and the final results are adjusted to the nearest available discrete value.

With no restrictions, the result of most optimisation problems would approach to the infinity or a zero value. Constraints are given in order to keep the results within a feasible domain and are commonly given by restrictions in terms of budget (quantity of used material), available space (boundary conditions and geometry), serviceability (displacements, frequency requirements) and/or intrinsic material properties (permissible strains and stresses) among others. Generally speaking, there are 3 types of constraints:

- inequality constraints
- equality constraints
- side constraints

Inequality constraints are those which impose either a lower or an upper limit on some quantities. Equality constraints represent specific requirements of a quantity taking a selected value while, the third type, the side constraints, impose at the same time an upper and a lower restriction.

$$\text{minimise } F(X) \quad (2.1)$$

$$\text{subject to: } g_j(X) \geq 0, \quad j = l, m \quad \text{inequality constraints} \quad (2.2a)$$

$$h_k(X) = 0, \quad k = l, l \quad \text{equality constraints} \quad (2.2b)$$

$$X_i^l \leq X_i \leq X_i^m, \quad i = l, n \quad \text{side constraints} \quad (2.2c)$$

with

$$X = \begin{bmatrix} x_1 \\ x_2 \\ \vdots \\ x_n \end{bmatrix}$$

where X denotes the vector containing the design variables. Commonly, minimisation problems are preferred to maximisation ones. However, a maximisation problem can be solved indirectly by minimising the problem with opposite value. In a similar way, the less-than constraints can be transformed into greater-than ones by multiplying them by -1 affecting only the sign convention in some of the final results.

When using constraints that do not correspond to the same order of magnitude (e.g. displacements and lengths) it results advantageous to represent them in a normalised form:

$$x_i \leq x_i^m \quad \text{becomes} \quad \frac{x_i^m - x_i}{x_i^m} \leq 1 \quad (2.3)$$

2.1.1.1 Variables of structural optimisation problems

Any structural system can be globally described by a set of quantities (lengths, number of elements, etc.). Some of these quantities such as loads or spans may be preassigned by the type of structure itself but any other quantity subject to modifications can be taken as a variable.

The selection of variables and preassigned parameters is made for a variety of reasons. It may be that the designer is not free to choose certain parameters, or it may be known from experience that a particular value of the parameter produces good results [Kirsch, 2012].

For real problems, design variables must consider plausible modifications of the structure. Such modifications can be divided into three types: [Christensen and Klarbring, 2008]:

- Sizing optimisation: the design variables are the thicknesses or the cross sections of the elements of a predefined structure. Generally, the design variables are governed by an inferior constraint of non-zero values or replaced by a greater-than relation (see figure 2.1a).
- Shape optimisation: in this case the structure is intended to be improved through modifications in the form, the contour of some part of the boundary of the structural domain. Shape optimisation does not alter the connectivity of the structure: new boundaries are not formed (see figure 2.1b).

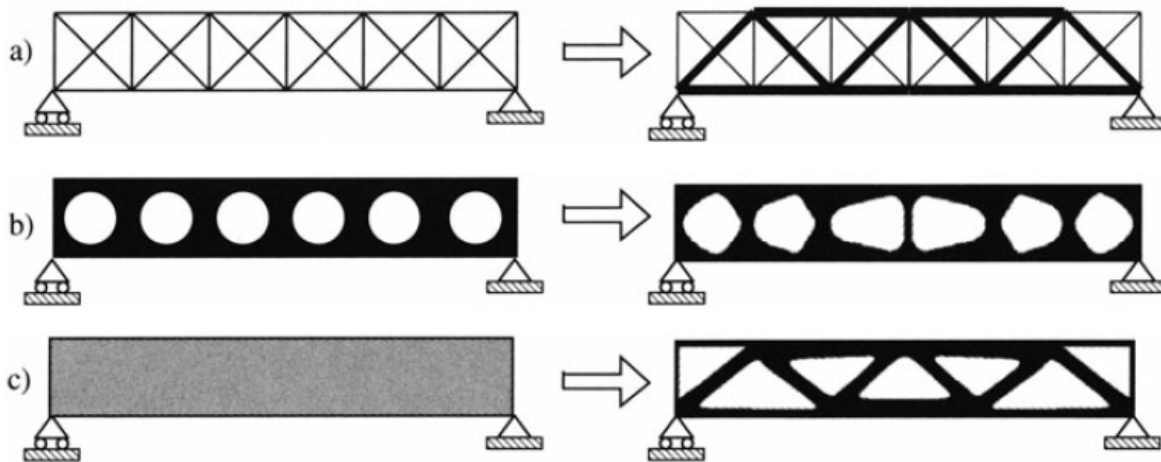


Figure 2.1: Three categories of structural optimisation: a) Sizing optimisation of a truss structure, b) shape optimisation and c) topology optimisation [Bendsøe and Sigmund, 2003].

- Topology optimisation: This is probably the most general form of structural optimisation. As in the sizing optimisation, the design variables are the value of the thicknesses or cross sections but this time allowing them to reach zero values. If pure topological features are optimised, the optimal values of the design variables should take only two values: 1 (the element exists) and 0 (the element is absent) (see figure 2.1c).

A fourth type of optimisation arises when the selection considers some characteristics of the material such as E , σ_y or ν . When treated as a continuous variable, the material selection can be used to study non-conventional materials such as polymers or fibre-matrix mixtures. On the other hand, due to the nature of conventional materials, this kind of problem may lead to optimal solutions that points out a non real material. When treated as discrete variables, the complexity of the problem may considerably be increased [Kirsch, 2012]. Given the vast quantity of possible materials and in order to reduce the complexity of the problem, a small list of possible materials must be specified.

2.1.1.2 Constraints of structural optimisation problems

Two common kinds of restrictions can be identified in structural problems: Constraints derived from considerations such as fabrication, aesthetics availability of structural profiles or thicknesses, etc. are called technological constraints or side constraints.

Constraints that derive from behaviour requirements are referred as behaviour constraints. Some examples are limitations on displacements, buckling or maximum stresses which in general are given by the design codes or specifications.

2.1.1.3 Behaviour variables

This type of variables are used as an indicator of the performance of the model; they are for instance quantities results of the structural analysis such as displacements, stresses or forces. Even if these variables are not always included within the optimisation procedure, their final value can be decisive for accepting or rejecting a given model.

2.1.1.4 Objective function for structural optimisation problems

The choice of the objective function (also referred as the merit function or cost criterion) directly influence the solution thus, it should be adapted for each specific case.

As concerns civil engineering structures, the total price is commonly seen as the most important criterion of construction and self weight is probably the most commonly used objective function due to the fact that it is readily quantified. Even though the weight of a structure is often of critical importance, its minimisation does not always lead to the cheapest model. And even more, the final cost does not only depend on weight but also on rather difficult to obtain data such as construction cost, fabrication, transportation, etc. In addition to the cost involved in the design and construction, additional factors such as operating and maintenance costs, repair costs, insurance may be also taken into account.

Other common objective functions for structural optimisation are displacements, vibration frequencies, stresses, buckling loads, and cost or even any weighed combination of these functions [Haftka and Gürdal, 2012].

Some approaches [Soltani and Corotis, 1988] consider the initial cost of the structure and the failure costs by assuming this last one as an association of the damage cost of a particular mode of failure and its probability of occurrence. Despite seeming conservative, this approach requires to solve the moral dilemma of what constitutes an appropriate failure damage and, for this reason, it will not be taken into account within this work.

2.1.2 Solution procedure

All points contained in the zone delimited by the constraints $g_i(X)$ are called feasible design and together form the feasible region $\Omega_{feasible}$. According to the nature and the number of constraints, an infinity of different feasible regions can be generated. Figure 2.2 shows some common types of feasible regions generated by generic two-variable design problems.

From the situations presented, four different cases may be considered. For figures 2.2d) and e) only one minimum exists. For figures 2.2b) and c) several local minima are generated but the only one providing the lowest value of the objective function is the solution of the problem. Case 2.2f) shows a feasible region formed by isolated sub-regions with at least one potential minimum included. Finally, case 2.2a) represents a situation where the constraints do not properly delimit, case that do not occur for properly proposed real problems.

For cases presenting linear objective functions and feasible regions bounded only by straight lines, the solution is a unique point placed at a vertex of the feasible region which can be determined by using any linear programming method [Winston and Goldberg, 2004]. In cases presenting linear constraints but a non-linear objective function, several local minima may be involved thus, more complicated methodologies must be applied.

As said in the last paragraphs, if a linear problem has an optimal solution, an extreme point of the feasible region must be an optimum. However, for problems presenting non-linear feasible regions, the optimal solution does not require to be an extreme point of the feasible region and local minima may appear. This difference is produced directly by the shape of the feasible region.

A domain Ω is said to be convex if any pair of points X_1 and X_2 , part of the limits of single constraint function, can develop a joining line completely inside the feasible domain.

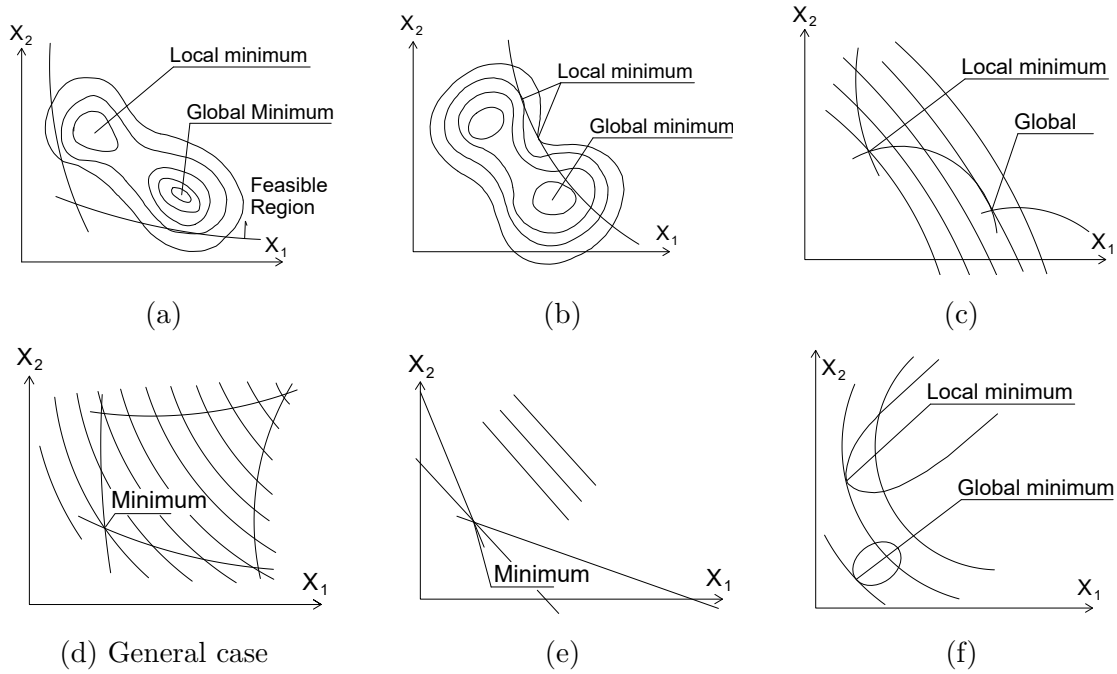


Figure 2.2: Shape of feasible region (adapted from [Adeli, 2002]).

A minimisation problem is referred as convex only if the objective function is convex and the constraints bound a convex domain.

Svanberg [Svanberg, 1981] identifies three principal constraints that lead to convex problems in structural optimisation:

- Symmetric displacement constraint. The displacement vector u_k of a node k has the same direction as the external load P_i

$$u_i = \mu P_i \leq u_i^U \quad k = 1, \dots, n \quad (2.4)$$

where u_i^U is an upper limit for the displacement at the i th node.

- Global displacement constraint. This constraint imposes a limit on the maximum displacement u_k to any component on the resultant vector displacement

$$\max u_i \leq u^U \quad (2.5)$$

- Lower limit of the smallest eigenvalue. The constraint places a lower bound, λ_m , on the smallest of the N eigenvalues of the structural stiffness matrix K

$$\lambda_m \leq \lambda_j \quad j = 1, \dots, N \quad (2.6)$$

Common constraints such stress or displacement related ones produce non-convex regions thus, the feasible regions for realistic structural optimisation problems are expected to be non-convex which is not always easy to verify. In cases presenting two or three variables, the design space is reduced to a plane or to a three-dimensional space. In the general case of n variables the design space becomes a n -dimensional hyperspace

In structural optimisation problems, the solution is commonly approached through numerical search techniques. These techniques start from an initial design and attempt to improve the value of the objective function by modifying the value of the design variables.

The formulations in design variables are solved in a so-called two-level "nested" scheme. The first level corresponds to the structural analysis and the evaluation of the constraints. The second level corresponds to the optimisation procedure.

Optimisation techniques divide the design space into *feasible* and *unfeasible* domains where the boundaries between this two domains are defined by the constraint functions. The feasible domain contains all the points associated to allowable values of the design variables. As one could expect, the imposed constraints influence the point of the optimum design commonly attracting it to the boundary between feasible and unfeasible domains. During the process, the value of the the normalised constraints (equation 2.3) may change, adopting a critical value equal to zero. The zero value on a normalised constraint describes a constraint either as an *active* or a passive *constraint*.

Intuitively, it can be assumed that all active constraints influence the final result but this is not always true [Haftka and Gürdal, 2012]. Some procedures use the Lagrange multipliers in order to measure the sensitivity of the results to changes in each constraint.

In the literature, one can find different propositions to regroup optimisation methods (eg. [Schittkowski et al., 1994, Hernández, 1993, Vanderplaats, 1984b]). Keeping in mind the distinctions made by S. Hernández [Adeli and Kamal, 1986], this text will introduce the ones that in a personal opinion can be seen as the most relevant methods of solution.

2.1.3 Exact solution tools

Differential and variational calculus have been referred as common methods used to find exact solutions to structural optimisation problems [Cherkaev, 2012, Fraternali et al., 2011]

2.1.3.1 Differential calculus for unconstrained optimisation problems

If no constraints are considered, a continuously differentiable objective function F reaches a maximum (or a minimum) at the stationary points X^* . This obtained is when the following condition is fulfilled.

$$dF(X) = \frac{\partial F}{\partial x_1} dx_1 + \frac{\partial F}{\partial x_2} dx_2 + \dots + \frac{\partial F}{\partial x_n} dx_n = 0 \quad (2.7)$$

The development of a sufficient condition of a stationary point X^* to be an extreme requires the evaluation of the Hessian matrix H of the objective function. If the Hessian matrix evaluated at X^* is positive-definite ($Q = x^T H x$ is positive for every x), the stationary point is a minimum. The stationary point is a maximum if H is negative-definite (Q is negative for every x) [Hancock, 1917].

For cases where the Hessian matrix is positive semi-definite (Q is non negative for every x), higher order derivatives must be evaluated to establish sufficient conditions for the stationary point. In order to verify such conditions, a computational check involving the determinants of all the principal minors must be performed either numerically or symbolically.

2.1.3.2 Lagrange multipliers

As always, in order to find the minimum of an objective function F depending on n design variables, the differential change must vanish

$$dF = \frac{\partial F}{\partial x_1} dx_1 + \frac{\partial F}{\partial x_2} dx_2 + \dots + \frac{\partial F}{\partial x_n} dx_n = 0 \quad (2.8)$$

In the same manner, the differential changes in the constraints are verified:

$$dh = \frac{\partial h}{\partial x_1} dx_1 + \frac{\partial h}{\partial x_2} dx_2 + \dots + \frac{\partial h}{\partial x_n} dx_n = 0 \quad (2.9)$$

Multiplying equation 2.9 by an arbitrary constant, λ , and adding the result to equation 2.8 leads to:

$$\left(\frac{\partial F}{\partial x_1} + \lambda \frac{\partial h}{\partial x_1} \right) dx_1 + \left(\frac{\partial F}{\partial x_2} + \lambda \frac{\partial h}{\partial x_2} \right) dx_2 + \dots + \left(\frac{\partial F}{\partial x_n} + \lambda \frac{\partial h}{\partial x_n} \right) dx_n = 0 \quad (2.10)$$

In order to vanish the elements inside each parenthesis one must determine λ which leads to a system of n equations and $n + 1$ unknowns (the n design variables plus the Lagrange multiplier). The additional equation needed to solve the system is given by the constraint relation ($h(x) = 0$). If multiple constraints must be treated, additional Lagrange multipliers shall be added for each of the constraint functions. The general formulation of an optimisation problem of one objective function, n design variables and, n_e equality constraints is thus equivalent to a n unconstrained problem with an auxiliary function (equation 2.11). Then the optimum design can be found by solving the system formed by equations 2.12.

$$L(X, \lambda) = F(X) + \sum_j^{n_e} \lambda_j h_j \quad (2.11)$$

$$\frac{\partial L}{\partial x_i} = 0, \quad i = 1, \dots, n \quad (2.12a)$$

$$\frac{\partial L}{\partial \lambda_j} = 0, \quad j = 1, \dots, n_e \quad (2.12b)$$

2.1.4 Optimality Criteria (OC) based methods

Considering a general structure discretised into m finite elements, the load-displacement relation is expressed in the framework of linear elasticity as:

$$[K]\{U\} = \{F\} \quad (2.13)$$

where $[K]$ is the global stiffness matrix, $\{U\}$ is the displacements and, $\{F\}$ the applied load vector.

The total weight, W , of a structure composed of m elements, can be calculated as:

$$W(a_i) = \sum_{i=1}^m \rho_i a_i \ell_i \quad (2.14)$$

where ρ is the mass density and $a_i \ell_i$ the volume of the i th element. The element length, ℓ_i , is considered constant while the cross sections, a_i , are taken as the design variables. The generalised constraints $g_j(X)$ applying to the structure can be written as:

$$g_j(a_i) = C_j(a_i) - \bar{C}_j \leq 0 \quad j = 1, \dots, p \quad (2.15)$$

where C_j is the actual value of the j th constrained value and \bar{C}_j is the upper limit value.

When treating displacement constraints, it is convenient to express the generalised constraints (equation 2.15) as a function of the flexibility coefficient E_{ij} :

$$F_j(A_i) = \sum_{i=1}^m \frac{E_{ij}}{a_j} - C_j \leq 0 \quad j = 1, \dots, p \quad (2.16)$$

with $E_{ij} = \{r\}_i [k]_i \{s^j\} a_i$ (or $E_{ij} = F_i U_i^j \ell_i / E_i$ for truss structures). In the previous expressions $\{r\}_i$ and $\{s^j\}$ are the displacement vectors generated at the i th element by the a vector $\{R\}$ and a virtual load vector $\{S^j\}$ associated to the j th constraint, F_i is the force in the i th bar.

Given the objective function to minimise, $W(a_i)$, and the constraints, $g_j(a_i)$, the Lagrange multipliers can be applied to the minimisation in the form:

$$W(a_i, \lambda_j) = \sum_{i=1}^m \rho_i \ell_i a_i + \sum_{j=1}^p \lambda_j g_j(a_i) \quad (2.17)$$

where λ_j are the Lagrangian parameters. Now, the local constrained optimum is obtained by differentiating the previous equation (2.17) with respect to the design variables a_i resulting in equation 2.18.

$$\frac{\partial}{\partial a_i} W(a_i, \lambda_j) = \rho_i \ell_i + \sum_{j=1}^p \lambda_j \frac{\partial}{\partial a_i} g_j(a_i) = 0 \quad i = 1, \dots, m \quad (2.18)$$

with $\lambda_j \geq 0$ and $\lambda_j g_j = 0$.

Substituting equation 2.16 into 2.18 leads to:

$$\sum_{j=1}^p \lambda_j \frac{E_{ij}}{\rho_i \ell_i A_i^2} = 1 \quad i = 1, \dots, m \quad (2.19)$$

The optimal structure must satisfy the optimality condition (equation 2.19) and the constraints (equation 2.15). When solving problems with only one constraint, the Lagrange multiplier can be explicitly defined and used to derive the recurrence relation for the design variable. When there is more than one constraint, the problem becomes more complex.

Since the obtained equations are non-linear, the solution schemes are based on the use of recurrence relations iterative in nature. In few words, the optimality criterion is used to derive a relation to modify the design variables while the constraints equations are used

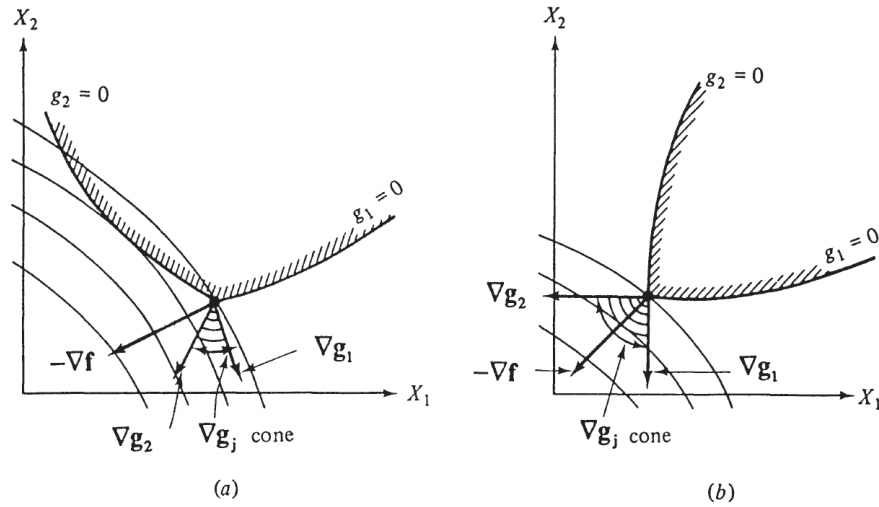


Figure 2.3: Graphical explanation of KKT conditions as seen in [Kirsch, 2012]

to obtain relations for the evaluation of the Lagrange parameters [Khot and B., 1979]. For truss structures, the allowable stress constraint can be directly replaced by a constraint on the deformation of each element.

2.1.4.1 Karush-Kuhn-Tucker based methods

Karush-Kuhn-Tucker conditions (KKT), sometimes referred as Kuhn-Tucker conditions, establish that the vector ∇F must have negative components for all gradients ∇g_i at a local minimum point. In other words, when some components of λ_i are non-positive, the current point cannot be a minimum.

$$\frac{\partial F}{\partial x_i} + \sum_{j=1}^J \lambda_j \frac{\partial g_j}{\partial x_i} = 0 \quad i = 1, \dots, n \quad (2.20)$$

and

$$\lambda_j \geq 0 \quad j = 1, \dots, J \quad (2.21)$$

A 2D graphical representation of the KKT conditions is given in figure 2.3. In the first situation, where $-\nabla F$ is not within the zone delimited by ∇g_i , the value of F can still be improved without violating the constraints. Thus the point is not a minimum. In the second situation, the vector $-\nabla F$ lies in the zone defined by the constraints.

Based on equation 2.20, and knowing that the first term of the left-hand side cannot be zero ($\frac{\partial F}{\partial x_i} \neq 0$), it can be stated that an equivalent expression for finding the minimum based on an iterative process is obtained by:

$$-\sum_{j=1}^m \lambda_{jk} \frac{\partial g_{jk}}{\partial x_i} \bigg/ \frac{\partial F_k}{\partial x_i} = T_{ik} \quad (2.22)$$

where T_{ik} will take a value of 1 at the minimum

Equation 2.22 is used as an indicator of proximity to the point of minimum and, according to the value of T_{ik} , a recurrence relation can be established of any element x_i of

design variables ${}^k X$ and ${}^{k+1} X$ at two consecutive iterations. A common recurrence relation [Khot and B., 1979] and expression to compute the Lagrange multipliers are shown in equations 2.23 and 2.24.

$${}^{k+1}x_i = [\alpha + (1 - \alpha)({}^k T_i)]^k x_i \quad i = 1, \dots, n \quad (2.23)$$

$$\sum_{i=1}^n \frac{\partial({}^k g_j)}{\partial x_i}({}^k x_i) \sum_{j=1}^m \lambda_j \frac{\partial({}^k g_j)}{\partial x_i} \bigg/ \frac{\partial({}^k F)}{\partial x_i} = \frac{{}^k g_j}{1 - \alpha} - \sum_{i=1}^n \frac{\partial({}^k g_j)}{\partial x_i}({}^k x_i) \quad (2.24)$$

where α is the relaxation factor that limits the step size between iterations. The usual value of α oscillates between 0.5 to 0.75 [Adeli, 2002].

Equation 2.24 represents a system of linear equations with non-negative solutions for all λ_i associated to the active constraints.

As it can be inferred, finding the values of the Lagrange multipliers is trivial to solve the optimisation problem and this task that can be achieved through an iterative process. A general process can be summarised in four steps:

1. Definition of an initial design ${}^0 X$.
2. Computation of the Lagrange multipliers λ_i , task that can be achieved through equation 2.24
3. Computation of values T_{ik} (see equation 2.22)
4. Update of the system using a recurrence relation (such as equation 2.23)

A first estimate or starting point ${}^0 X$ of each design variables ${}^0 x_i$ is needed. This starting point gets the iterative procedure improved by a loop generated by points 2 to 4 until the relative or absolute convergence is achieved. If the initial point is very far from the minimum, the procedure may present difficulties to converge. The same difficulties are expected if the subset of active constraints changes frequently from one iteration to another.

2.1.5 Methods based on mathematical programming

2.1.5.1 Linear programming

A large variety of types of optimisation problems can be found in almost any book of optimisation techniques [Foulds, 2012] or Operational research [Hillier, 2012]. Despite its versatility, its applicability in the field of structural design can sometimes be reduced. The standard form of LP problems is defined by a linear objective function with linear equality constraints and non-negative design variables defining altogether a (possibly unbounded) convex polytope. Although structural design problems are rarely linear, linearisation strategies can be introduced to fit some special cases.

The general LP statement is:

$$\text{minimise} \quad F = C^T X \quad (2.25)$$

$$\text{subject to: } g_j = A_1 X - b_1 = 0 \quad (2.26a)$$

$$h_k = A_2 X - b_2 \leq 0 \quad (2.26b)$$

where the vectors b_1 , b_2 , and C and the matrices A_1 and A_2 are all parameters whose dimensions match the dimensions and X , h_k and g_j . For these cases, the objective function contours are straight intersecting lines and the solution will be found at the intersections of the active constraints.

Probably the most popular method to solve linear problems is the well-known Simplex Method (including its revisions) [Dantzig, 2016]. This method, tests adjacent vertices of the feasible region in a sort of sequence so that at each new vertex tested, the objective function improves or unchanges but does not decrease. The simplex method has been presented as an efficient tool [Wright and Nocedal, 1999], generally taking $2m$ to $3m$ iterations (being m the number of constraints) to converge. However, the effort to obtain the solution increases exponentially for the worst case [Klee and Minty, 1970].

Briefly explained, the simplex algorithm minimises a linear objective function (equation 2.25) subject to equality constraints (equations 2.26)

The first step consists in transforming the problem into a system of linear equations of a standard form. The objective function takes the form of $f(X) = 0$ and slack variables, whose value is constraint to be equal or greater than zero, are added to the current constraint equations.

The solution is achieved by starting from an initial "guess" and improving through an iterative process based on the Gauss-Jordan procedure.

Other type of procedures for LP are the interior point methods. These type of methods construct a sequence of strictly feasible points lying in the interior but not belonging to the boundaries in order to converge to the solution. Interior point methods such as Karmarkar's or Mehrotra's ones [Karmarkar, 1984, Mehrotra, 1992] have been proved effective but the experience with their application to real problems is still very limited [Hernández, 1993].

2.1.5.2 Methods of feasible direction

Originally developed by Zoutendijk [Zoutendijk, 1960] Methods of Feasible Directions (MFD) are intended to give solution for NLP (non-linear programming) and LP (linear programming) problems by moving from a feasible point to an improved feasible point.

Starting from a feasible initial point (or design) 0X , the process is carried out in an iterative scheme improving the value of the objective function at each step k ideally conducting to the problem's solution *X . Given a feasible point, a plausible direction kS and a step size α are chosen. The choice of these two last parameters is made in such a way that two properties must be respected: 1) the new point ^{k+1}X (equation 2.27) must remain within the feasible domain and 2) the value of the objective function at ^{k+1}X is better (lower in a minimisation problem) than the objective value at kX . After having determined such feasible direction, a one-dimensional optimisation problem is established and then solved to determine how far to advance.

$$^{k+1}X = ^kX + \alpha(^kS) \quad (2.27)$$

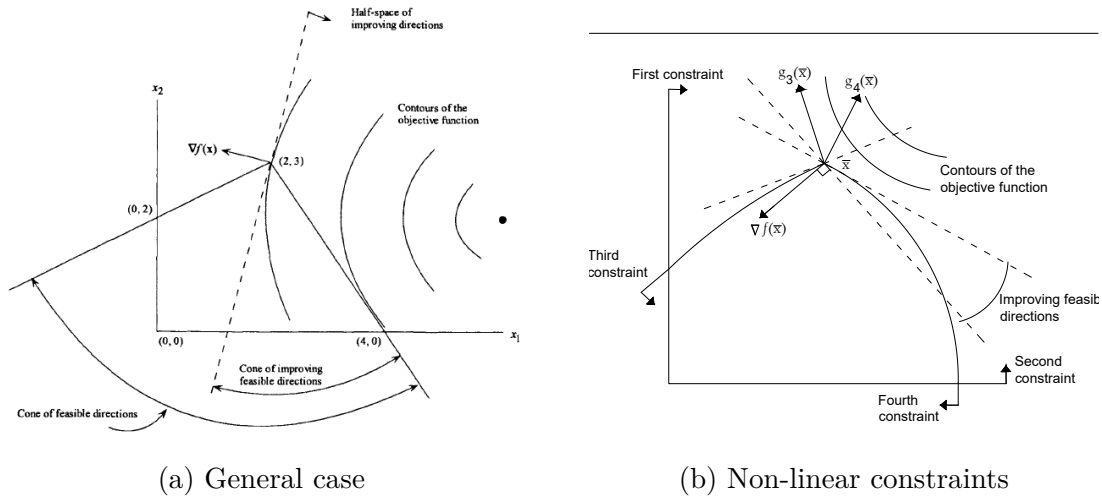


Figure 2.4: Improving feasible directions (modified from [Bazaraa et al., 2013]).

Considering a NLP problem, the Zoutendijk algorithm consists in the following steps:

1. Feasible direction ${}^k S$. Letting the set of active (binding) constraints $I = \{j : g_j({}^k X) = 0\}$, a Finding-Direction-Sub-Problem (FDSB) is stated under the form:

$$\text{minimise } z \quad (2.28)$$

$$\text{subject to: } \nabla({}^k X)^T S - Z \leq 0 \quad (2.29a)$$

$$\nabla g_j(X)^T S - Z \leq 0 \quad \text{for } j \in I \quad (2.29b)$$

$$-1 \leq S_i \leq 1 \quad \text{for } i = 1, \dots, n \quad (2.29c)$$

The process continues according to the solution vector ${}^k S$ and value ${}^k Z$. If ${}^k Z = 0$, stop. Otherwise the algorithm moves to step 2

2. Step ${}^k \alpha$. The step is then proposed to be the solution of the following line search problem:

$$\text{minimise } F({}^k X + \alpha({}^k S)) \quad (2.30a)$$

$$\text{subject to: } 0 \leq \alpha \leq \alpha_{max} \quad (2.30b)$$

where $\alpha_{max} = \sup\{\alpha : g_j({}^k X + \alpha({}^k S)) \leq 0 \text{ for } i = 1, \dots, m\}$.

The recurrence relation (equation 2.27) is applied and step 1 is repeated until convergence.

The main drawback that the MFD presents is that it does not present a closed algorithmic map [Bazaraa et al., 2013]. This can sometimes lead to solutions that do no

lie in the feasible region, violating one or more constraints, and hence presenting problems of convergence. Some modifications have been proposed to overcome this problem ([Topkis and Veinott, 1967, Vanderplaats, 1984a, Vanderplaats and Moses, 1973]), one of the simplest consisting on the addition of the logic condition:

$$[{}^k X + \alpha({}^k S)] \in \Omega_{feasible} \quad (2.31)$$

2.1.5.3 Successive linear approximation approach

For this type of approach, at each iteration, a direction-finding linear program is set up based on the first-order Taylor series approximations to the objective and constraint functions. If the solution is found in the direction S , the process stops. Otherwise the process decides between iterate ${}^{k+1}X = {}^k X + \alpha({}^k S)$ or reduce the stepbounds. Originally presented by Griffith [Griffith and Stewart, 1961], this method presents robustness for large-scale problems and may be easily implemented.

2.1.5.4 Methods based on mathematical programming

Ideally, the Shape optimisation problem is a subclass of topology optimisation, but their implementations are based on very different techniques, hence are commonly treated separately in the literature [Kirsch, 2012]. Now, regarding the relation between topology and sizing optimisation, they are related for practical considerations even if from a fundamental point of view they are very different.

2.1.6 Simultaneous analysis and design

In some design problems it has been found advantageous [Schmith and Fox, 1965] to simultaneously integrate the analysis and design procedures within the optimisation process. This problem statement is referred as the integrated formulation or Simultaneous Analysis and Design (SAND). This approach considers both design variables X and behaviour ones Y and treats them in the same manner.

The SAND approach eliminates the need for the iterative analysis of the structure at the expense of a larger size optimisation problem. This is a great advantage when dealing with structures requiring a sort of non-linear analysis but in general, it represents major shortcoming. The additional variables and equality constraints makes the approach less attractive in many optimal design problems where elastic analysis models are considered.

2.1.7 Convergence

The results obtained by the implementation of numerical algorithms are sequence of points vectors idealised as a generalised function or mapping. In short, the application of an algorithm A over an arbitrary set of points ${}^k X = \{x_1 \dots x_m\}^T$ would generate a sequence ${}^{k+1}X$:

$${}^{k+1}X = A({}^k X) \quad (2.32)$$

Theoretically, the sequence ${}^k X$ should converge to a minimum ${}^* X$. Generally, the algorithm should present a steady progress while iterating sets ${}^k X$ away from ${}^* X$. Once approaching to a minimum, a rapid convergence is expected.

According to P. Papalambros [Papalambros and Wilde, 2000] there are two distinct characteristics of convergence behaviour; global convergence is understood as the ability of the algorithm to reach the neighbourhood of the minimiser ${}^* X$ starting from an arbitrary initial point ${}^0 X$ located far from ${}^* X$. The second one, the local convergence, refers to the ability to approach ${}^* X$ rapidly from a starting point (or iterant ${}^k X$) already placed in the neighbourhood of ${}^* X$.

Based on the difference between continuous iterations, an error can be defined under the form ${}^k \epsilon \triangleq {}^k X - {}^* X$. Convergence of the sequence ${}^k X$ to ${}^* X$ means that the limit of ${}^k \epsilon$ is zero. The rate of convergence can be defined by measuring the decrease in the error within subsequent iterations. The usual rates of convergence are expressed in terms of an asymptotic convergence ratio as expressed below:

$$\|{}^{k+1} X - ({}^* X)\| \leq \gamma \|{}^k X - ({}^* X)\|, \quad 0 < \gamma < 1 \quad (\text{linear}) \quad (2.33a)$$

$$\|{}^{k+1} X - ({}^* X)\| \leq ({}^k \gamma) \|{}^k X - ({}^* X)\|, \quad ({}^k \gamma) \rightarrow 0 \quad (\text{superlinear}) \quad (2.33b)$$

$$\|{}^{k+1} X - ({}^* X)\| \leq \gamma \|{}^k X - ({}^* X)\|^2, \quad \gamma \in \mathbb{R} \quad (\text{linear}) \quad (2.33c)$$

To sum up, global convergence is directly related to reliability (or robustness), while local convergence corresponds to efficiency on the applied algorithm.

2.1.7.1 Termination

A common optimisation algorithm tends to reach the solution when the error, ϵ , equals zero but this solution is not always reachable nor necessary. The iterative process is terminated when no improvement can be done on the value of the objective function without violating the constraints. However this is not the only possible solution. Some methods stop the iterative procedure when the progress on the improvement becomes slow, while others base their decision on KKT conditions [Arora, 2004]. The criteria of stopping the iterative process should correspond to the following five situations:

- no improvement can be done on the value of the objective function.
- slow progress is made from iterations k to ${}^{k+1}$
- an acceptable number of iterations have been done
- an acceptable solution does not exist
- an infinite loop has been generated

Ideally the best way to determine to stop or not the process would be a test comparing directly the current values and the optimal ones $|{}^k x_i - {}^* x_i| \leq \epsilon_i$, where ϵ_i are small values determined by the user. Given that for most cases these values corresponding the optimal solution are not known, a useful test is:

$$|{}^k x_i - {}^{k+1} x_i| \leq \epsilon_i, \quad i = 1 \dots m \quad (2.34)$$

Many algorithms are also constructed in such a manner that $\{\nabla^k f\} \rightarrow \{0\}^T$ indicating a stationary point that is most of the times (a exception for hidden saddles) also a minimiser.

$$\|\nabla^k f\| \leq \epsilon \quad (2.35)$$

Precedent equation (2.35), together with a satisfactory positive-definiteness of the Hessian evaluated at ${}^k X$, seems to be a reliable index for the termination with the disadvantage of the restiveness of its application to problems with large numbers of variables.

When solving constrained problems, apart from convergence tests, an acceptable constraint violation is allowed by setting:

$$\|g_j\| \leq \epsilon \quad (2.36)$$

being g_j the vector off all active constraints.

In reality, determining the proper termination criteria seems to be a matter of experience and expertise and is itself a subject of study [Kirsch, 2012].

2.2 Continuum optimisation

Within the structural design, three typical problems can be defined: namely sizing, shape and topology optimisation problems. The goal of sizing problems is to determine the optimal distribution of thicknesses or cross sections of the elements conforming an existent linear elastic structure. The optimal "size" minimises or maximises the objective function normally expressed as a physical quantity such as the peak stress, displacement, external work (compliance), etc. For the case of shape optimisation, the domain of the structure is taken as the design variable. The goal here is to find the optimum shape. Finally, topology optimisation may redefine the connectivity of the domain.

Within the structural optimisation domain, two types of optimisation can be defined according to the treated structure: discrete and continuous. For inherently discrete structures (skeletal structures), finding the optimum design consists in determining the optimum number, positions, mutual connectivity and individual cross section of the structural members.

For continuum structures, the shape of both internal and external boundaries as well as inner cavities may be simultaneously optimised following a predefined objective function and constraints. According to [Eschenauer and Olhoff, 2001], two sub-classes of continuum optimisation can be distinguished :

1. Material optimisation or Microapproach. For this type of approach, a fixed FE (finite element) mesh is used to describe the initial geometry (or the admissible design domain). Typically, the mesh has a rectangular shape with elements evenly distributed and the constraints are assumed to attain constant values at the nodes of the mesh. For the analysis, the characteristics of the FE such as Young modulus E and material density ρ are based on the physical modelling of a porous microstructure (made up of solid material and void) whose orientation and density are described by

continuous variables along the admissible domain. The optimisation consists in the deciding whether each element should contain material or not. To achieve this, the material within each element is associated to a design variable defined between 0 and 1; 0 considers a void or a very weak material while 1 represents a solid material [Bendsøe and Sigmund, 2003].

The final result can be graphically represented showing a rough description of the optimum outer and inner boundaries (see figure 2.5).

2. Geometrical continuum optimisation or Macroapproach. This class of optimisation proceeds with a FE analysis considering fixed characteristics for the materials of the elements associated to a non-fixed mesh. The topology of the optimum structure is achieved by growing/reducing material or inserting holes. The first method starts from the hypothesis that the optimal design is obtained as a subset of the design domain. The second method iteratively proposes holes at specific points on the structure continuously modifying the boundaries of the geometry.

Even if some articles have been published showing Strut-and-Tie models found through continuum-type optimal topology, [Almeida et al., 2013, Shobeiri, 2016] this practice remains controversial. From the point of view of mechanics, the characteristics of the discrete and continuum structures are very different, and from the point of view of the practical implementation, there is no criteria for constructing truss topologies from the results of optimal finite element solutions [Starčev-Čurčin et al., 2013]. In addition, due to the characteristics presented by the interaction concrete-reinforcement and according to some studies [Swan et al., 1999], a more adequate ST model would be found through a discrete optimisation purely based on truss structures.

2.3 Discrete optimisation: ground structure approach

Past decades can be considered to be the apogee for the development of algorithms for structural optimisation, mainly for weight minimisation problems. Most of generated algorithms have been initially developed for truss cases and then generalised for the treatment of more complex structures [Farshi and Alinia-Ziazi, 2010].

The objective functions presented in truss optimisation are usually dependant on the design variables, while constraints can be expressed in both behaviour and design variables leading to a non-linear relation that normally requires Non-Linear Programming (NLP) approaches for a direct mathematical solution.

Initially proposed by Dorn [Dorn, 1964], the ground structure approach reduces the complexity of a topology optimisation problem by considering a truss with a preexisting quantity of potential elements, m , linked at the nodes, n , of a fixed grid. The initial, or ground structure, is characterised by a high degree of connectivity that in some cases produces an element for the combination of any two nodes on the grid, having a quantity of elements m equal to $n(n - 1)/2$, while the degree of freedom N is only of the order $2n$ or $3n$ (for planar and 3-D trusses) (see figure 2.6).

The ground structure approach arises as a simplification of the optimisation problem. Once the initial truss has been proposed, its solution depends on the type of the addressed problem.

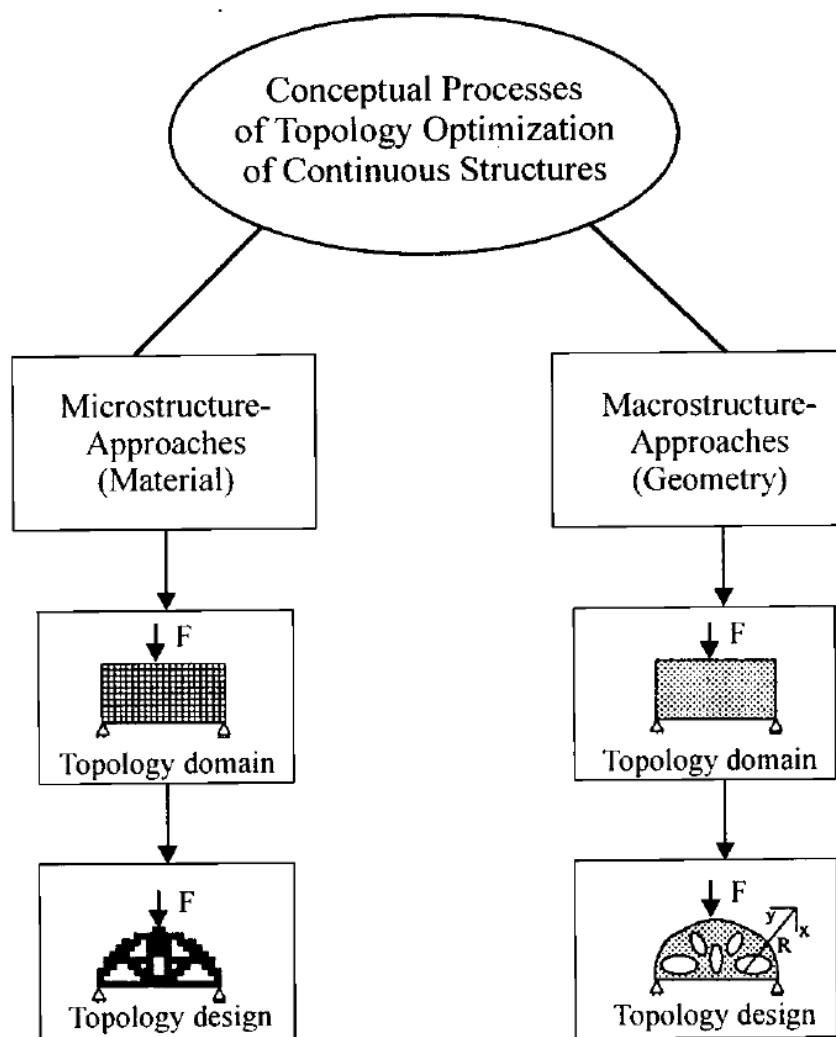


Figure 2.5: Conceptual processes of optimisation of continuum structures (as seen in [Eschenauer and Olhoff, 2001])

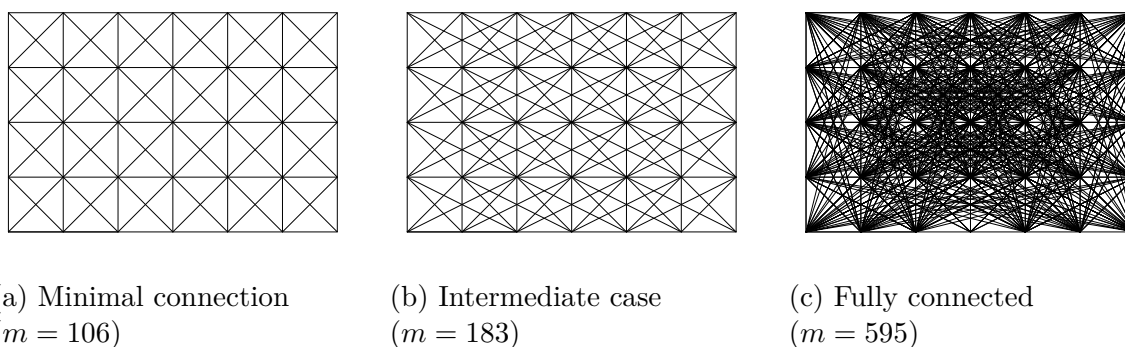


Figure 2.6: Three possible ground structures for a 4×6 grid ($n = 35$)

The methods based on mathematical programming can also be found in the literature [Lamberti and Pappalettere, 2000]. A vast range of techniques exists for determining the optimum according to the specific problem. LP is commonly used for problems exhibiting linearity in their statements [Ringertz, 1985], otherwise quadratic and non-linear methods must be used [Bekdaş et al., 2017]. Specific cases, such Integer Programming (IP), take into account discrete integer values which can be desired in a size optimisation when availability of the real structural profiles is reduced.

While a large number of available procedures rely on NLP approach showing good results for typical cases [Sedaghati and Esmailzadeh, 2003], [Adeli and Kamal, 1986] or [Arora and Haug, 1976], some other proposed algorithms are based on the Optimality Criteria (OC) as a shortcut to find optima in a limited way [Venkayya, 1978, Venkayya, 1971, Fleury, 1979].

When applied to truss problems, the optimal solution is found iteratively with a structural reanalysis to account for changes in load distribution. The efficiency of OC methods has been shown to be weakly dependent on the number of design variables holding an advantage over mathematical programming techniques in that they are not restricted to locally optimal solutions in the vicinity of the initial design. However, in structures with a high degree of statical indeterminacy, changes in load distribution may mean the approach still fails to locate the global optimum.

While some works prefer the use of the well known force method, most of the visited literature prefers the use of a simple formulation based on the displaced method. The use of one formulation or the other is largely a matter of taste and availability of a suitable computer program [Przemieniecki, 1985].

One last visited methodology is the so-called Full Stressed Design (FSD).

2.3.0.1 Fully stressed design (FSD) technique

The FSD is an intuitive optimality criteria based on the following simple statement: "For the optimum design, each member of the structure must be fully stressed under at least one of the design load conditions" [Ganzreli, 2013].

Within each iteration, the elements increase, reduce or keep the value of their cross sections according to the supported stress: when they do not support the allowable stress the section is increased, whereas the section is reduced if the supported stress is inferior. Otherwise, the section remain unchanged. In order to avoid stability problems carried out by zero-section elements, an inferior gauge is commonly adopted, so that the optimal solution must accept that some members are not fully stressed.

Considering the general problem (equation 2.14) and the premises described in above paragraph, the problem can be expressed as:

$$\text{minimise: } W(X) = \sum_{i=1}^m \rho_i a_i \ell_i \quad (2.37)$$

$$\text{subject to: } \sigma_i \leq \sigma_{in} \leq \bar{\sigma}_i, \quad n = 1, 2, \dots, n \quad (2.38a)$$

$$u_i \leq u_{in} \leq \bar{u}_i, \quad j = 1, 2, \dots, J \quad (2.38b)$$

$$a_i \leq a_{in} \leq \bar{a}_i, \quad i = 1, 2, \dots, m1 \quad (2.38c)$$

The solution procedure given in [Li, 1990] proceeds by including a scaling factor, ξ (equation 2.39), which is used as an indicator to individually identifies the current active constraint governing the element's cross section.

$$\xi = \max \left(\frac{u_{jn}}{\bar{u}_j}, \frac{\sigma_{ij}}{[\sigma]_i}, \frac{-\sigma_{in}}{\phi_i[\sigma]_i} \right) \quad (2.39)$$

When the active constraint is the stress-related one, the cross section at the i th element for the design at iteration n is going to be updated in the following manner:

$${}^{k+i}(a_i) = {}^{k+i} \left[\max \left(\frac{\sigma_{in}}{[\sigma]_i}, k\mu_i \right) ({}^k a_i) \right] \quad (2.40)$$

In the other possible case, when the active constraint is a displacement constraint the update must be computed as follows:

$${}^{k+i}(a_i) = {}^{k+i} \left\{ \left[\frac{V}{\bar{u}_j} \left(\sum_{P=1}^n \sigma_P^q \sigma_P^j \ell_P / E_p \right) \left(1 / \sum_{P=1}^n \ell_p \right) \right]^\eta a_i \right\} \quad (2.41)$$

where η is a relaxation parameter used to control the stability and convergence of the method and commonly takes a value between 0.1 and 0.2 [Li, 1990].

The algorithm showing the solution procedure is summarised in the flux diagram showed in figure 2.7.

Strictly speaking, the FSD is not really an optimisation method but an automatic technique of design. This technique is applicable to design for strength only and cannot deal with more general types of constraints such as displacement-based constraints.

The FSD is principally used for statically determinate design problems in which strength considerations govern over stiffness, nevertheless its use is proved to solve also statically indeterminate structures within few analyses [Razani, 1965]. For highly redundant structures, due to the large number of possible fully stressed designs, the FSD algorithm may diverge from the solution or oscillate about the optimum. Latter difficulty can be avoided by restricting the evolution of the cross section to a determined percentage of their current value [Vanderplaats, 1984b].

As seen in figure 2.7, the algorithm increases the size of over-stressed members and reduces the size of under-stressed ones, reanalysing and iterating until the convergence is achieved. However, Mueller [Mueller and Burns, 2001] demonstrates that this procedure may exclude a set of feasible designs in which some members will respond to an increase in size by attracting greater stress.

The first complication derives from the fact that the element cross section, a_i , could approach or even reach a zero value, which has obvious repercussion on the diagonal of the stiffness matrix. To overcome this, the possibility of zero cross sections is no longer permitted and in most cases, an inferior limit, a_{min} , is imposed for a_i ($a_i > 0$ or $a_i \geq a_{min}$).

A non-zero lower bound will generally produce "secondary" elements whose only purpose is often only to guaranty the non-singularity condition on the stiffness matrix and to avoid inner mechanisms on the structure. Such elements are often erased or simply ignored at the last stage of the optimisation, [Ohsaki and Swan, 2002]. This decision implies that most

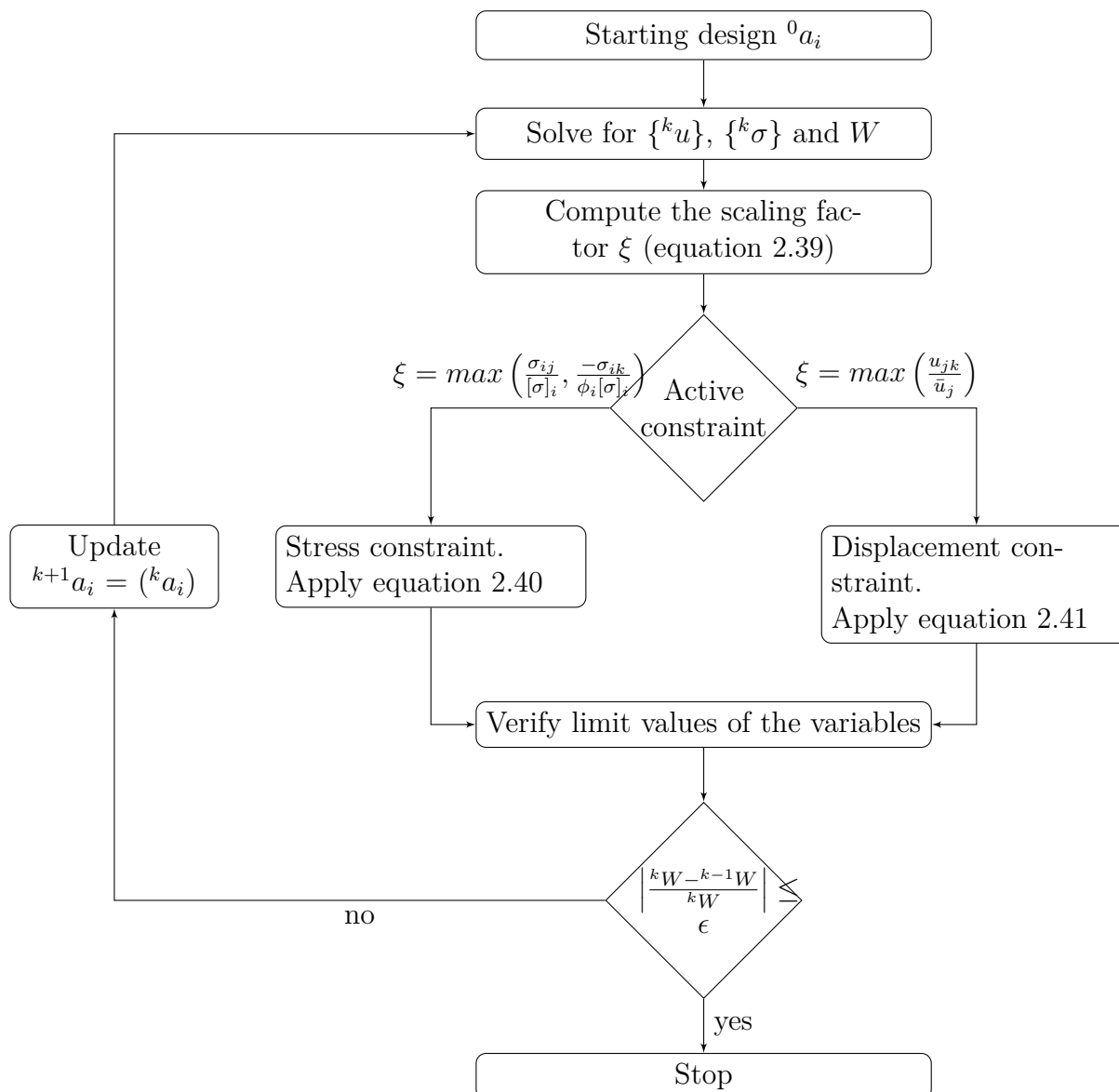


Figure 2.7: Flowchart design procedure using FSD (inspired from [Li, 1990]).

optimal designs have a singular matrix and present potential mechanisms when described as a part of the ground structure leading to the second listed complication.

The third complication is related to the choice of the ground structure. The ground structure approach may or may not lead to the optimal structure according to the group of nodes proposed (quantity and position) and the set of allowed elements; the optimal structure appears to be limited by the original geometrical restrictions and possible connections (figure 2.8).

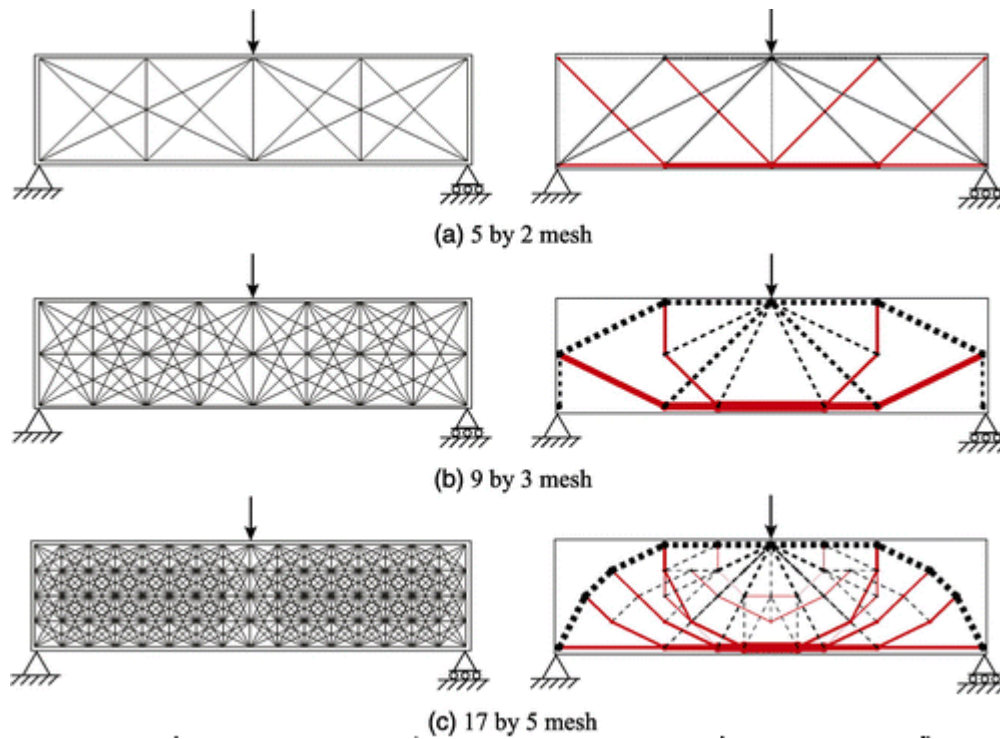


Figure 2.8: ST models obtained from 3 different ground structures [Gaynor et al., 2012].

2.3.1 Special cases of the ground structure approach

2.3.1.1 Geometric optimisation

Generally, the position of the nodes of a truss structure depends on the position of the supports, loads, the available profile's length, the constructive procedure, the aesthetics, and are also strongly dependant on the engineer's criteria. The engineer is of course sensed to provide a model that fulfils the service criteria but also, a model that is economically feasible.

The geometric (or shape) optimisation is meant to find the optimum layout of a truss through the optimum nodal coordinates. Hence, this optimisation problem is defined by the minimisation of an objective function in terms of a series of unknown nodal coordinates [Gil and Andreu, 2001].

Even though the ground structure approach has been proved a powerful tool for computing ST models allowing the optimisation to be seen as a relatively simple sizing problem, it comes against many difficulties principally related to: 1) the singularity of the stiffness matrix, K , 2) the stability of the optimised structure, and 3) the optimality of the structure *per se*.

2.3.1.2 Material optimisation: truss optimisation considering different types of materials

Concerning classic applications, the minimal weight of a truss structure is computed based on a model that considers a certain number of materials with same yield stresses for tension and compression. A generalisation of this approach may consider the cases where one or

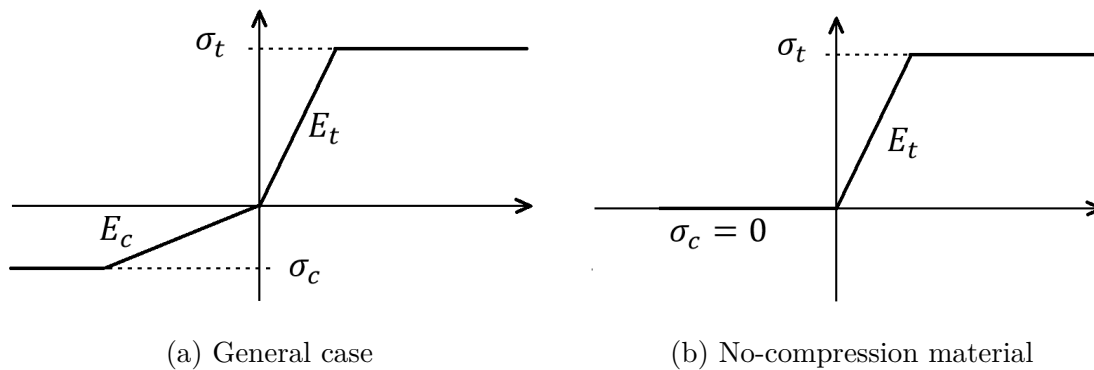


Figure 2.9: Piece-wise linear stress-strain relations (modified from [Achtziger, 1996])

more of the considered materials present different properties for negative and positive stresses.

Figure 2.9 depicts a material where the absolute yield stress σ_c and σ_t (stresses of compression and traction) are different, in the same manner E_c and E_t may be different [Achtziger, 1996]. This "equivalent" behaviour considers the case where two materials are present in a structure. One branch of the stress-strain relation represent the behaviour of the bars in compression while the other concerns the elements in compression.

A key point of this kind of optimisation must be the correct handling of the property-assignment scheme. However, the nature of the forces at each element is not available at the beginning of the process. Thus, this difficulty must be stated on the formulation of the problem.

2.4 Summary

Most optimal design studies applied on skeletal structures deal with cross-sectional design variables. However, due to the weight reductions that can be gained by modifications of the structural configuration [Gil and Andreu, 2001], a growing quantity of scientific papers interested in shape optimisation have been published in recent years. Yet, there are some basic difficulties involved in this type of optimisation. One major complication is related to the need of declare the existence or absence of structural elements. Another complication, and probably the most important, involves the choice of the starting selection of nodes and elements; the selection of the ground structure.

So far, the procedure to select a ground structure seems to rely on the designer experience. Intuitively, if the nodal positions are fixed, the choice of a saturated ground structure would lead to the best results. In this manner, the geometric optimisation is "replaced" by a large quantity of potential (fixed) nodes in the ground structure. The selection of the "best nodal coordinates" is indirectly made by vanishing those nodes only attached to elements whose cross section approximates to 0. From an opposed point of view, if nodal positions are also implicitly included in the variable vector, a sparse ground structure is preferred.

From a practical point of view, optimisation formulations that simultaneously improve topology and geometry may lead to reasonable structures presenting the disadvantage of being a highly non-linear problem and, in some cases, with disjointed design spaces. On the

other hand, pure ground structure optimisation generally its simple performed. However, it has been shown that such approach frequently leads to singular unstable structures or to structures with a considerable high quantity of secondary elements.

In an attempt to obtain reasonable structures through a simple algorithm, avoiding the complications related with mixed design vectors, some methodologies are presented as 2-part optimisation problems.

The optimum solution can be obtained by the application of a stress-ratio method over a fixed geometry followed by a geometric optimisation. In the first instance, this process will allow to "reduce" the structure by decreasing the section of non-trivial elements. Once the sizing procedure is completed, the optimisation of the geometry is implemented.

The proposed procedure combines the ground structure approach with a subsequent iteration procedure that alternates between the member sizing optimisation (cross sections as variables) and the shape modification (node coordinates as variables).

In addition, [Vanderplaats, 1984a] developed a technique where the stress-ratio method was used to size the structure while keeping the topology fixed and the steepest descent method was used to move the nodal coordinates while keeping the sections fixed. Using two separate design spaces reduces the design variables at each sub-problem and simplifying the global optimisation. The main drawback was that the algorithm was not able to automatically to add or delete members or joints during the design process frequently producing ill-conditioning problems.

According to the reviewed literature, a suitable way to threat truss optimisation problems would be an hybrid algorithm able to sequentially threat the structure and a subroutine capable of delete or insert elements without compromising the stability of the Stiffness matrix and the whole structure.

Chapter 3

Computational aided approach through locally weighted regressions

In recent years, several approaches have been proposed in order to ease the application of the Strut-and-Tie method. While some methodologies treat the problem as a continuous optimisation, some others prefer the ground structure and truss optimisation to create an acceptable reinforcement layout.

One of the main difficulties of this last approach, based on the truss optimisation, is how to define the initial structure: the initial number of elements, connectivity and, the most important, how to determine the number and position of the nodes.

The objective of this chapter is to present in detail the proposed computer aided process to acquire Strut-and-Tie models for the reinforcement bi-dimensional and three-dimensional concrete structures.

This chapter contains two important sections. The first one presents and describes the algorithm of the proposed method. The second section intends to clear out some points of the behaviour and the performance of the process seen on the test campaign.

Approche assistée par ordinateur par régressions localement pondérées

Au cours des dernières années, plusieurs approches ont été proposées afin de faciliter l'application de la méthode Bielle-Tirant. Alors que certaines méthodologies abordent le problème en tant qu'une optimisation continue, d'autres préfèrent la structure de base et l'optimisation du treillis pour créer un schéma de ferrailage acceptable.

L'un des principales difficultés de la dernière méthodologie, basée sur l'optimisation d'une ferme, est de définir la structure initiale : le nombre initial d'éléments, la connectivité et, surtout, la façon de déterminer le nombre et la position des noeuds.

L'objectif de ce chapitre est de présenter en détail le l'algorithme proposée pour l'acquisition de modèles Bielle-Tirant pour des structures planes ou tridimensionnelles en béton armé.

Ce chapitre consiste en deux sections. La première présente et décrit l'algorithme de la méthode proposée. La deuxième section vise à éclairer certains points du comportement et la performance du processus vu sur la campagne de tests.

3.1 Basis and description of the algorithm

The procedure here presented has three main purposes:

- to ease the generation of ST models based on the linear-elastic stress field distribution
- to propose both a fully automatic approach and a rational one based on the experience of the engineer
- to present a fast and low cost (in terms of computational effort) option to assess the need of steel reinforcement respecting the EuroCodes

Despite the previously discussed limitations that a ST based on its linear elastic stress field may have. It was decided that, according to some sources such as [Chae and Yun, 2016], [Schlaich et al., 1987] and the [British Standards Institution, 2005], a strut-and-tie model can be developed for a given element based on its linear elastic (uncracked) stress field, used to identify from it a possible resisting truss model. Accepting that plausible ST models can be produced through the application of structural optimisation techniques, the project proposed a scheme based on weight minimisation. Within this work, discrete representations (FE models including only bar-type elements) have been preferred over the so-called continuous optimisation. This decision was principally based on the structural behaviour of a ST system (according to the EuroCodes) and also, based on the advantages that this type of representation have in terms of its simplicity of treatment and the direct extraction of the final results.

Since the beginning, the construction of the initial ground structure was one of the major difficulties to overcome. In order to automatise the process, the selection of the nodes, as well as the construction of the ground structure, is based on the linear elastic stress field of a FE analysis of the structure. This selection allows to generate an initial truss structure and proceed to optimise it.

The algorithm has been divided in five subroutines that include the analysis and the post-process of a model. The included subroutines proceed to fulfil different tasks:

1. input of the geometry and the boundary conditions
2. analysis of an initial continuous model of the structure and post-processing of the results
3. construction of the ground structure based on the trajectories of the principal stresses product of the previous subroutine
4. reduction of the truss optimisation
5. construction of the resultant ST model and reinforcement proposition

These five subroutines will allow the user to determine a ST model

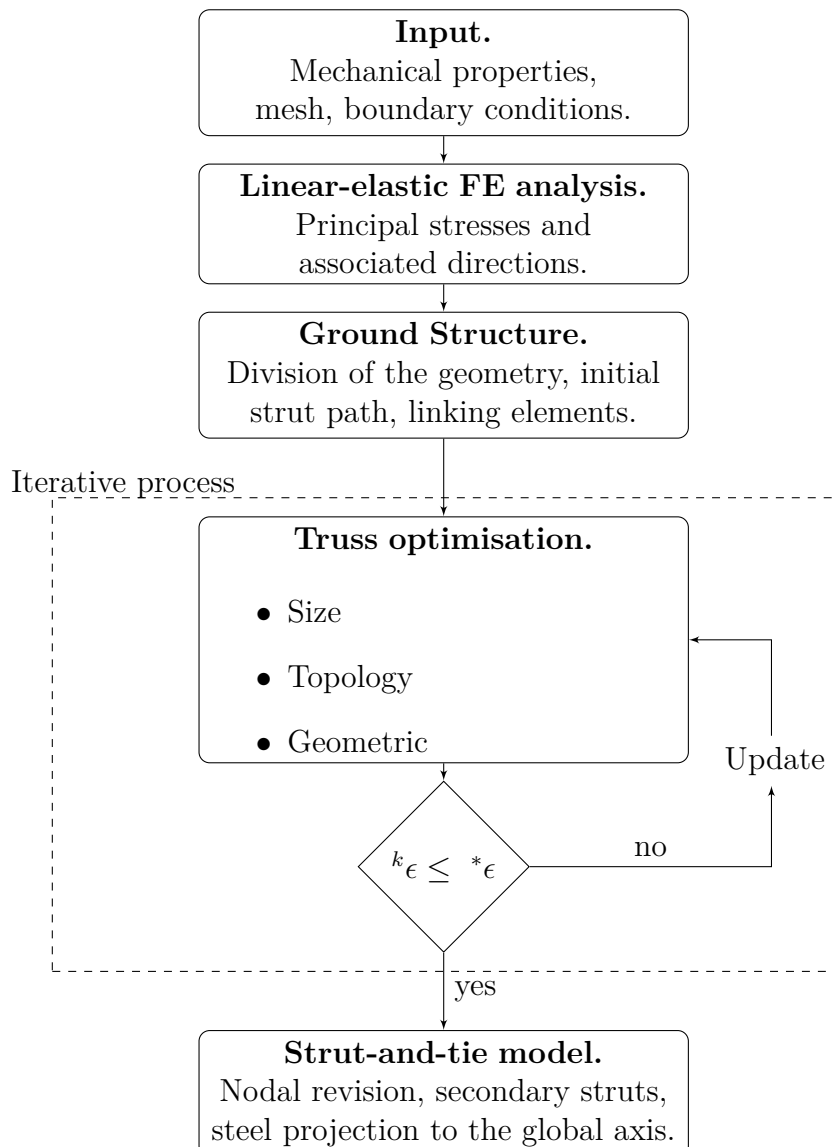


Figure 3.1: Flowchart showing proposed the design procedure

3.1.1 Input

The input required for the algorithm depends on whether an initial FE analysis is needed or, the user already posses the results of an analysis carried out on a specialised software.

For the case where the initial finite element analysis is desired to be treated by the algorithm, the input data matches the requirements of any other FE solver: the geometry depicted by a nodal list and a connectivity matrix, the list of materials, and the boundary conditions. On the other hand, the algorithm can post-treat the results obtained by software such as ANSYS and Code-Aster. For this case, additionally to the previous lists, the input must contain the resultant principal stresses computed at the element's Gauss points.

The subroutine reads the available information and stocks it as matrices and vectors in Matlab environment and inside a file where further results are also saved.

3.1.2 Linear-elastic FE analysis

If the data does not include the result lists, the initial analysis has to be performed. The assembling of the global stiffness matrix K , and the solution of the FE model are performed considering simple 2D-4-node quadrangular model for those elements defined by 3 or 4 nodes and 3D-8-node brick type for those elements defined by up to 8 nodes. If different elements are desired, the option to read existent results instead of perform the initial analysis should be chosen.

The FE analysis is performed within a classic fashion like routine where the global stiffness matrix is iteratively assembled from the individual element stiffness matrices according to the connectivity matrix.

```

function [U]=assem_solve (DoF,Geom,Mat)
%%%%%%%%%%%%%%%%%%%%%%%%%%%%%%%%%%%%%%%%%%%%%%%%%%%%%%%%%%%%%%%%%%%%%%%%%%%%%%
%% Inner variables
% K_global .- Global stiffness matrix.
%   k_m .- Element stiffness matrix.
%   DoF .- Degrees of freedom vector [True False].
%   P .- Load vector.
%   U .- Global displacement vector.
%   Geom .- Cell containing nodal list and connectivity matrix
%   Mat .- Material properties
%% Required subroutines
% elem_stiff .- Computes the element stiffness matrix
%%%%%%%%%%%%%%%%%%%%%%%%%%%%%%%%%%%%%%%%%%%%%%%%%%%%%%%%%%%%%%%%%%%%%%%%%%%%%%
K_global = zeros(num(DoF)); %Prelocating global stiffness matrix
U = zeros(num(DoF),1); %Prelocating displacement vector
for m = 1:num_of_elem
    k_m = elem_stiff(Mat,Geom,m); %Element stiffness matrix
    K_global=K_global+k_m ;
end; %Assembling the matrix
U(DoF==True)=P(DoF==True)/K(DoF==True,DoF==True); %Solve for U

```

Listing 3.1: Stiffness matrix assemble

The results of an initial linear elastic finite element model constitute the base of the proposed algorithm.

3.1.3 Ground structure

Knowing that the initial number, position and length of the elements are characteristics of the ground structure that directly affects the computing effort and the final results, the first concern was to be able to create a base structure with enough elements to provide a reasonable system but avoiding a prohibitive large number of elements. Another important difficulty was related with the length and the position of the elements. To overcome this, the ground structure is proposed according to the results on a linear elastic finite element analysis. These results such as the direction field and stress levels are used as predictors of the characteristics of the final model.

The first step of the algorithm is to delimit zones of the structure where plausible elements can be placed. The division of the geometry has been established under two main principles: 1) the resultant sub-domains must not contain potential structural nodes, and

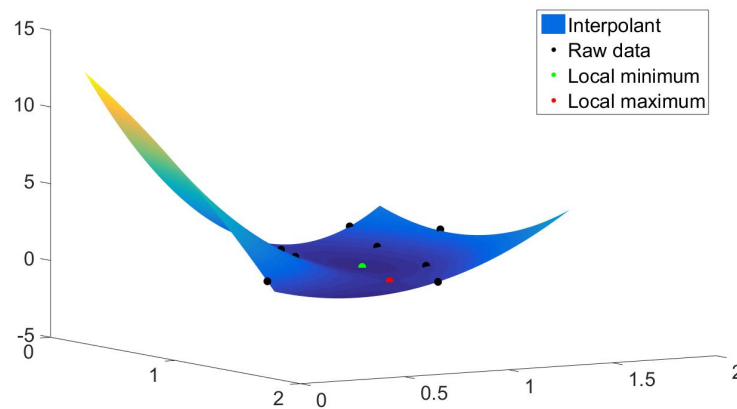


Figure 3.2: Polynomial interpolation over 8 random XYZ triplets (second degree function of two variables of the form $f(x, y) = \alpha_1 x_i^2 + \alpha_2 x_i y_i + \alpha_3 y_i^2 + \alpha_4 x_i + \alpha_5 y_i + \alpha_6$).

2) the principal direction of the minor stresses at each sub-domain must be developed along a remarkable preponderant direction.

3.1.3.1 Local maximum of stress fields

Based on existent recommendations (principally found in [Schlaich et al., 1987, ACI-318, 2008, Davidovici et al., 2013, El-Metwally and Chen, 2017]) and some previous results found in documents such [Wahlgren and Bailleul, 2016, Shah et al., 2011], the nodes of the ST model are initially placed on the stress concentrations of the FE model. Among the different methods to compute the local maxima and minima two options are available in the algorithm:

- **Differentiation via interpolation.** After having constructed an interpolating polynomial from the data, an approximation of the derivative at any point can be obtained by a direct differentiation of the interpolant.

For the differentiation via interpolation, the first stage is to construct an interpolating polynomial from the data. An approximation of the derivative at any point can be then obtained by a direct differentiation of the interpolant.

Based on a formula presented by Saniee [Saniee, 2008], the differentiation proceeds through the construction of a polynomial function approximately describing the stress field along axis X and Y . The locals are the computed through the Hessian matrix.

Besides its questionable application over stress fields of real structures, its principal limitation lies in the computational effort required to construct the polynomial. Being n the quantity of triplets on the available data, the procedure requires the solution of $n + 1$ square matrices of nxn elements.

- **Grid based numerical differentiation.** After having performed a linear interpolation of the data to approximate the values at the intersections of the grid, the local maxima/minima are searched over parallel planes along the and axis through a numerical algorithm.

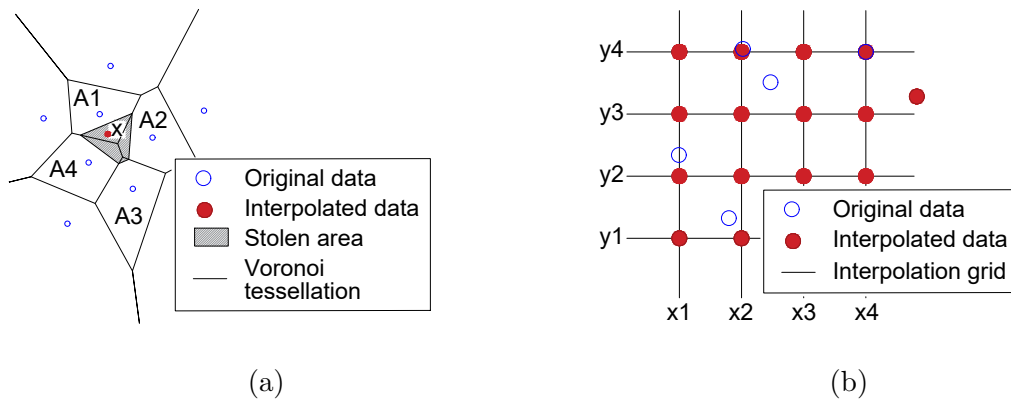


Figure 3.3: Grid based numerical differentiation: (a) Natural neighbours [Boissonnat and Cazals, 2000] and, (b) Grid interpolated data

Intuitively, the directional derivative can be computed by selecting one variable and numerically differentiate the function keeping the other variables fixed. Selecting a list of fixed values for one variable implies that the differentiation neglects those results that are not strictly placed along the selected value which leads to two possibilities: **1)** the differentiation is done along all the values of the variables or **2)** just some values are selected. To avoid this, the numerical differentiation is done over a grid of data obtained by a natural neighbour interpolation [Sibson, 1981] of the form:

$$\sigma(x, y, z) = \sum_{i=1}^n w_i \sigma(x_i, y_i, z_i) \quad (3.1)$$

where $\sigma(x, y, z)$ is the estimate value of the stress at coordinates (x, y, z) , $\sigma(x_i, y_i, z_i)$ and w_i are the data values and their associated weights located at (x_i, y_i, z_i) . The weights are calculated superposing two Voronoi tessellations (refer to section 3.1.3.2), one of only the data coordinates and another one including both the data and the interpolation coordinates, and computing the "stolen" area at each surrounding zone [Ledoux and Gold, 2005].

After having performed the interpolation of the data to approximate the values at the intersections of the grid, the local maximum/minimum are searched over parallel planes along the and axis through a numerical partial derivatives.

The partial derivatives are sensed to give the slope of some function f at any point (a, b) in the directions parallel to the coordinate axes. From the definition of partial derivatives (equations 3.2) given by [Levy, 2010], it can be appreciated that the partial derivative $\partial f / \partial x$ is obtained by fixing the value of y to a constant b and differentiating the function $f(x, b)$ at $x = a$. In the same manner, the partial derivative with respect to y is obtained by fixing $x = a$ and differentiating the function $f(a, y)$ at $y = b$.

$$\frac{\partial f}{\partial x}(a, b) = \lim_{h \rightarrow 0} \frac{f(a + h, b) - f(a, b)}{h} \quad (3.2a)$$

$$\frac{\partial f}{\partial y}(a, b) = \lim_{h \rightarrow 0} \frac{f(a, b + h) - f(a, b)}{h} \quad (3.2b)$$

3.1.3.2 Division of the geometry

Within a manual application of the STM, the structural engineer must decide the length, inclination and position of each structural element. With the same spirit, here, the algorithm is intended to identify potential zones of development of a single compressive element (strut). To this purpose, a division of the geometry was proposed under few premises:

1. The resultant division must be influenced by the coordinates of potential structural nodes (local maximum of stress fields).
2. Each subdivision must be big enough to be able to contain one straight element within its limits.
3. At the same time, it must be small enough to present a clearly preponderant direction of σ_{III} (considering only the results of the initial FE model located at the interior of each division).

The Voronoi diagram, also known as Voronoi tessellation, is the partition of an space into a finite number of regions based on the distance between points in a specific subset of known data; the "seeds" x_i ($i = 1, \dots, n$). Each seed, x_i , is surrounded by a convex polygon $V(x_i)$ delimiting a Voronoi cell, which is defined as a set of points x that are closer to x_i than to any other seed x_j ($j \neq i$) (see equation 3.3).

$$V(x_i) = \{x \in \sigma : d(x, x_i) < d(x, x_j), \forall j \neq i\} \quad (3.3)$$

where, for this case, $d(x_1, x_2)$ represents the Euclidian distance measured between point x_1 and x_2 .

The Voronoi cells corresponding to the seeds at the boundary of the convex hull of all the sites are infinite. However, for the purpose of this work, only the parts of the Voronoi within the analysed structure (feasible domain), $\Omega_{feasible}$, are needed. Hence, the Voronoi diagram with respect to the given domain can be defined as the intersection of the Voronoi diagram and the domain, Ω , referred as of the clipped Voronoi diagram [Park et al., 2006].

$$V(x_i)_{clipped} = V(x_i) \cap \Omega_{feasible} \quad (3.4)$$

Computing the clipped Voronoi diagram in a convex domain requires to compute the intersection of each Voronoi cell and $\Omega_{feasible}$.

An important number of algorithms for computing clipped Voronoi divisions are available. For this project, the Multi-Parametric Toolbox [Kvasnica et al., 2004] was used and nested into Matlab functions in order to achieve the desired diagrams on the geometry of the analysed structure.

Based on the clipped Voronoi tessellation, the division of the geometry is performed. Considering the coordinates of the local maxima and minima of the principal stresses as the seeds, the division allows to delimit zones where the direction field of the principal minor stress of the contained nodes tends to present a preponderant unique direction. In order to make sure that these seeds will be placed at the limits of a region and not

inside a sub-domain, a small disturbance is introduced over the position of the seeds. This disturbance is included by replacing the original selected seeds by two new seeds result from the intersection of a circle, of an arbitrary infinitesimal radius and centred at the original seed's coordinates, with the boundaries of the geometry.

3.1.3.3 Initial struts' direction assessment

Previous step is intended to directly delimit the length and distribution of the compressive elements of the skeletal structure. In this work, the inclination of each individual element is assumed parallel to the principal stress directions and their values are obtained from them (this hypothesis is classical in the development of STM).

Considering that the struts shall approach the distribution and direction of the minor principal elastic stress, θ_{III} , the inclination of each strut, $\theta_{s,i}$, is approximated taking into account a weighted contribution of the principal direction, $\theta_{III,j}$, of the finite elements included in the current Voronoi cell.

The chosen approximation, equation 3.9, is based on a Locally Weighted Least Square Regression (loess). The estimate of θ_s at the centred of the cell, $C(XYZ)$, uses the n observations whose distance d is closest to C . That is, starting from the previously defined neighbourhood ($V_{x,i}$), each included point is weighted according to its distance from C ; points close to C have large weight, and points far from C have small weight [Cleveland and Devlin, 1988].

$$\theta_s = f(\theta_{III,j}) + \epsilon, \quad j \in V(x_i) \quad (3.5)$$

$$\text{Fit } A \text{ to minimise: } \epsilon = \sum_{j=1}^1 w_i (\theta_s(X, Y) - A^T \theta_{III,j})^2 \quad (3.6)$$

$$\{a \ b\}^T = (\{P\}^T [W] \{P\})^{-1} (\{P\}^T [W] [\theta_{III,j}]), \quad j \in V_{x,i} \quad (3.7)$$

Where w_i is the local weight assigned to the data x_i , $[W]$ is the diagonal weight matrix, $\{P\}$ is the data set vector containing the explanatory variables and $\{a \ b\}^T$ corresponds to the vector containing the coefficients of the regression.

For this case, the weight is given by a parabolic kernel function (equations 3.8). This function is intended to reduce (or eliminate) the reliance on the values laying at boundaries of the cells; principally, those nodal results near the mechanic raisers that could bring "noise" to the regression.

$$W_i = W_{X,i} W_{Y,i} W_{Z,i} \quad (3.8a)$$

$$W_{X,i} = 1 - 3 \left(\frac{d(x_j, C)_X}{l_X} \right)^2 - 2 \left| \frac{d(x_j, C)_X}{l_X} \right|^3 \quad (3.8b)$$

$$W_{Y,i} = 1 - 3 \left(\frac{d(x_j, C)_Y}{l_Y} \right)^2 - 2 \left| \frac{d(x_j, C)_Y}{l_Y} \right|^3 \quad (3.8c)$$

$$W_{Z,i} = 1 - 3 \left(\frac{d(x_j, C)_Z}{l_Z} \right)^2 - 2 \left| \frac{d(x_j, C)_Z}{l_Z} \right|^3 \quad (3.8d)$$

Additionally to the kernel function, the *loess* also requires a specification of neighbourhood size. The chosen neighbourhoods, Ω_i , are selected as cuboids whose maximum interior diagonal connects the minimum and the maximum of the coordinates of the current cell.

Placing the kernel function over a cuboid zone of dimensions l_X , l_Y and l_Z (sides measured along X , Y and Z respectively) and centred at the coordinates (C_X , C_Y and C_Z) the local weight of the data subsets within the zone Ω_i is given, according to their spatial positions on the geometry (X , Y and Z) by the product of the parabolic distributions.

$$\theta_{s,i} = a(\theta_{III}) + b, \quad j \in V(x_i) \quad (3.9)$$

For this approximation to be implemented there are some conditions that the data must satisfy:

- **Cuboid-base sub-domains.** Since the base-shape of the chosen kernel function presents a cuboid projection, this function is ideally applied on this type of zones.
- **Singularities located at the boundaries of the regression zones.** Regarding the kernel function as a filter, the aim of this filter is to reduce the weight that the singularities could have on the regression, which can be only done if those points are at the boundaries.
- **Small angular dispersion coefficient.** A small angular dispersion allows applying the current model of regression over the selected angular data. This aspect results advantageous inasmuch as is not necessary to apply a sort of angular regression that could imply a heavy iterative procedure [Fisher, 1995].

Within this step, the subroutine implemented to approach the initial strut inclination which is computed based on the direction of the major principal stresses of the elements found in the subdomain through the *loes*. This approach is adopted for subdomains presenting a small angular dispersion and a significant quantity of available data. The initial strut at subdomains presenting either a large angular dispersion or a small quantity of data (less than 10) is then associated to the mean value of the circular directions $\bar{\Theta}$.

$$\bar{\Theta} = \arctan 2 \left(\sum_{j=1}^n \sin \Theta_j, \sum_{j=1}^n \cos \Theta_j \right) \quad (3.10)$$

where Θ_j represents the angle of the principal direction of the n elements found inside the subdomain.

3.1.3.4 Branch-like generation of struts

Last sub-routines propose and distribute the struts within the structure but the connection between the elements is not done yet.

Once the inclination of the struts have been computed at each zone, Ω_i , an iterative "branch-like" algorithm is implemented for the generation of the struts.

Starting from the coordinates of the seeds that correspond to the local maximum stress, the algorithm takes an initial node, N_i , and projects a straight line, following the slope

calculated for the contouring zone. The projected line is cut at the limits of the current zone generating an ending node N_f . The next iteration takes the previous final node as the new initial one, and proceeds in the same manner to calculate another final node. The procedure continues for all the seeds until the boundaries of the geometry have been reached by the generated “branches”. Hence, the strut generation algorithm produces branches that start at the coordinates of concentrated loads and compressive stress concentrations, and diffuses throughout design domain. Even though two or more branches could pass through common zones, until this step, these branches do not necessarily share common nodes. Therefore, a nodal merging procedure has been implemented at this state.

3.1.3.5 Linking elements

Similarly to the case of struts, the ties are expected to approximate the distribution of the major principal elastic stress σ_I . Besides, these elements should also be adapted to the already existing strut path.

Starting from the premise that the punctual concentration of major stress provides a reliable index of the position of the ST nodes in pure traction, the distribution of the ties is obtained by considering each concentration point as a birth node which is attached by a straight line to every existent node contained by the closest local minima.

Considering all possible connections may produce a structure with a high degree of potential trusses hence, a reduction of the quantity of potential elements is a desirable step before the optimisation.

Starting from the premise that the principal struts have been already created during the branch-like procedure, the linking elements will produce principally potential traction elements. A simple way to reduce the quantity of elements on the ground structure has been found to apply a restriction on the "linking" phase: an elements is created between two existent nodes if the resultant element is inside the the feasible region but outside the zones delimited by the α -shape defined by the local minima of σ_I .

[Edelsbrunner et al., 1983] introduced α -shapes as the shape of a point set at a given level of detail, α . With this definition and assuming that any loading system will generate at least one zone where the behaviour is dominated by the minor principal stress over the major one. The algorithm constructs a zone bounded by straight line segments defined between 2 coordinates of local minimum. The constructed zone does not require to be connected, but points that are close together are in the same component of the shape. Conversely, a component of the shape cannot contain a large region void of points [Van Kreveld et al., 2011].

3.1.4 Optimisation procedure

The three first sub-routines depicted in figure 3.1 are meant to propose the ground structure. The proposed structure is characterised by presenting the structural nodes at the coordinates (or nearby) the coordinates where the ST nodes are expected to be. At this point, the quantity of potential elements do not allow to clearly identify a feasible ST model. Furthermore, the straight elements lack of fundamental characteristics such as the area.

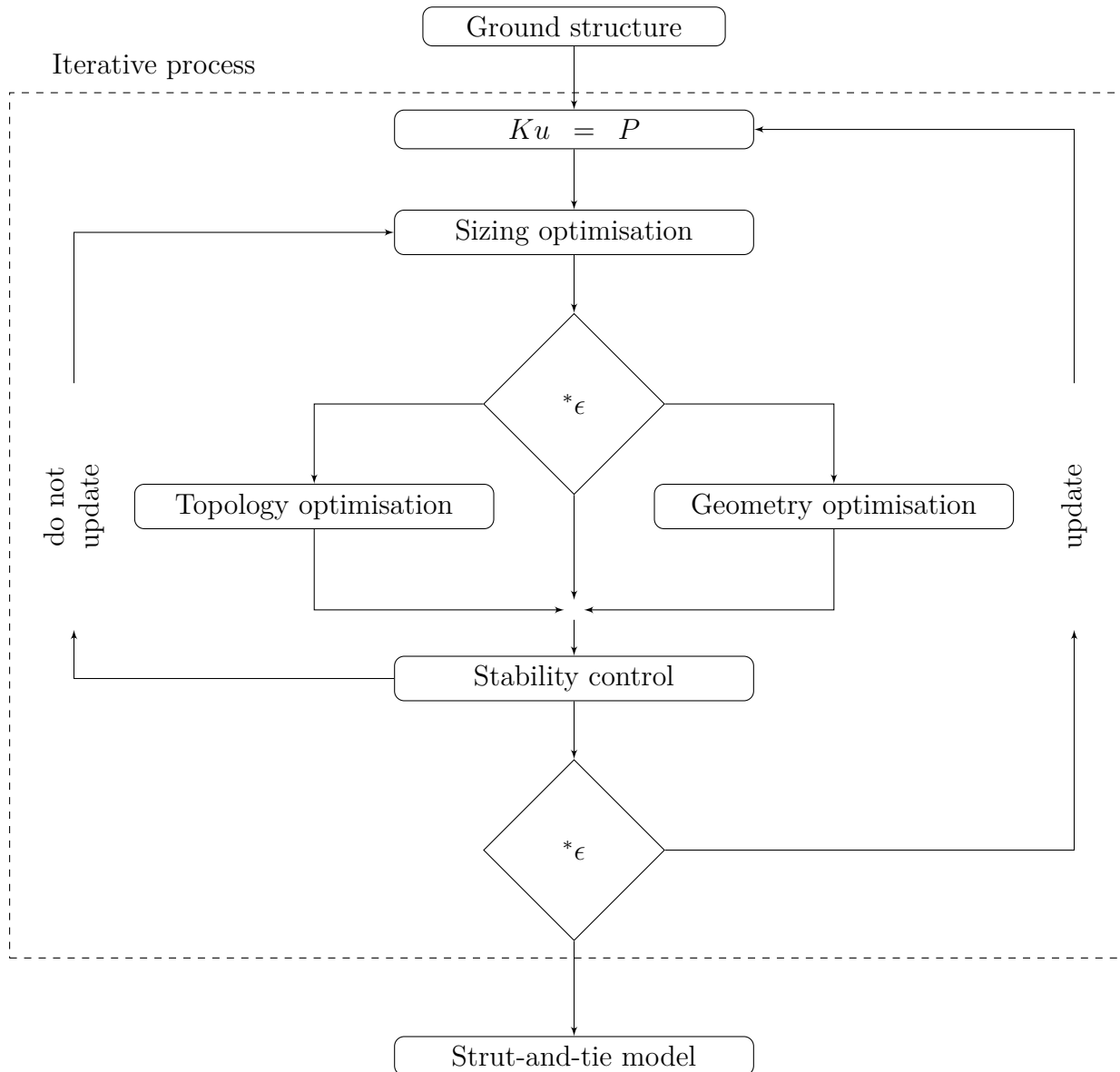


Figure 3.4: Flowchart of the proposed truss optimisation

In order to decrease highlight a ST model from the ground structure it was implemented a optimisation scheme able to reduce the quantity of elements, to choose the material of each member (steel or concrete) and most important, to assess cross sections.

3.1.4.1 Initialisation

An initial configuration built by a total of m elements can be now stated based on the strut path and the tie distribution.

At the very early stages of the Thesis, the initial cross section of the elements was intended to be based on an energetic equivalence between the initial FE model and the ground structure. The equivalence was made by computing the strain energy associated to the compressive stresses only, $\Psi_{EF}^{\{-\}}$, within the FE model and calibrate it with the energy of the deformation of the proposed struts $\sum \Psi_S^{\{-\}}$.

considering that for a general body the strain energy to a compressive state of stress can be computed as:

$$\Psi^{\{-\}} = \frac{A}{2} \left[\lambda \left(\epsilon_I^{\{-\}} + \epsilon_{II}^{\{-\}} \right)^2 + 2\mu \left((\epsilon_I^{\{-\}})^2 + (\epsilon_{II}^{\{-\}})^2 \right) \right] \quad (3.11)$$

Analogously, in the case of a straight element undergoing an axial compressive force, the strain energy can be easily expressed in terms of the force, F , cross section, a_i , length, ℓ , strain, ϵ , and its Young's modulus, E as:

$$\Psi^{\{-\}} = \frac{1}{2} E (\epsilon^{\{-\}})^2 \quad (3.12)$$

Considering that the struts are proposed and delimited within an individual Voronoi zone, Ω_i , the equilibrium is made individually for each strut; the strain energy from the FE considers only the nodal results from the n nodes contained inside the limits of the current zone leading to:

$$\sum_{j=1}^n \frac{A}{2} \left[\lambda \left(\epsilon_I^{\{-\}} + \epsilon_{II}^{\{-\}} \right)^2 + 2\mu \left((\epsilon_I^{\{-\}})^2 + (\epsilon_{II}^{\{-\}})^2 \right) \right]_{\Omega_j} = \frac{1}{2} E a \ell (\epsilon^{\{-\}})_{S, \Omega_j}^2 \quad (3.13)$$

So far, the axial strain of the struts $\epsilon_{S, \Omega_j}^{\{-\}}$ is unknown but, looking for the compatibility of displacements between the FE model and the ST one, the strain of each strut is estimated as the nodal displacement between the 2 nodes closest to the strut edges divided by their initial Euclidean distance leaving the cross section, a , as the only unknown.

$$a = \frac{\sum_{j=1}^n \frac{A}{2} \left[\lambda \left(\epsilon_I^{\{-\}} + \epsilon_{II}^{\{-\}} \right)^2 + 2\mu \left((\epsilon_I^{\{-\}})^2 + (\epsilon_{II}^{\{-\}})^2 \right) \right]_{\Omega_j}}{E \ell (\epsilon^{\{-\}})_{S, \Omega_j}^2} \quad (3.14)$$

This attempt to predict the cross section of the struts was rapidly discarded for two main reasons: 1) the operations needed involved three-dimensional nodal research which requires high computational efforts and 2) the results were, for most of the cases, too far from the final result which was translated into the need of more iterations or even the non-convergence.

For instance, the guess value of cross sections is proposed as a constant vector of value $a_{initial}$. Considering the fact that the selection of the initial cross sections may affect the performance, or even the solution of the optimisation, $a_{initial}$ may consider a realistic steel distribution. The user should chose a value that produce elements that individually fit into the boundaries of the geometry.

The initial model considers that all elements are made out of steel. This consideration is only made once. During the iterative process, the selection of the material is done based on the sign of the force obtained at previous iterations. The material models correspond to linear-elastic hypothesis whose behaviour law is assumed with Young's moduli, E_i , and Poisson's ratio, ν , assigned according to the idealised selected materials.

3.1.4.2 Optimisation scheme

At this point, the problem has been reduced to a quite simple topology optimisation of a truss model with a relatively low number of potential structural elements where the objective function is to reduce the volume of the sum of the elements $V = \sum_{i=1}^m a_i \ell_i$. The treatment of the problem is proposed to be done through a tree-part truss optimisation:

- **Sizing problem.** Cross-section area of each element is applied as a design variable with a non-zero lower bound condition, [Li, 1990].

Taking into account that, in general, the elements withstanding compression possess a small slenderness ratio, the effects of buckling are neglected. Thus, the previously presented FSD (fully stressed design) can be simplified. At each iteration, the equilibrium is verified through the relation $Ku = P$, and the cross sections are replaced with values according to the axial stress ratio.

The optimised cross sections are bounded by a maxima and a minima values. While the maximum value commonly depends on available cross sections, the choice of the minimum value does not only rely on manufacturing limitations. As said before, due to the nature of the stiffness matrix, the minimum cross section cannot attain a zero value but neither an arbitrary "small" one. Depending on the solving procedure and the available numerical precision, the difference between the smallest and the largest root of a matrix may be used to determine its singularity. Matrices with large condition numbers are difficult to invert accurately [Greene, 2003].

$$\text{Condition number} = \kappa(A) = \left(\frac{\text{maximum root}}{\text{minimum root}} \right)^{1/2} \quad (3.15)$$

Although there is not a specific limit on the condition number to determine the singularity of a matrix [Pyzara et al., 2011], for practical purposes some restrictions were imposed. The minimum value that a cross section may take at the k -th iteration is equal to the value of the largest cross section, computed at iteration $k-1$ divided by 10^6 . This value has found to be significantly small to represent a neglectable element but to be sufficiently large to avoid numerical problems providing an inexpensive damping to the inversion.

- **Topology optimisation.** A dichotomous optimisation is applied to the elements included in the percentile with the less important cross section. The elements included in this percentile that are not required to maintain equilibrium for that particular geometry and loaded condition are eliminated, [Kirsch, 1989].

The sizing optimisation allows the selection of a group of elements presenting active constraints; the elements whose cross-section is equal to the minimum permitted. The basic combinatorial problem of topology design is applied over this group of elements. Similarly to the case of a lower zero bound, removing all the elements with active constraints may imply that the stiffness matrix is not necessarily positive definite and the state of displacement vector U cannot be computed accurately.

To overcome this difficulty, the solution procedure is proposed in two phases: 1) the first phase assembles the stiffness matrix with all the elements whose cross-section

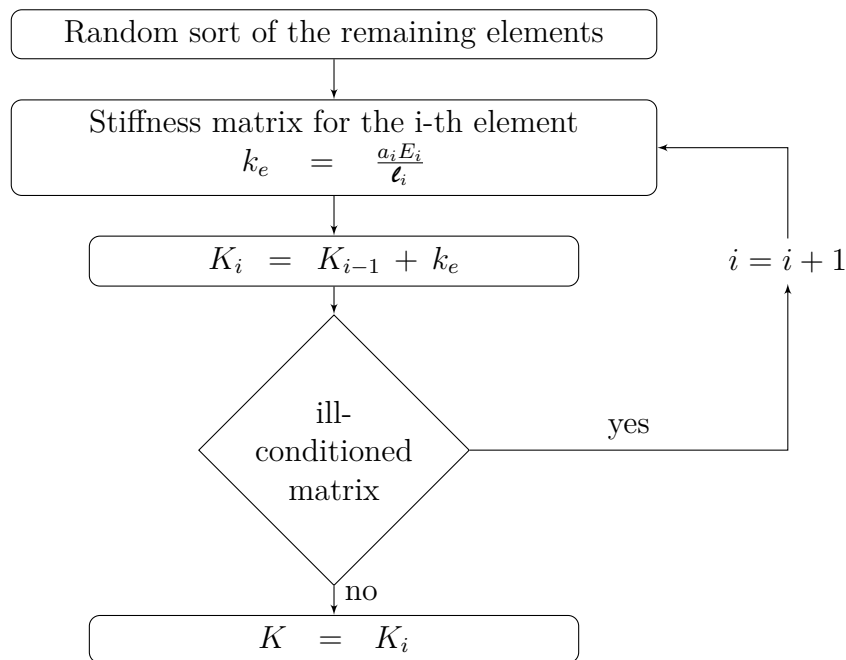


Figure 3.5: Element suppression flowchart

is superior to the minimum, and 2) the second phase randomly adds the rest of the elements verifying that the stability of the stiffness matrix. The second phase continues until the algorithm determines that no ill-condition is presented in the problem and eliminates the reminder elements . The process is achieved through the modification to the assembling subroutine (see flowchart 3.5) by adding a logical operation that verifies the section of the current element and the conditioning of the matrix once the current element has been added.

Even though suppressing all the elements presenting active constraints have little repercussion on the conditioning of a stiffness matrix associated to a fully populated structure, for a problem with sparsity and bandedness, erasing elements becomes a trivial task. The presented subroutine guaranties the invertibility of the matrix and erases non-trivial elements reducing the quantity of elements in the final structure and also reducing the need of computational effort for further iterations.

- **Geometric optimisation.** As stated before and according to [Bendsøe et al., 1994], the resultant topologies can be very sensitive to the layout of nodal points. This makes it natural to consider an extension of the ground structure approach and to include the optimisation of the nodal point location for a given number and connectivity of nodal points.

The optimisation of the nodal coordinates is based on the feasible direction method. The algorithm is intended to find a step and a direction, within the limits of the original structure, and updating the vector x of nodal coordinates.

In general, the displacement of the nodal coordinates leads to two complications:

- nodal coordinates found outside the geometry the considered geometry
- bars with infinitesimal lengths or "melting nodes"

To overcome the first complication logical restrictions were imposed. The algorithm limits the final position of the nodes accepting the optimised coordinates if and only if they are included within the geometry. For cases where the optimum coordinates are found outside the geometry, the algorithm retains the computed direction α and scales the step S to fit the structure. This allows keeping a classic formulation for a geometric optimisation and, at the same time, it allows to directly include spatial restrictions.

The second complication is linked with bar elements whose length is or approaches to zero thus, their stiffness $K = Ea/\ell$ approaches to the, computationally speaking, infinite or is simply undefined.

According to [Achtziger, 2007], melting nodes can be frequently observed; in some zones, the nodes tend to approach to the supports avoiding long elements with important stresses. Nevertheless, the melting nodes can cause ill-conditioning, their presence can also be useful to control the number of elements in the structure.

From a practical point of view, one solution to threat this problem is to define a minimum for the length of the elements. Another solution to work-around this problem is to formally exclude the melting nodes from the structure.

For this work an alternative process was stated. An element presenting both, an infinite stiffness and an infinitesimal length suggest that the initial and ending node of such element may be merged into one single node. According to a distance specified by the user or by the used precision (h), a subroutine selects the melting nodes and evaluates if they can or cannot be merged. If the geometry considering the merge leads to a stable structure, the suppression of the element proceeds and the model is updated. Alternately, if the merge leads to an unstable structure at the current iteration, the length of the element is increased.

3.1.5 Termination

The termination of the algorithm can occur in two different manners:

1. the current error, ${}^k\epsilon$ attains the prescribed threshold ϵ_i
2. the number of iterations has reached the prescribed maximum

3.1.6 Acquiring the strut-and-tie model and reinforcement

At this point, the cross sections and the associated material of each element are known. A skeletal structure has already been defined from the reduction of the initial ground structure but this reduced structure sometimes possesses "repeated" elements; elements that share both initial and final nodes one another. Even if those elements do not affect the model, their existence may produce interpretation errors as they represent different bodies occupying the same space. This is simply avoided by searching those groups of elements sharing nodes and, if it is the case, merge each group into one single element whose area equals the sum of the group. This step provides a skeletal structure with a reduced quantity of elements that correspond to the specifications for a ST model prescribed by the Eurocode.

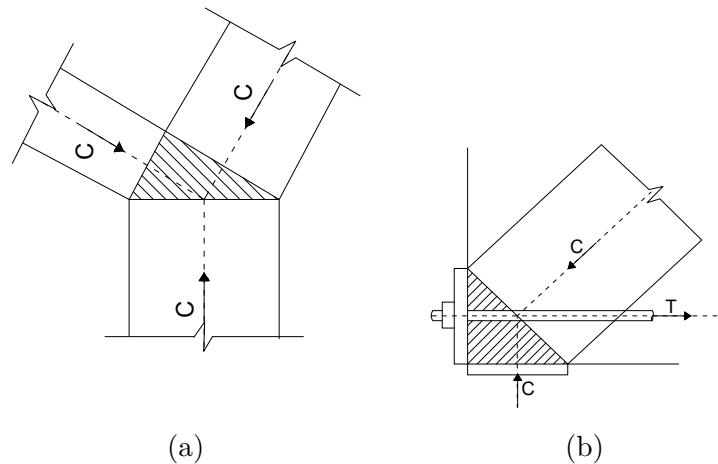


Figure 3.6: Hydrostatic nodes: (a) CCC node geometry and (b) Tension force anchored by a plate

3.1.6.1 Nodal revision

The nodal revision is done through a subroutine that isolates each node and geometrically evaluates if it is able to resist the arriving forces. Considering that all joints behave under hydrostatic hypothesis, the dimension of each node is approached according to the next criteria:

- Tension ties are anchored behind the node and considered struts.
- The area of the converted strut is equal to the area of concrete surrounding the tension tie reinforcement and having the same centroid.

In other words, the tensile force induced by the ties is replaced by a compressive force in the opposite face of the node. The resultant force is considered to act over a surface computed under the same principle as the elements in compression: $a = F/\phi\sigma$. Considering that all the elements are conceived as prismatic geometries whose cross section was computed considering the concrete's allowable compressive strength, the resultant nodes present are subjected to the same stress level at all their faces.

Based on the geometry obtained, a further verification of the bearing capacity of the nodes can be approximated through a linear elastic FE analysis. The principal stresses are compared to the concrete's allowable compressive strength using a Mohr-Coulomb failure criterion.

3.1.6.2 Reinforcement

Considering the distribution of the steel reinforcement to follow the ties could result, from a constructability point of view, in an impractical solution. In addition to present the skeletal model, the algorithm proposes a solution that projects the ties to the principal axis in order to obtain a more classical steel distribution.

A subproblem is stated for all considered ties where the oriented steel must replace the existent element in the following fashion:

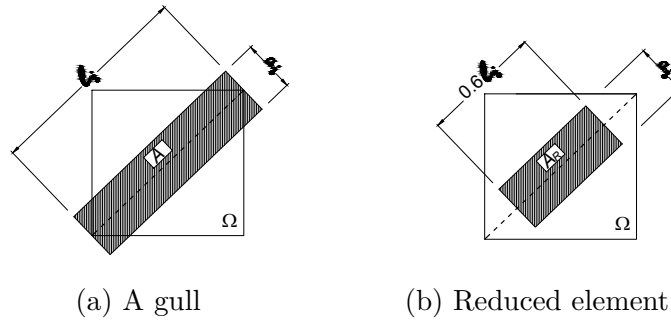


Figure 3.7: Schematic representation of element's length reduction and space verification

$$\text{minimise} \quad W(X) = a_x \ell_x + a_y \ell_y \quad (3.16)$$

$$\text{subject to: } a_x f_y \geq a_i f_y \cos \theta \quad (3.17a)$$

$$a_y f_y \geq a_i f_y \sin \theta \quad (3.17b)$$

where a_x and a_y are the total steel areas needed along axis X and Y respectively; ℓ_x and ℓ_y are the geometrical projections of the tie's length over the reinforcement axis.

Equations 3.16 and 3.17 represent a simple optimisation problem that is solved within the same subroutine.

3.1.6.3 Cross section verification

The final verification is made on the dimensions of each element. At this step, the individual geometry of the final struts and ties, A , is contrasted with the hole geometry, Ω . In order to verify if the selected section fits the geometry, a Boolean operation is implemented:

$$(A_R \cup \Omega) == \Omega \quad (3.18)$$

if the precedent statement is not true, the analysed element overpasses the feasible section and an alert is printed

The nodes located at the geometric boundaries may be attached to elements that appear to be slightly outside the permitted geometry. In reality, boundary nodes are shifted towards the the interior of the geometry due to the concrete cover thickness.

Given that the algorithm does not consider a coverage thickness, most of the elements located near the boundaries could be wrongly considered "outside" the geometry. To overcome this, only a percentage of the total length of the element is matched with the feasible section, Ω .

3.1.7 Outputs

The principal outputs of the algorithm are those associated with the quantity of reinforcement, the position of the ties and nodes but also, the evolution of the optimisation process. The outputs can be divided into three different groups.

The first type, and maybe the most important, groups the results of each iteration of the geometry from the ground structure to the final ST model. Available on list format (.txt) and on Visualization Toolkit (VTK), the results include the geometry (nodal list and connectivity matrix); geometric characteristics of the elements such as length and cross section; and the force developed at each bar. Additionally, data related to the nodal revision is also included: geometry of the nodes and type of node (CCC, CTC, etc.). These results are saved at each iteration into file named OUTPUT.

The second type corresponds to results that are stocked only in form of text such as the reinforcement computed from the projection of the ties over the principal axis. If a FE analysis was performed, the initial mesh, global displacements, stresses and principal stresses can also be found in the OUTPUT file. Other intermediate results are also associated to this group. Useful data of the iterative process such as the convergence rate and the evolution of the total volume are also presented in text format.

The last type has been associated to results that are contained only in a non-interactive visual representation. This information such as the Voronoi division, the subdomains and the local maximum/minimum of the principal stresses is only depicted in a Joint Photographic Experts Group format (.jpeg). Although, the backup of this information was not considered important, the data can be directly read and saved from the Matlab's interface.

3.2 Illustrative example

In this section, the proposed approach is used to find the ST model of a first planar example inspired by the work of [Zhong et al., 2016]. For simplicity and for illustrative purposes the algorithm is applied over 3 idealised anchorage zones shown in figure 3.8.

Different cases have been chosen. Whether the geometry is the same for the three cases, the load location changes from one case to another as seen in figure 3.8. The length of the structures is $L = 6\text{m}$, the width is $b = 3\text{m}$ and the considered thickness of the elements is $t = 0.2\text{ m}$. The effect of the prestressing tendons has been simplified into one concentrated load $F = 5\text{ KN}$. The considered eccentricities, e , are 0, 0.75, and 1.35 meters. The three models are considered fixed at the opposite side of the force. Regarding the material, the Young's modulus, E , and the Poisson's ratio, ν , were specified according to a concrete of $f_{ck} = 35\text{MPa}$: $E = 34.5\text{GPa}$ and $\nu = 0.3$ (values extracted from the reference [Zhong et al., 2016]).

For this example, a simple linear-elastic finite element model was built and evaluated in software ANSYS (ANSYS[®] Academic Research Mechanical, Release 18.1). In the mentioned software, a planar representation of the structure was built up using a regular mesh consisting in 1800 4-node plane stress elements (figure 3.9a). The load was represented by a unique punctual force. Concerning the support, all degrees of freedom were suppressed for the nodes at the base zone. Plane stress hypothesis were considered during the procedure.

3.2.1 Input

After having imposed the respective boundary conditions and solving some results were extracted. The information extracted from ANSYS software was the nodal list (NLIST in

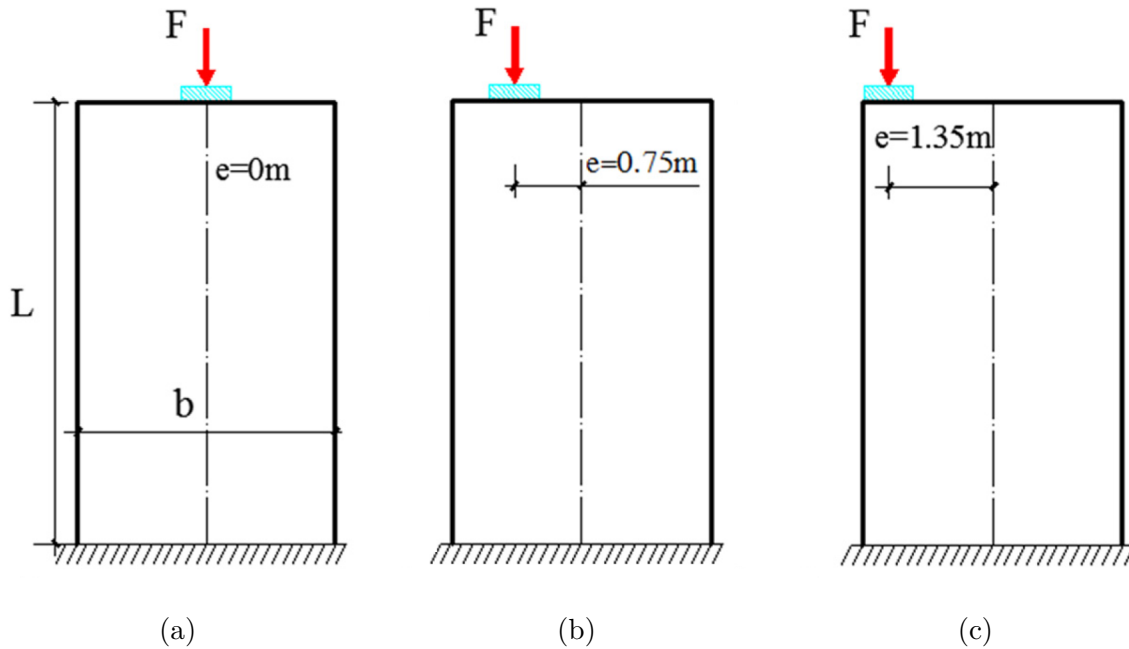


Figure 3.8: Anchorage zone models [Zhong et al., 2016]

ANSYS environment), the connectivity matrix (ELIST), the principal stresses computed at the Gauss points and also smoothed at the nodes (PRESOL and PRNSOL respectively) and the direction field of the principal stresses (PVSOL). This information, schematised in figures 3.9 and 3.10, is the starting point to develop the ground structure.

3.2.2 Ground structure

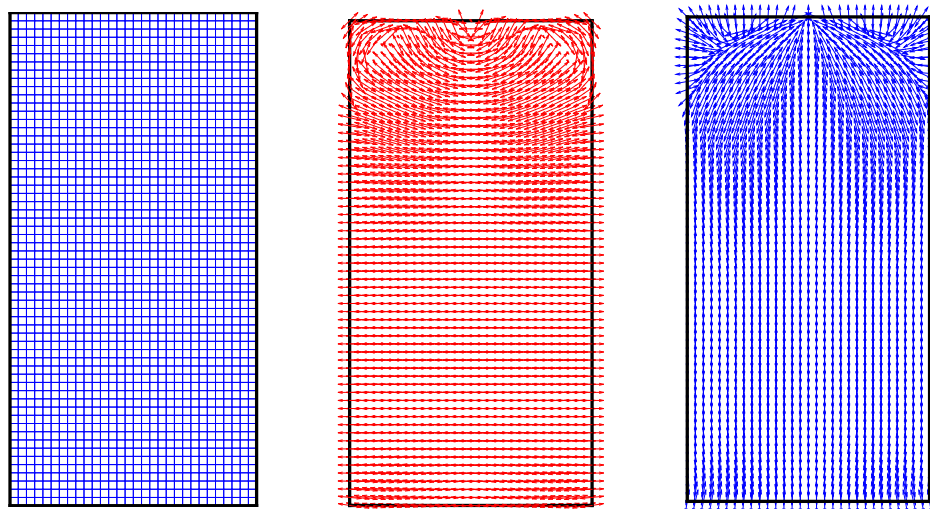
As mentioned in precedent paragraphs, the picks and the valleys presented in the principal stress fields are taken as indicators of the presence of the nodes of a suitable ST model. For the current test, the grid based numerical differentiation was preferred over the differentiation via interpolation and the results.

In figure 3.11 they are shown the principal stress fields all over the structural element developed under the specified boundary conditions and in subfigure 3.11a the peaks and valleys detected by the code are also shown.

Taking the local maximum and minimum as seeds for the Voronoi division and the geometry as the feasible region, the division is performed. For this case, 20 cells were found during the performed division (refer to subfigure 3.12a).

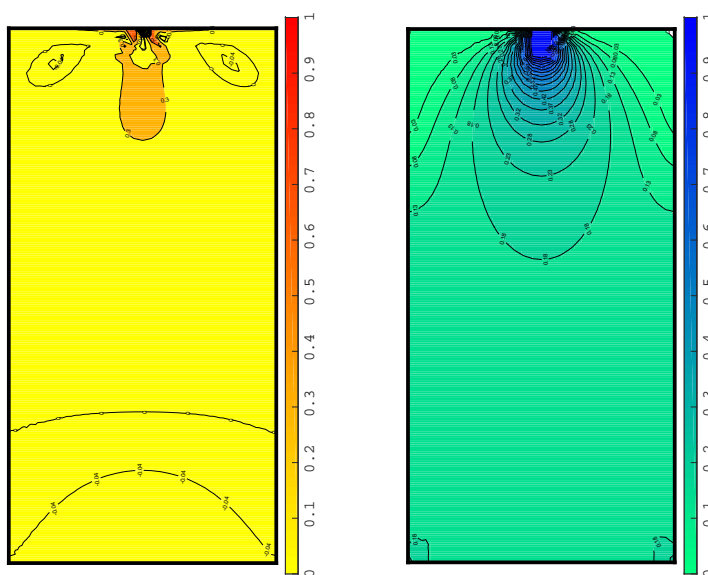
Following the presented methodology, the *loess* was applied at the centre of every cell. Considering the principal directions of the all the elements found in the cell, the regression was applied and the results are schematised in figure 3.12b.

The initial strut path (subfigure 3.11d) was achieved through the sub routine described in the previous chapter. An initial node is selected (node containing a maximum of σ_{III}) and a straight line is developed until finding the limits of a cell).



(a) Mesh (b) σ_I direction field (c) σ_{III} direction field

Figure 3.9: Schematic representation of the needed: mesh and principal stress direction fields



(a) Normed σ_I contours (b) Normed σ_{III} contours

Figure 3.10: Schematic representation of the needed data: principal stress fields

3.2.3 Truss optimisation

Figure 3.4 depicts the flowchart of the implanted optimisation procedure. The algorithm was conceived in such a way that the application of the sizing optimisation is mandatory

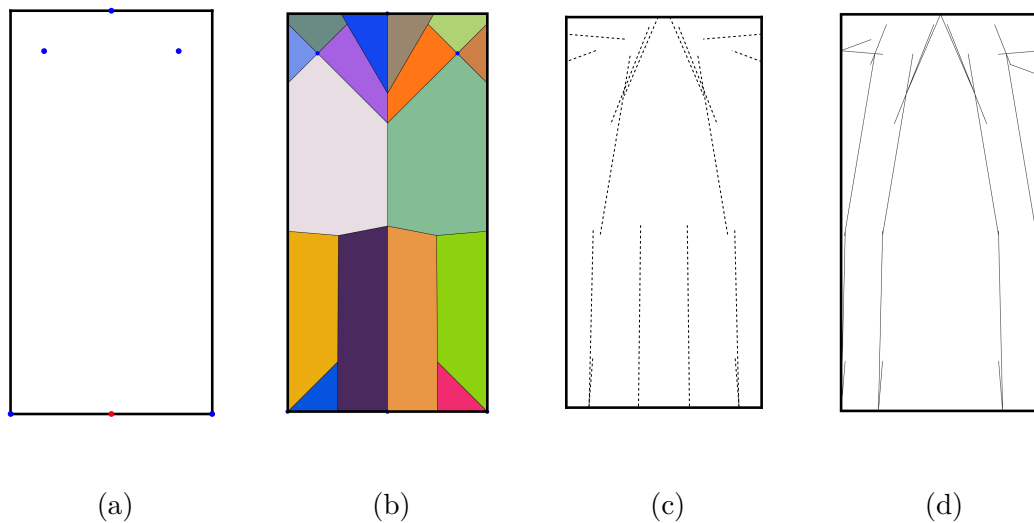


Figure 3.11: Strut path generation: (a) Computed Voronoi seeds, (b) Clipped Voronoi division, (c) Associated direction strut direction and (d) Initial strut path

while the application of topology and geometry optimisation is optional. In other words, the algorithm gives the possibility to the user to apply a simply sizing optimisation or mixed schemes; sizing-topology, sizing-geometry, or sizing-topology-geometric.

Figure 3.13 shows the results obtained through the application of 2 mixed schemes: sizing-topology and sizing-topology-geometric. The principal difference between the results obtained by the two different mixed schemes lies in the quantity of elements conforming the final Strut-and-Tie model. More subtle differences are found in the nodal coordinates. A mean distance of 5.8cm was found in the position of the nodes from a model to the other.

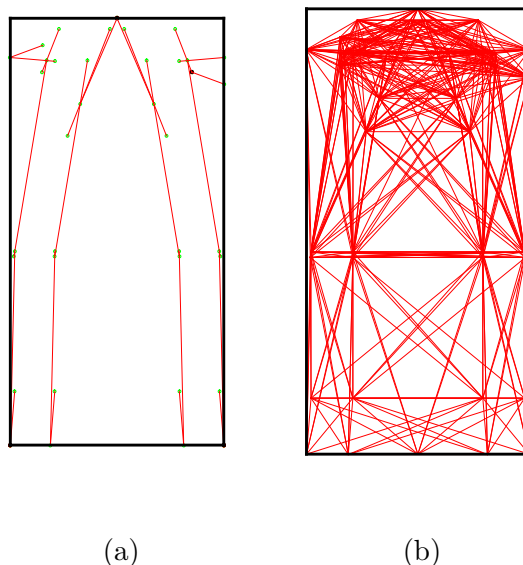


Figure 3.12: Ground structure development: (a) merged strut path and (b) proposed ground structure ($m=447$).

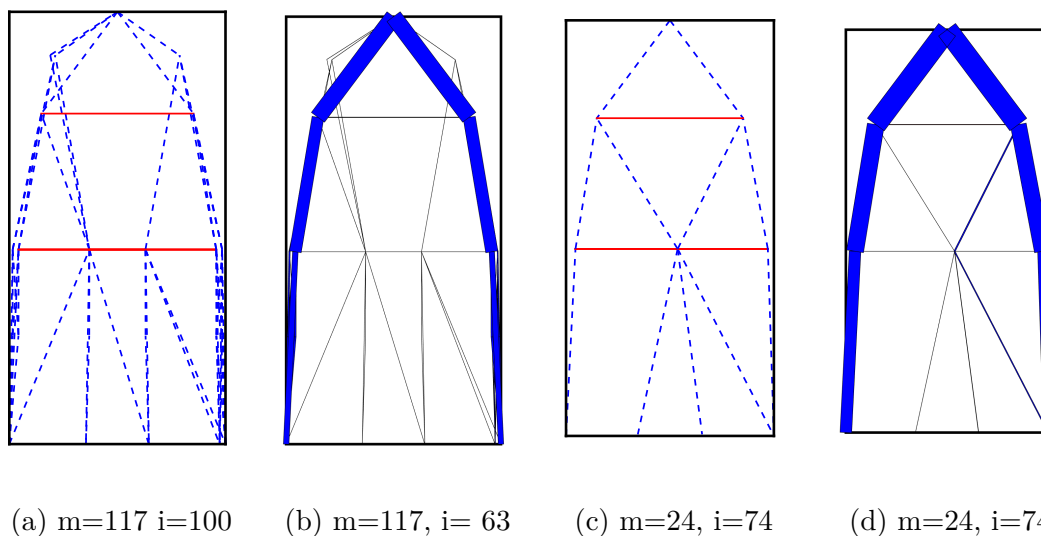


Figure 3.13: Anchorage Strut-and-Tie models obtained from a fine mesh. Figure (a) shows the results obtained through an optimisation scheme considering only size and topology techniques; figure (c) shows the results obtained through an optimisation scheme considering size, topology, and geometric techniques. Figures (b) and (d) are graphical representations of the associated cross sections corresponding to (a) and (c) .

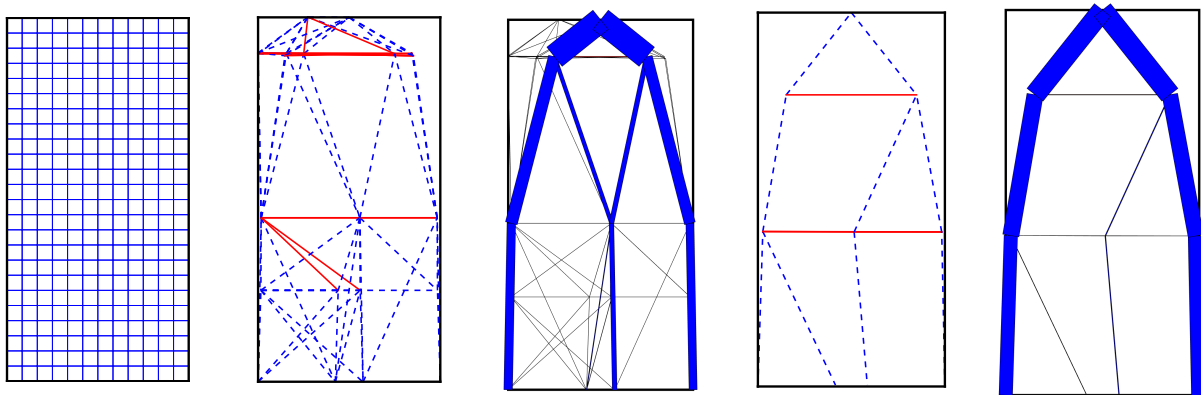
3.2.4 Mesh sensibility analysis

One of the issues found when treating local zones is use of models that are not well detailed or just not appropriate.

The proposed topology of the previous example is obtained through the approach presented within this document. The numerical results are shown in figure 3.13 and the numerical results well evaluate and reflect the load-transfer mechanisms, such as transverse tensile stresses, caused by force spreading. It is well known the issue of mesh-dependency

of the results in the finite element method; a problem referring to the contrast in the solutions for different mesh sizes or democratisation, fact that can decrease the reliability of the numerical results. Being based on the FEM, it is natural to expect certain mesh-dependency on the proposed approach. In order to have an idea of how the choice of the initial mesh can influence the final results, the same example was performed with different initial meshes and the results are presented in figures 3.14 and 3.15. Similarly to the results presented in the previous section, the figures show the results achieved by the application of mixed schemes sizing-topology and sizing-topology-geometric.

Along with the mesh discretisation showed in 4.2, another two different meshes were used for the purpose of comparison, as shown in figures 3.14a and 3.15a. Figures 3.13, 3.14 and 3.15 show the obtained ST schemes for the three different meshes, in blue dashed lines represent members in compression and other continuous red lines represent members in tension.

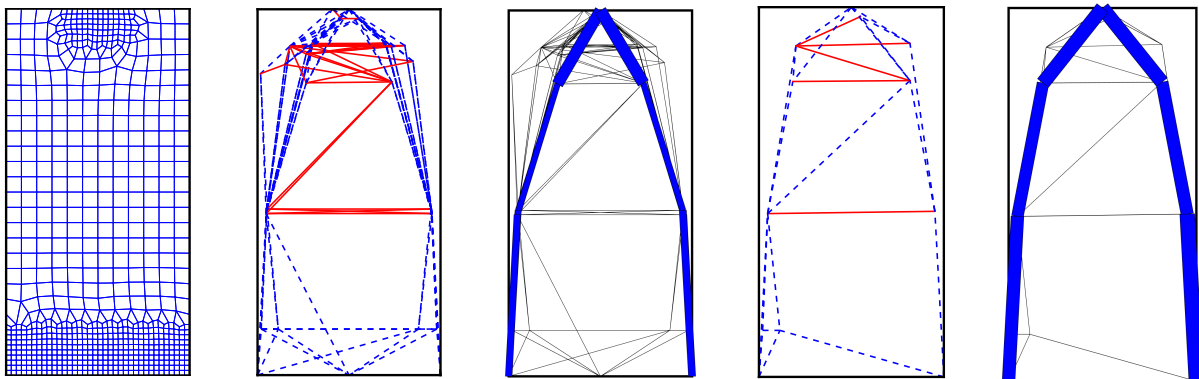


(a) 288 elements (b) $m=84, i=46$ (c) $m=84, i=46$ (d) $m=21, i=74$ (e) $m=21, i=74$

Figure 3.14: Anchorage Strut-and-Tie models obtained from a coarse mesh. Figure (a) shows the results obtained through an optimisation scheme considering only size and topology techniques; figure (c) shows the results obtained through an optimisation scheme considering size, topology, and geometric techniques. Figures (b) and (d) are graphical representations of the associated cross sections corresponding to (a) and (c) .

As it can be observed, the results obtained from different initial meshes do not radically differ from one model to another when treated with the full optimisation scheme (sizing-topology-geometric). This can be explained by the fact that the initial FE mesh is used only as mean to propose the initial truss system. If the algorithm is able to find similar local maximum and minimum from the principal stress fields, the Voronoi division will define the same zones for the initial system.

Although the number of elements may not be the same from one model to other, it can be appreciated that the obtained differences are mainly found in secondary elements remaining the principal elements as a constant for the three different systems. Additionally it can be pointed out that the position of the nodes present a good consistency in the results specially for size-topology-geometric schemes (subfigures (e)). Even though the final nodal coordinates are not exactly the same, the largest discrepancy between models has been found to be about 15 centimetres which, arguably, does not impact a structure whose smallest dimension is equal to 3 meters.



(a) 723 elements (b) $m=130, i=66$ (c) $m=130, i=66$ (d) $m=28, i=90$ (e) $m=28, i=90$

Figure 3.15: Anchorage Strut-and-Tie models obtained from a locally refined mesh. Figure (b) shows the results obtained through an optimisation scheme considering only size and topology techniques; figure (c) shows the results obtained through an optimisation scheme considering size, topology, and geometric techniques. Figures (b) and (d) are graphical representations of the associated cross sections corresponding to (a) and (c) .

In general, the obtained ST models show consistently the same characteristics of load-transfer mechanisms, such as the force-spreading and transverse tensile stresses. Despite being computed from different initial meshes, figures 3.13e, 3.14e and, 3.15e present huge similarities in terms of quantity, distribution and position of principal elements. Small differences remarkable in the quantity of "secondary" elements; elements that are present only for stability issues or ill-conditioning in the stiffness matrix. The presence of this elements, having a neglectable cross section area, do not affect the behaviour of the whole structure. Therefore, a conclusion can be safely drawn that mesh sizes have little influence on the final model and results.

3.2.5 Literature results

Figure 3.16 shows the proposed Strut-and-Tie models. As in previous figures, the blue dashed lines represent members in compression and the continuous red lines represent elements in tension; the original figures were adapted to respect this colour pallet.

Given the strong similarities found in the models computed in the previous section, the comparison is done considering only the model obtained from size-topology-geometric optimisation scheme starting with the coarse mesh (figure 3.14).

It can be observed that although the number of members is different from one model to another, the burst deep shows a good consistency in terms of load-transfer mechanisms and length. The main differences can be summarised into three points:

1. **Force-spreading.** The force spreading mechanism shows consistency with the model presented by Schlaich; for the case of the model presented by Zhong, the difference is due to a discretisation of the load (2 point load instead 1 punctual one).
2. **Burst deep.** The three showed topologies present close values for the parameter d_{burst} 1.46, 1.35, and, 1.41 meters for model (a), (b) and, (c) respectively. With

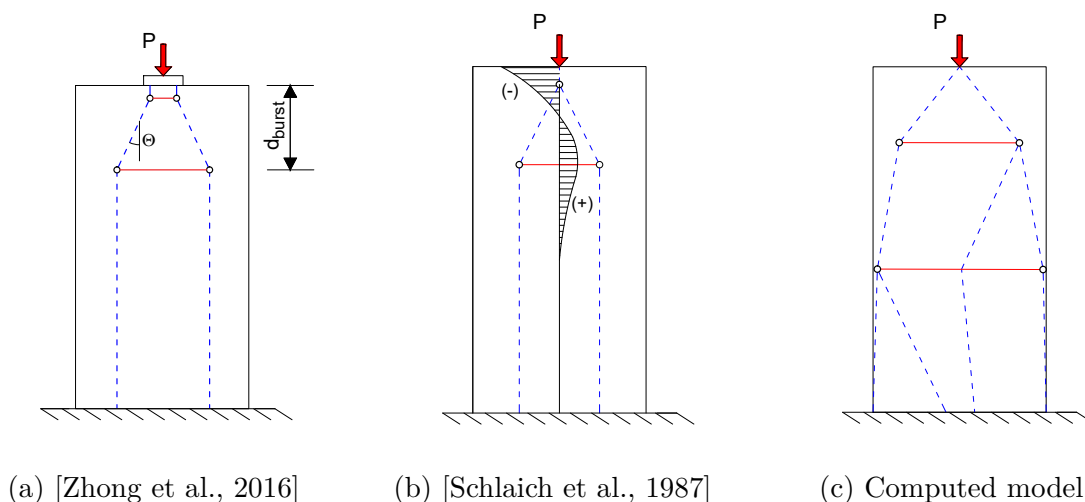


Figure 3.16: Different Strut-and-Tie model propositions

respect to the angle Θ , the proposed model presents a value of 37 degrees; inclination 10° greater than the presented by the cited authors (26° reported by Zhong and 28° by Schlaich).

3. **Transverse tensile elements.** Beyond the burst deep is where the most remarkable differences arise. Whether the literature models show just two straight struts, the computed model propose a continuity of the of the load-transfer mechanism presenting short elements following a natural spreading of the force.

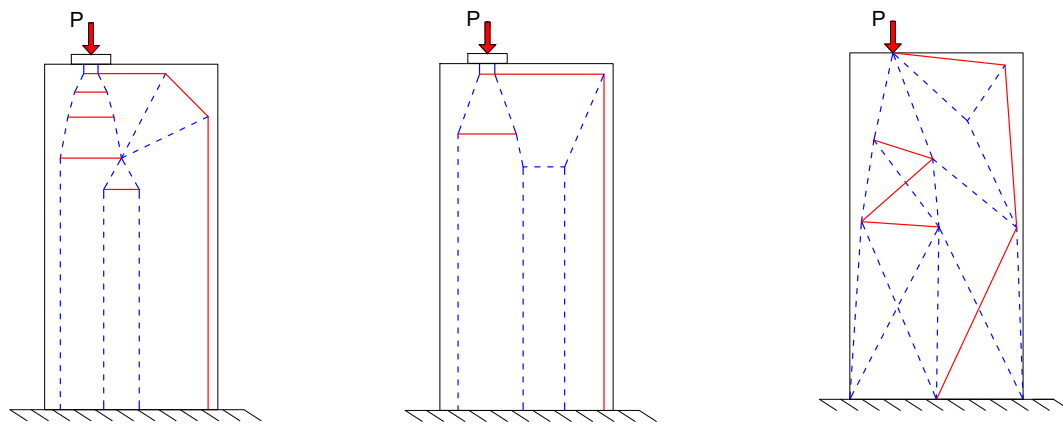
The differences presented in the first and second point of the previous list refer to small variations that, given the size of the analysed element, are acceptable in actual structures. For the third point, the literature results propose long strut elements (more than 4 meters long) that, according to the EuroCodes, may need further detailing an even secondary strut and ties.

3.2.6 Different load cases

Similar analysis were performed for the load cases (b) and (c) showed in figure 3.8. Intermediate results can be found in the annexes and the final ST models are presented in the subsequent figures.

It can be observed that this is so far the model that differs the most from the literature examples. Even though the models present strong similarities in terms of load-transfer mechanisms, the mere existence of some elements in the proposed model brings effects of compression in a zone that do not consider struts in the other two models (right support in figures 3.17 (a) to (c)).

The differences presented in this model come from the fact that, for this case, the automatically obtained Voronoi seeds did not allow a satisfactory geometry division (clipped Voronoi division) and some seeds were need to be added manually to the algorithm to continue the procedure. The present results permit to state that the present approach is highly sensitive to the number and position of the Voronoi seeds. In case of not being



(a) [Zhong et al., 2016] (b) [Aashto L.R.F.D., 1998] (c) Computed model

Figure 3.17: Comparison of different Strut-and-Tie model propositions(anchorage $e=0.75m$)

satisfied with the final results, it was decided to let the user the liberty to add, erase or modify the proposed Voronoi seed hence adapting a computer aided scheme over a fully automatic one.

3.3 Behaviour of the algorithm

3.3.1 Linear-elastic FE analysis

The included solving procedure is a very basic algorithm that assembles the matrix K and then solves for $Ku = P$. The assemble follows an iterative scheme that do not present any complications if the inputs follow the predefined format. Similarly, the available solution subroutines are simple and show good performance.

3.3.2 Ground structure

From the different step needed to arrive to the ground structure, two of them should be mentioned.

Is worth to mention that the subroutine that computes the maxima/minima is highly dependant on the difference of the "peaks" and their surroundings. Given that the mesh-size directly affects this difference, the selection of the threshold defining a peak or valley is given to the user. Despite this, the tests show that selecting a threshold between 5% and 10%, in addition to the change in the sign of numerical derivative, provides good results.

3.3.3 Truss optimisation

When applying the topology and the geometric subroutines, the algorithm presents a good performance and a fast convergence. However, when the vector of design variables also includes nodal coordinates, the algorithm may become unstable and, according to the experience, a solution may or may not be found.

Aiming to stabilise the algorithm, three parameters should be carefully controlled.

Firstly, small values of S (step) are preferred. Based on the hypothesis that the nodal coordinates of the ground structure are close to the optimal coordinates, it results natural that just a small variation on the position of the nodes is expected. Thus according to the tests, limiting S to attain values inferior to 10cm (depending on the dimensions of the analysed geometry) can be considered as a reasonable limit step.

An aspect worth to point out is the effect that the random elimination of bar elements during the topology optimisation, produce a light disparity of the results found when "running" multiple times the exact same example. Even though this can be seen as a huge drawback concerning the robustness of the algorithm, the difference found between two different runs of the same example do not significantly affect the final results.

3.4 Summary

As it was pointed out, the proposed methodology is based on an organised list of subroutines that allow to automatically obtain feasible ST models from common linear-elastic FE analysis. The initial FE planar analysis intends to serve as a link between the structural engineer, used to this type of analysis, and the rational approach ST.

The performed analyses show that:

1. the proposed methodology keeps the "spirit" of the manual ST models being obtained through linear-elastic stress fields
2. the obtained results approach to the geometries obtained by different methods and authors
3. the use of different mesh sizes have little influence on the final model and results

So far the results clearly show the capabilities for finding feasible ST systems but the gains in terms of reinforcement still remain unsaid. Next chapter addresses to this issue and compares usual practice techniques to compute the reinforcement of a D-region.

Chapter 4

Comparative example

In previous chapter, the proposed approach was described and a simple bi-dimensional literature case was used to compare the obtained results.

Even though the automatic generation of feasible planar Strut-and-Tie Models can be advantageous, a wide variety of structures present geometries or boundary conditions that can limit the application of planar models. Besides, due to the graphical limitations, classical reinforcement schemes based on ST models remain applicable only to considered 2D structures where the effects in a third direction are just omitted. When facing 3D problems, within the industrial context, the geometries are commonly reduced to mere surface representations based on shell or plate type elements and the need of steel reinforcement is directly computed through an algorithm based on generalised forces such as Capra-Maury.

Specifically, within the nuclear civil works, industrial constraints have imposed an immoderate use of plate and shell formulations. The size of the buildings, its structural behaviour as well as the need of efficient auditable methods, are just some aspects that have encouraged this practice.

This chapter is intended to compare results from the industrial practice and those possibly achieved through the use of the rational approach STM while applied on local zones; pointing out the advantages of the implementation of detailing stages during the design procedure. To this purpose a literature example treated from three points of view:

1. ST model computed from a planar representation
2. Capra-Maury algorithm applied over a surface model representation
3. ST model computed from a full 3D solid element representation

It is worth to mention that in no case the computation time will be a subject of study. This decision has been taken under two premises: 1) the main purpose is to evaluate the viability of the proposed algorithm and, 2) the code was written in MATLAB that, arguably, may induced a slow execution [Aruoba and Fernández-Villaverde, 2015].

Exemple comparative

Dans le chapitre précédent, l'approche proposée a été décrite et un simple cas de littérature bidimensionnelle a été utilisé pour comparer les résultats obtenus.

Même si la génération automatique de modèles planaires Strut-and-Tie réalisables peut être avantageuse, une grande variété de structures présentent des géométries ou des conditions aux limites qui peuvent limiter l'application de modèles planaires. En outre, en raison des limitations graphiques, les schémas de renforcement classiques basés sur les modèles ST restent applicables uniquement aux structures 2D considérées où les effets dans une troisième direction sont simplement omis. Face aux problèmes 3D, dans le contexte industriel, les géométries sont souvent réduites à de simples représentations surfaciques basées sur des éléments de type coque ou plaque et le besoin de ferrailage est directement calculé par un algorithme basé sur des forces généralisées comme Capra-Maury.

Plus précisément, dans les travaux de génie civil nucléaire, les contraintes industrielles ont imposé une utilisation immodérée des formulations de plaques et de coques. La taille des bâtiments, son comportement structurel ainsi que le besoin de méthodes auditables efficaces ne sont que quelques aspects qui ont encouragé cette pratique.

Ce chapitre vise à comparer les résultats de la pratique industrielle et ceux éventuellement obtenus grâce à l'utilisation d'une approche rationnelle appliquée aux zones locales; souligner les avantages de la mise en œuvre des étapes de détail au cours de la procédure de conception. A cet effet, un exemple de littérature traité de trois points de vue:

- 1. algorithme Capra-Maury appliqué sur une représentation de surfacique du model*
- 2. BT calculé à partir d'une représentation planaire du modèle*
- 3. BT calculé à partir d'une représentation d'un modèle solide 3D*

Il est important de mentionner que le temps de calcul ne sera en aucun cas un sujet d'étude. Cette décision a été prise sous deux prémisses: 1) le but principal est d'évaluer la viabilité de l'algorithme proposé et, 2) le code a été écrit dans MATLAB qui, sans doute, peut induire une exécution lente [Aruoba and Fernández-Villaverde, 2015].

4.1 Example selection

With the aim of having a direct comparison with existent approaches, it was chosen to apply the proposed algorithm to the classical problem of a corbel withstanding a punctual load. The example was inspired by [Almeida et al., 2013] where a 2D FE model of the geometry was treated by a Smooth Evolutionary Structural Optimisation (SESO). The structure was conceived to support a concentrated load, P of 0.5 MN, being fixed at both ends of the column. An initial thickness of 30 cm, along the third direction, was assumed for the element. The Young's modulus, E_c , of 28.5 GPa and the Poisson's ratio, ν , was taken equal to 0.15.

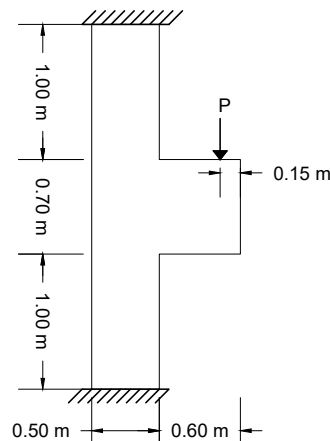


Figure 4.1: Planar corbel initial model

Table 4.1: Considered materials

Material	Young's modulus [GPa]	Poisson's ratio	Compressive strength [MPa]	Tensile strength [MPa]
Steel	210	0.3	434	434
Concrete	28.5	0.15	25	0

4.2 2D planar model

The first performed analysis is based on a planar model of the structure where a ST model is aimed to be obtained using the proposed approach.

For this case, a relatively coarse mesh consisting in 708 planar four-node elements (figure 4.2a) was preferred over the original one creating a model. Nodal displacements constraints were placed in the zones of the supports, and finally, a concentrated load, P , was placed according to figure 4.1. The material constants were also directly taken from the original model and are shown in table 4.1.

Similar to the previous examples, the procedure was applied and graphical results associated to the subroutines are shown in figures 4.2. As mentioned in the precedent chapter, the picks and the valleys presented in the principal stress fields are taken as indicators of the presence of the nodes of a suitable ST model.

In figures 4.2b and 4.2c are shown the principal stress fields all over the structural element developed under the specified boundary conditions and in subfigure 4.2f the detected peaks and valleys are depicted.

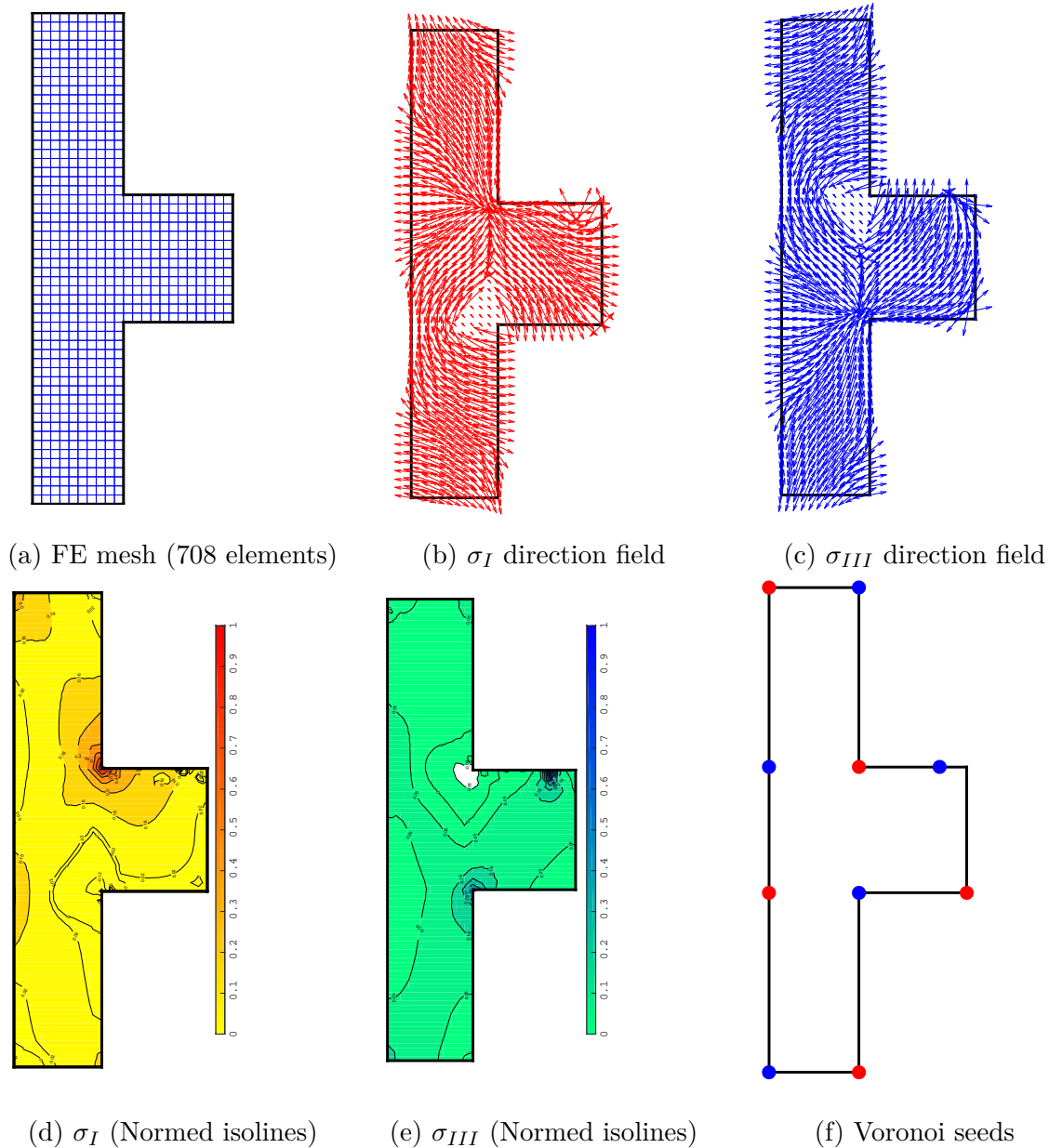


Figure 4.2: Schematic representation of the needed data

Taking the local maxima and minima as seeds for the Voronoi division and the geometry as the feasible region, the division is performed. For this case, 20 cells were found during the performed division 4.3a.

Following the presented methodology, the *loess* was applied at the centre of every cell. Considering the principal directions of all the elements found in the cell, the regression was applied and the results are schematised in figure 4.3b.

The initial strut path (subfigure 4.3c) was achieved through the sub routine described in the previous chapter. An initial node is selected (node containing a maxima of σ_{III})

and a straight line is developed until finding the limits of a cell.

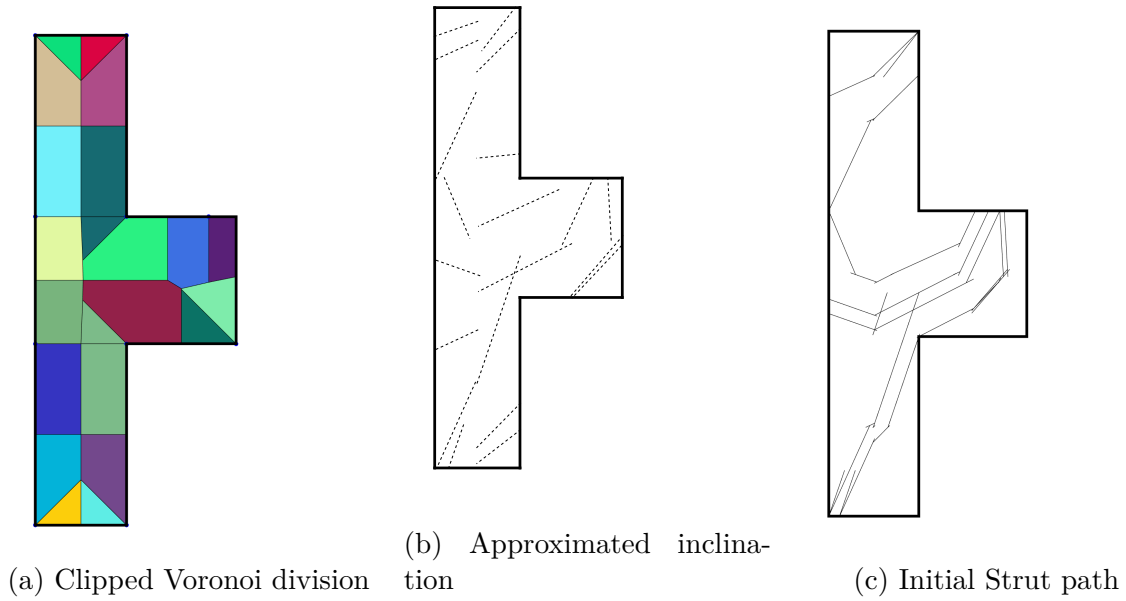


Figure 4.3: Strut generation subroutines

Based on the prior strut path, linking elements are placed and the ground structure is proposed.

For the presented example, the hybrid size-topology-geometry optimisation scheme was preferred and the final geometry is shown in figure 4.5a.

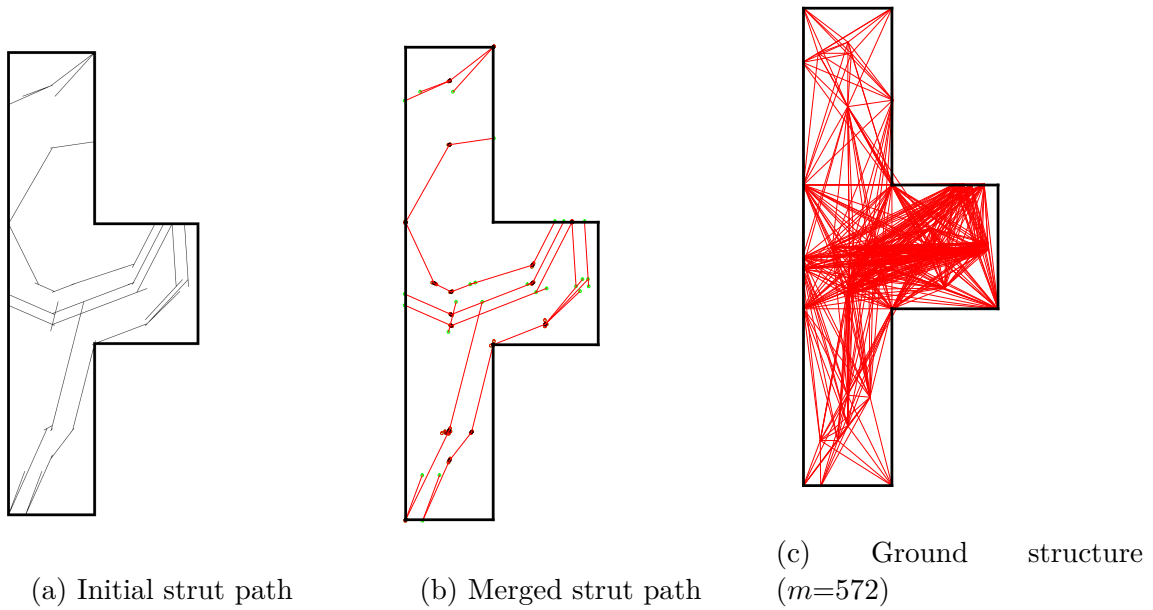


Figure 4.4: Ground structure

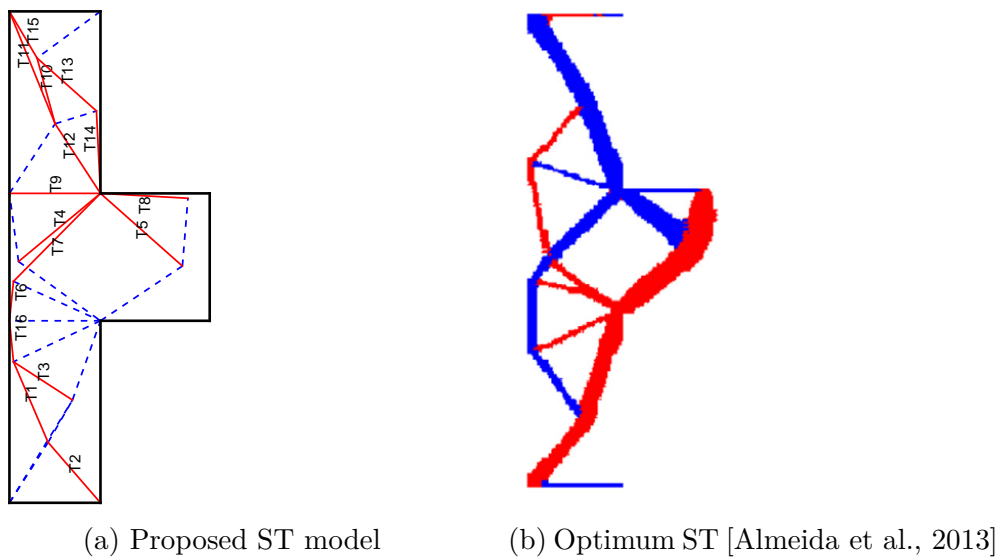


Figure 4.5: Different ST models for the corbel case. Figure (a) depicts the ties in red and the struts in blue; figure (b) is presented with shifted colours

The nodal revision consist in a graphical projection of the element considering their actual cross section. While elements in compression (struts) are directly considered, elements in tension are replaced by an equivalent strut arriving at the opposite face of the node. Being all elements designed at full stress, and being the geometry of the nodes directly computed from the intersection of the elements, the stress attained at nodal zones equals the concrete's strength design.

Figure 4.6 depicts the geometry of a CCT node produced by the intersection of three elements of the final ST model.

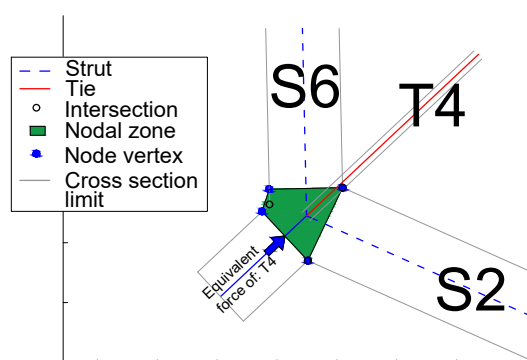


Figure 4.6: Nodal geometry

As it can be appreciated, the proposed model (4.5a) present a good geometry in terms of repetition of members and nodal position compared to the optimal design achieved by the SESO approach (4.5b). Both models, also present strong similarities with the model proposed by Schlaich and similar repetition of tensile elements.

Tables 4.2 and 4.3 contain the information of the ties for the model depicted in figure 4.5a. The first table presents the needed steel considering the Strut-and-Tie model as a skeletal structure. The second output, table 4.3, corresponds to the results of a more realistic model that considers the cross sections distributed along the principal axis X and Y as it is usually done in the construction field. This last result is achieved through the optimisation subproblem stated in section 3.1.6.2.

Table 4.2: Steel reinforcement for the ST model

Tie	Force [KN]	Required reinforcement [cm ²]	Length [cm]	Total reinforcement [cm ³]
T1	109.8	2.44	48	117.12
T2	89.66	1.99	44	87.67
T3	60.68	1.35	38	51.24
T4	7.9	0.18	58	10.18
T5	376.23	8.36	60	501.64
T6	152.18	3.38	21	71.02
T7	165.06	3.67	67	245.76
T8	60.23	1.34	48	64.25
T9	52.51	1.17	50	58.34
T10	60.68	1.35	37	49.89
T11	111.21	2.47	66	163.11
T12	154.7	3.44	45	154.7
T13	304.15	6.76	43	290.63
T14	144.83	3.22	45	144.83
T15	128.1	2.85	30	85.4
T16	163.26	3.63	22	79.82
Total				2175.59

Table 4.3: Steel reinforcement for the planar ST model: projection over the X and Y axis [cm³]

Tie		Force [KN]	Required steel [cm ²]	Length [cm]	Total reinforcement [cm ³]
T1	X	43.3	0.96	19	18.28
	Y	100.9	2.24	44	98.66
T2	X	58.7	1.3	28	36.52
	Y	67.8	1.51	33	49.72
T3	X	50.9	1.13	32	36.2
	Y	3.33	0.07	21	1.55
T4	X	6.1	0.14	45	6.1
	Y	5	0.11	37	4.11
T5	X	281.5	6.26	45	281.5
	Y	249.7	5.55	40	221.96
T6	X	15.5	0.34	2	0.69
	Y	151.4	3.36	21	70.65
T7	X	116	2.58	47	121.16
	Y	117.4	2.61	48	125.23
T8	X	60.1	1.34	48	64.11
	Y	3.3	0.07	2	0.15
T9	X	52.5	1.17	50	58.33
	Y	0	0	0	0
T10	X	29.5	0.66	9	5.9
	Y	107.3	2.38	36	85.84
T11	X	58.2	1.29	25	32.33
	Y	143.3	3.18	61	194.25
T12	X	166	3.69	24	88.53
	Y	254.8	5.66	38	215.16
T13	X	108	2.4	32	76.8
	Y	96.4	2.14	29	62.12
T14	X	6.3	0.14	2	0.28
	Y	127.9	2.84	45	127.9
T15	X	125.6	2.79	15	41.87
	Y	212.2	4.72	25	117.89
T16	X	16	0.36	2	0.71
	Y	162.4	3.61	22	79.4
Total					2323.9

For comparative purposes, in this and further examples, the considered geometry is divided into four regions according to table 4.4: the arm, the forehead, the joint and the foot.

Table 4.4: Steel reinforcement for the planar ST model: need of steel reinforcement per zone [cm³]

	X reinforcement	Y reinforcement	Total
Arm	345.61	222.1	567.71
Forehead	274.88	803.17	1078.05
Joint	157.11	199.99	357.1
Foot	91.71	229.33	321.04
	$\Sigma = 869.31$	$\Sigma = 1454.59$	$\Sigma = 2323.9$

Figure 4.7 shows the PI history attained by the structure along the the optimisation process. The PI decreases with the removal of lowly stressed elements from the corbel at the same time that the error measured between continuous iterations, ϵ , also is reduced.

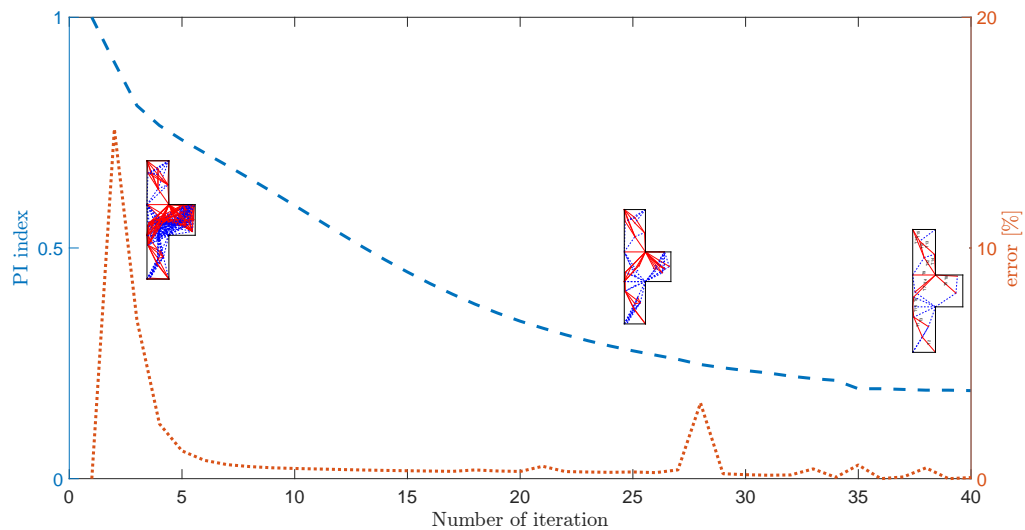
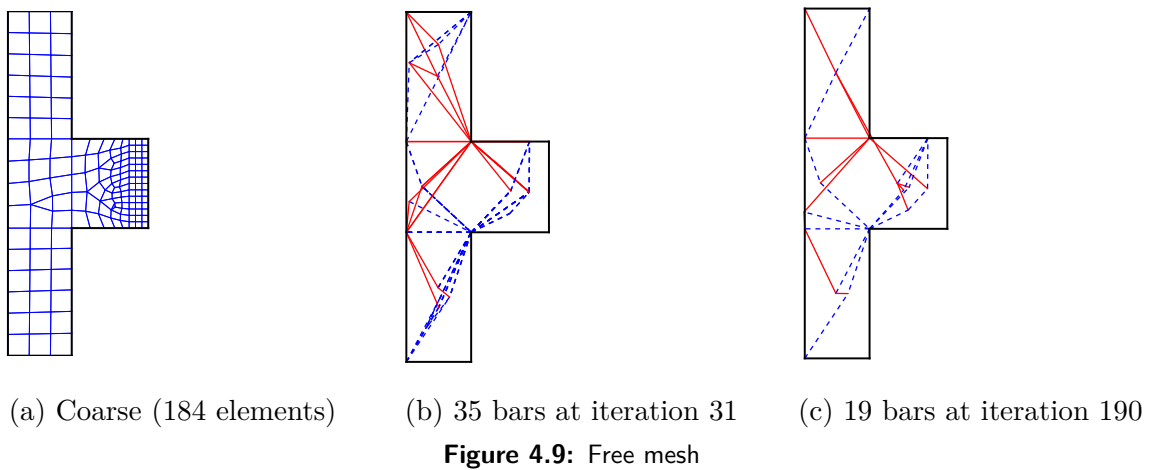
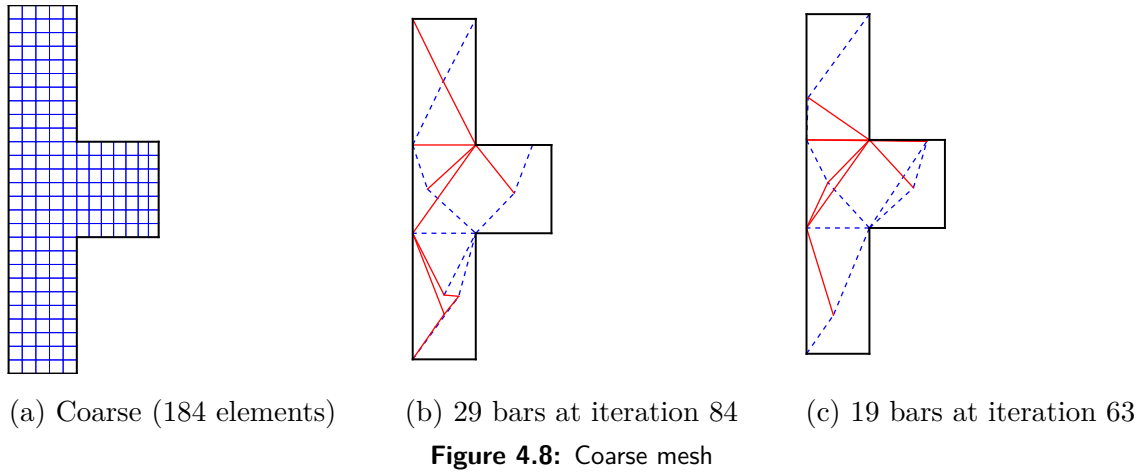


Figure 4.7: Optimisation evolution

With the same aim as in the previous examples, two variants of the mesh discretisation were used to perform the same analysis (same materials and boundary conditions) and the results are plotted in figures 4.8a and 4.8b.



In general, the differences found in the results of the application of the algorithm over different meshes do not drastically modify the final ST model. Hence, as in the previous chapter, the statement that the obtained ST models show consistently the same characteristics of load-transfer mechanisms regardless the initial FE mesh remains true.

4.3 Surface model representation

For comparison purposes, the selected example was modelled in Code_Aster 13.4 software (included in Salome-Meca2017.0.2 for Windows). Code_Aster is a multi-physics software of simulation principally developed for mechanical analysis and acoustics.

The choice of Code_Aster was principally based on 3 aspects:

1. open software
2. built-in steel reinforcement computation algorithm
3. used by EDF in the nuclear context

In order to be consistent with the industrial practice, it has been chosen to model the corbel with a heavily coarse mesh constructed by elements of nearly 0.5 meters per side. This choice has been guided by the will of modelling a simple object exhibiting a typical D-region discretisation found in structural junction. With that in mind, the presented model can be seen as a local extract of bigger structural representation.

The shell-element model was built, calculated and then post-processed by means of Code_aster software. The software includes a function able to calculate reinforcement densities in shell and plates elements as a function of the elements of reduction: the generalised forces.

The result (referred as **FERRAILLAGE** in the data structure) can be accessed in text form or directly plotted within SALOME_MECA interface.

At the Ultimate Limit States that is considered, the software operator **CALC_FERRAILLAGE** only calculates the bending reinforcement areas. The shear reinforcement has been hand calculated and was added to the calculated values. The field of reinforcement that is obtained through these two operations per each element is then:

- a longitudinal reinforcement density in the X direction of the element for the lower face of the element (**DNSXI**);
- the equivalent for the top face (**DNSXS**);
- a longitudinal reinforcement density in the Y direction of the element for the lower face of the element (**DNSYI**);
- a longitudinal reinforcement density in the Y direction of the element for the lower face of the element (**DNSYI**);
- the equivalent for the upper face (**DNSYS**);
- stress in concrete **SIGMBE**;
- deformation in **EPSIBE** concrete.
- transverse reinforcement density (**DNST**);

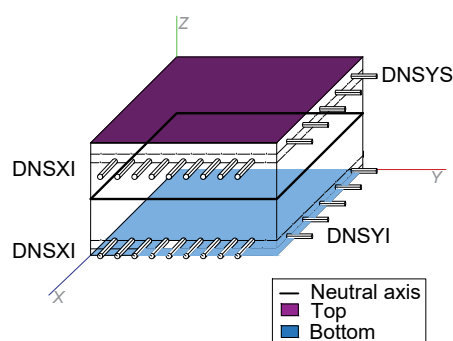


Figure 4.10: Computed components of reinforcement given in local coordinates

The densities of reinforcement are calculated according to the method of Capra-Maury. These densities are expressed in surface units per linear length of shell. For example, if the mesh in meters (with data of basic characteristics and coherent material), the densities will be expressed in m^2/m .

As mentioned, the used software bases its reinforcement computation algorithm in the results obtained from the shell or plate FE representative models. For the presented case, the corbel, an accepted 3D representation would be the construction of a planar representation. A vertical and a horizontal decks developed along the principal axis of the structure, defined by the "column" and the "arm", and attached at a "joint" zone (see figure 4.11).

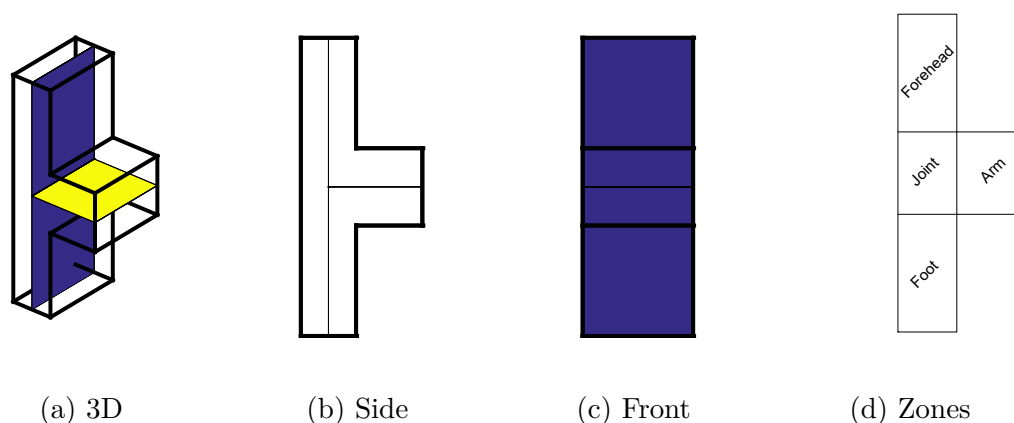


Figure 4.11: Views of model representation in Code_Aster software

Following the previous representation, a model was constructed using 14 shell elements of constant thickness (0.50m and 0.70m, respectively, for the elements conforming the column and the arm). The load of 0.5MN was considered distributed along the deep of the element. Finally, fixed supports were considered at the bottom and at the top of the geometry. A graphical representation of the model can be seen in subfigure 4.12a.

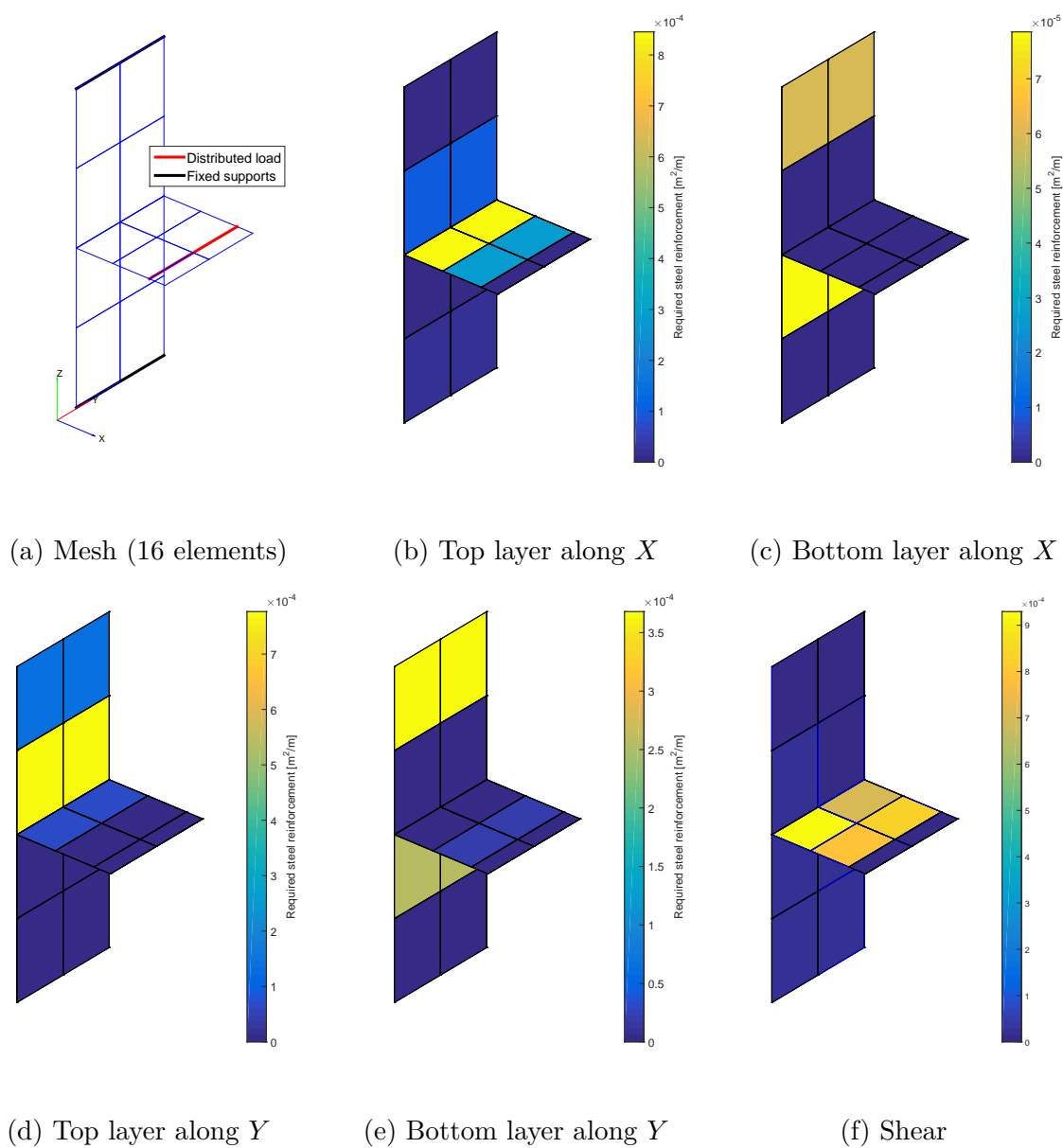


Figure 4.12: Capra-Maury computed required steel reinforcement (Coarse mesh).

The quantities of computed steel reinforcement were distributed into 4 zones and the results are presented in the next table.

Table 4.5: Computed need of steel reinforced per zone (coarse model) [cm³]

	XS	XI	YS	YI	SW	Total
Arm	55.11	0	0	3555.56	154	3764.67
Forehead	0	98	239.22	607.11	0	944.33
Joint	35	230.22	29.44	508	125.22	927.89
Foot	17.81	111.11	0	0	0	128.92
Total	107.92	439.33	268.67	4670.67	279.22	5765.81

Precedent results are attained via a model representation that intends to mimic a common mesh discretisation found in overall structural models. Assuming no singularities are present, meshes dictated by overall models present an acceptable accuracy and might be costly efficient for global behaviour objectives, yet their use for local zones and detailing is highly questionable.

Following the good practices, in this context, a coarse model can be used for pre-design purposes and after, local zones must be isolated and refined in order to proceed with the detailing stage. Nevertheless, the coarse representation would be kept.

Worthy to mention is the fact that even if the selected discretisation may probably not be the most appropriated for the problem, due to the size of nuclear facilities and their correspondent buildings, the FE mesh herein used represents a common case industrially used. Further, the selection of Finite Element representation may not be the best option neither for local zones.

In order to decide when to use shell elements, there exist different thumb rules presented by several authors; [Johnson, 1986] presents three criteria to justify the use of shell elements:

1. By observation (surface area / thickness ratio)
2. By failing to create a useful, or accurate, 3D solid model
3. By discovering that the shell assumptions are wrong

The selected corbel presents surface area / thickness ratios of 1.21 and 2.7 respectively for the arm and the column. These values remain far from the application of shell elements (being 10 the minimum acceptable value for surface area / thickness ratio [Johnson, 1986]). Additionally, due to the geometry, shell elements can "overlap" at corners affecting the precision of the results. Stiffness is still quite good, but stress at joints is not accurate even for thin elements [Moaveni, 2011].

4.4 Remarks

Due to its relative ease of implementation, most of the structures are analysed and designed in similar fashion as the one presented. The advantages of the use of shell elements to model structural elements, results mainly from time-saving due to reduced number of

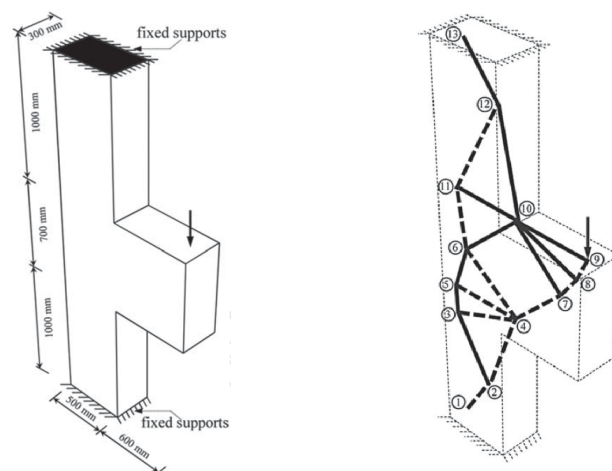
finite elements (and consequently the equations to solve). However, the shell elements are limited to thinner features. There is not an specific limit of the application of surface elements but a good approximate would be the ratio span / thickness [Bisch, 2013]. If the ratio is at least 20 times, the bodies are candidates for surface elements otherwise, the use of this type of elements need further justifications.

In an oversimplified definition, a shell addresses to a solid that presents a dimension considerably smaller than the other two dimensions. Physically, and according to the theory of structures, this fundamental characteristic allows the allusion to the hypotheses that entail the simplification of the behaviour of three-dimensional bodies into the one of a 2D body. Seldom, when modelling local zones, questionable simplifications are done. Shell elements are used to model entire geometries indiscriminately. Whether it results reasonable for static analysis of planar elements such as slabs or walls, its implementation for regions presenting weak span/thickness ratios or geometric discontinuities is debatable.

For structural elements where the third direction cannot be neglected, solid element discretisations are preferred.

4.5 3D brick model

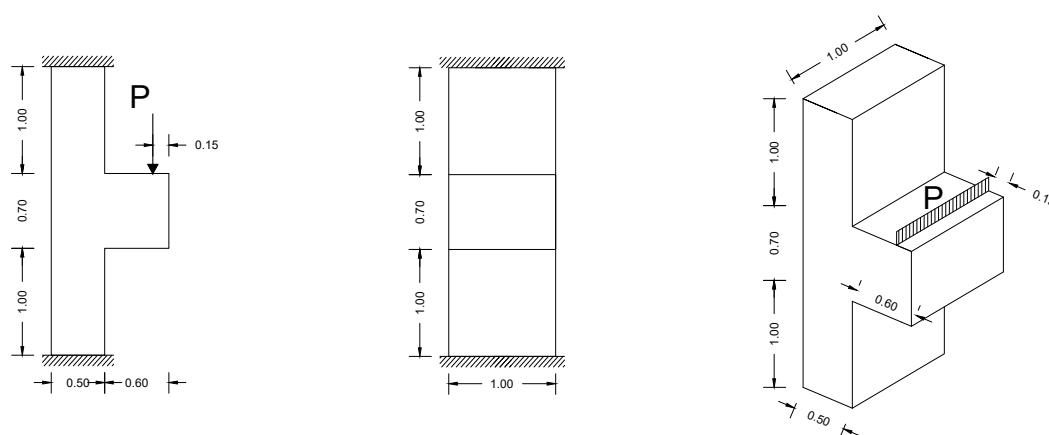
As showed by [Shobeiri, 2016], due to the relatively small thickness of the element, the development of a strut-and-tie model over a three-dimensional representation of the studied case would not be influenced by transverse effects (see figure 4.13).



(a) 3D model representation (b) Obtained ST model

Figure 4.13: ST model found through Bi-directional Evolutionary Structural Optimisation [Shobeiri, 2016]

In order to increase the effects of the load along the third direction, it was decided to modify the thickness of the original model according to figure 4.14. The corbel was assumed to present a one-meter thickness instead of the original 0.3m. Regarding the load, an equivalent linearly distributed pattern was preferred over then punctual one.



(a) Side view (b) Front view (c) 3D view

Figure 4.14: Three-dimensional model representation

A linear-elastic model consisting of 4200 8-node brick elements was built (figure 4.15a), the boundary conditions and the load were applied and, finally, the stresses were found. With the associated results, the algorithm was run and the obtained results are shown.

Figures 4.15 and 4.16 show some intermediate results product of the different steeps that conform the algorithm.

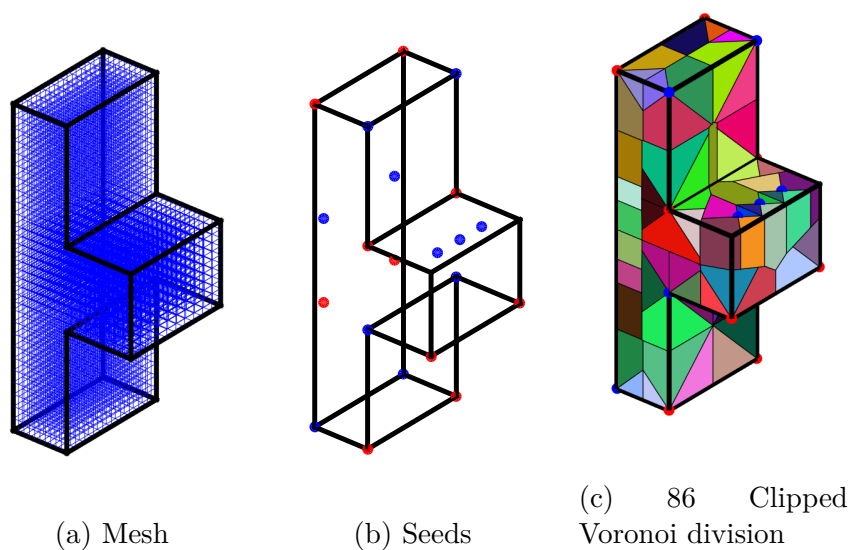


Figure 4.15: Caption

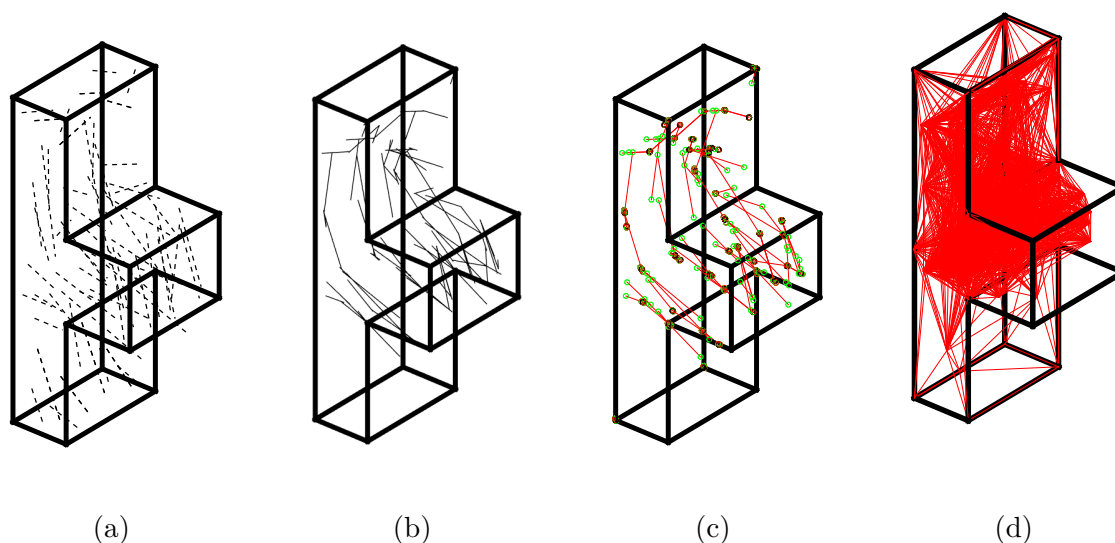


Figure 4.16: (a) directions associated to the Voronoi zones, (b) initial strut path, (c) merged strut path and (d) ground structure ($m = 1919$)

As in previous examples, two types of optimisation schemes were performed: size-topology and size-topology-geometry optimisation schemes.

After 260 iterations, the output of the first optimisation scheme shows a highly populated structure. Even though the algorithm reduced to almost 35% the quantity of the elements (690 elements) in the structure, it seems not to be sufficient to directly obtain a suitable ST model. In order to visualise the results, a filter needed to be applied. All the elements whose cross section results inferior to the arbitrary value of 0.6cm^2 were erased from the plotted images.

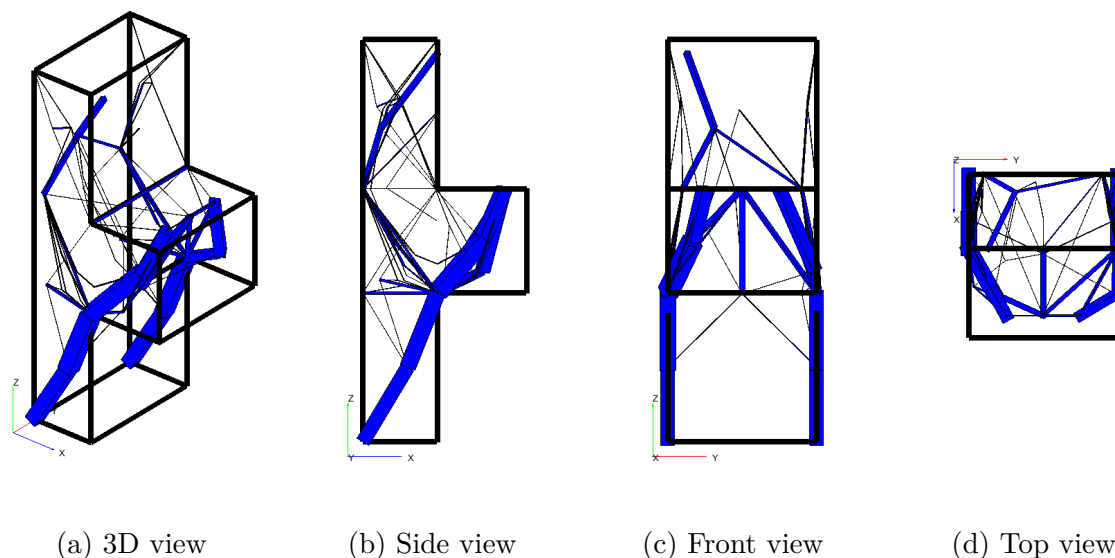


Figure 4.17: Filtered Strut and tie model resultant of a size-topology scheme ($m = 88$)

Figure 4.17 shows the "filtered" ST model obtained through a size-topology optimisation scheme. This image represents the actual sizes and distribution of the elements conforming the proposed ST model. As in can be appreciated despite of having performed the filter, there are still few elements whose existence may be not necessary for the structure. Hence, in order to obtain a simpler ST model, a manual intervention may be a good option at this state.

Another alternative is to apply the full optimisation scheme (size-topology-geometry).

Figures 4.18 and 1.17 show the results obtained through the application of the full optimisation scheme (size-topology-geometry) to the ground structure previously presented (figure 4.16d) .

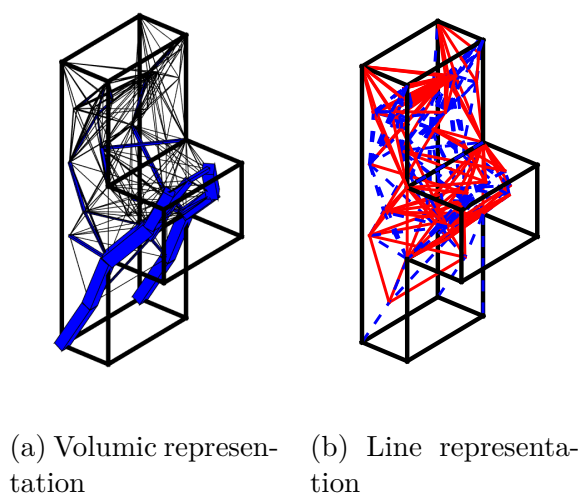


Figure 4.18: Strut-and-tie model resultant of size-topology-geometry optimisation scheme ($m = 247$)

Again, but this time after 329 iterations, the output shows a highly populated structure. The scheme improved the results obtaining a final structure containing only 247 elements (representing a 12% of the initial quantity). Despite the fact that the second optimisation

scheme allows a huge reduction regarding the quantity of elements of the initial structure, the results are still far from being directly presented as a suitable ST model. At this point, a minor manual intervention would be the ideal way to reveal the final ST model.

The proposed manual intervention is carried out by modifying the position of some nodal coordinates. For this case the priority was given to those nodes generating inconsistency in the symmetry along Z axis. From this point, after having performed the modification of nodal coordinates, the optimisation scheme was retaken. The process continued for 120 iterations (additionally to the 329 already performed) and ended with a final structure formed of only 86 elements (figure 4.19). The connectivity matrix and the nodal list are included in the annex C.

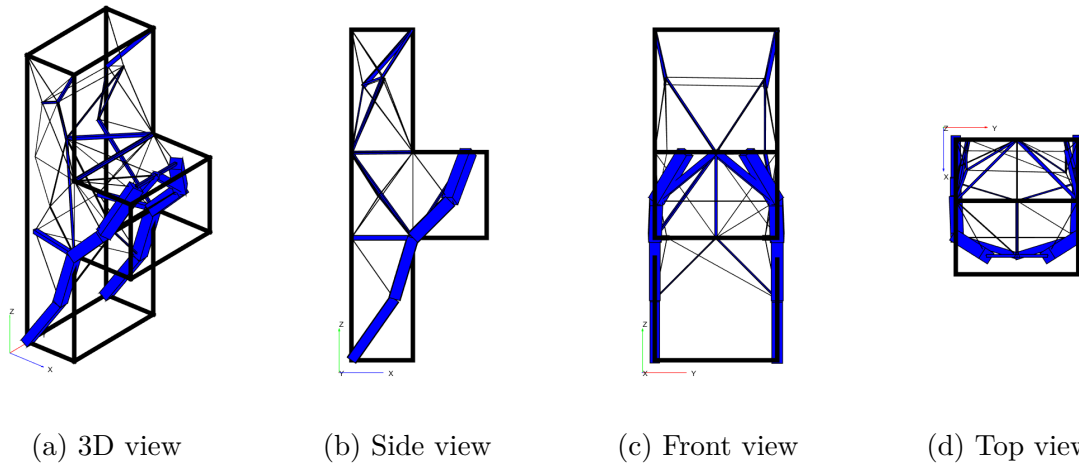


Figure 4.19: Manually modified Strut and tie model resultant from a size-topology-geometry scheme ($m = 86$)

Table 4.6: Computed need of steel reinforced per zone (3D ST) [cm^3]

Zone	Total
Arm	927.3
Forehead	1086.83
Joint	382.33
Foot	198.63
Total	2595.1

4.6 Results

The following table presents the total need of steel reinforcement per zone for the four different models presented: the surface representations where the steel reinforcement was computed using the Capra-Maury algorithm, the planar and the solid representations treated through the computer aided ST approach.

Table 4.7: Comparative table of need of steel reinforcement per zone [cm³]

Zone	CM (coarse)	ST (2D)	ST (3D)
Arm	3764.67	567.72	927.3
Forehead	944.33	1078.05	1086.83
Joint	927.89	357.1	382.33
Foot	128.92	321.04	198.63
Total	5765.81	2323.9	2595.1

Table 4.8: Comparative table of need of steel reinforcement per zone. kg of steel per cubic meter of concrete

Zone	Volume [m ³]	CM (coarse)	ST (2D)	ST (3D)
Arm	0.42	70.36	10.61	17.33
Forehead	0.50	14.83	16.93	17.06
Joint	0.35	20.81	8.01	8.58
Foot	0.50	2.02	5.04	3.12
$\Sigma = 1.77$		$\bar{X} = 27.01$	$\bar{X} = 10.15$	$\bar{X} = 11.52$

*The density of steel was taken as 7.85 g/cm³

As it can be inferred, the quantities herein presented, are raw results and should be arranged and smoothed before going to the blueprints. These arrangements may slightly increase the shown reinforcement densities.

4.7 Discussion

From the results obtained several conclusions can be done. The comments will be divided into two topics:

1. the capabilities of the algorithm
2. the quantity of reinforcement

4.7.1 Capabilities of the algorithm

So far, the developed algorithm fulfils the most important criteria established for this work

- **Standard FE modelling.** Described before, the application of the approach starts with a normal linear-elastic finite element model (bi- or three-dimensional). From the results obtained, the algorithm is able to propose and to design a suitable ST model.

- **Rational-based approach.** All the sub-routines were inspired in the practice of the engineer and remain close to the steep followed during a fully manual ST approach.
- **Accordance to with codes of construction.** Similar to the previous point, the algorithm and some choices (such as the selection of the nodes of the ST system) were made based on the thumb rules found in the construction manuals.
- **Computer aided ST model computation.** Even if a fully automatic design approach was the goal at the earliest stage of this project, a computer aided approach was found sufficient.

From the examples exposed, we note that the algorithm is able to identify feasible ST models from a self created ground structures. As it can be appreciated, the worked examples tend to present a good behaviour for planar structures however, some complications have been encountered in 3D cases:

- **Asymmetrical results for symmetrical problems.** As seen in the presented example, slight asymmetries can be found in the final distribution of elements. The source of this disparities is linked to the use the *loess* regression to approach a feasible inclination based on the principal stress field direction. As explained in the previous chapter, the application of the *loess* losses its applicability for groups of angles presenting an important angular distribution. Factor that has been easily overcome on 2D but yet, it disturbs the results for 3D cases.

Initially, in an effort to counter the "noise" brought by the *loess* regressions, the geometry optimisation was implemented. This optimisation scheme provided advantages such as the capacity of merging existent nodes in the structure and directly contributes to the mesh-low dependency but, due to its nature, it increases the quantity of operations to achieve an iteration highly influencing the next point.

- **Time consumption.** Even though it has been said that computation time would not be considered, a comment should be made for the application of size-topology-geometry optimisation scheme in 3D structures. While the feasible values and restrictions for cross sections remain unchanged when passing from a bi-dimensional problem to a three-dimensional one, the number of plausible nodal positions and restrictions increase. The time consumption is widely affected by specially three-dimensional Boolean operations needed to verify if the a plausible nodal modification remains inside the feasible domain (structure).
- **Manual intervention.** Whether a manual intervention would be unavoidable on a computer aided approach, for the reasons already expressed, this intervention is desired to be as minimal as possible. In order to obtain the final ST model for the 3D brick model, a hand intervention was required. The use of a filter on the cross sections or the manual modification of some nodes was necessary, in spite the fact of having appreciable improvements compared to the initial ground structure (in terms of volume and elements reduction).

4.7.2 Quantity of reinforcement

From table 4.7 it can be appreciated that current practices may lead to an important increase in the quantity of need of steel when detailing D-regions. Steel reinforcement quantity drops to half when using a more appropriated approach such as the Strut-and-Tie Method.

The validity and, in consequence, the results of a surface-element-based model such as the one presented here is debatable, yet it represents a quotidian engineering practice. Besides, it has been shown that the shear strength of reinforced concrete local elements computed using STM, predicts good accuracy judged from comparison with test results [Zechmann and Matamoros, 2002, Hofer and McCabe, 1998]. Thus a rational approach would be preferred over a design through CM algorithm or similar.

Another advantage that the Strut-and-Tie Method presents over CM is the easiness to pass the steel need to the blueprints. While the results of CM often need a smoothing process, the ties can be directly proposed as a steel reinforcement pattern.

Concluding remarks

Review of contributions

Chapter 1 presents a summary of the current practice engineering design addressed to reinforcement computation. In this chapter, efforts were made to point out the benefits of rational approaches, specifically the strut-and-tie approach, to threat local members. These techniques present the advantage of allowing a designer to follow the forces through a structure with discontinuities (either static or geometric) which formerly were beyond the scope of engineering practice based on the flexural theory. So far, one of the main drawbacks of its application is the need of highly skilled structural engineers for a manual approach or, the need of important resources in terms of computational effort for an, arguably, less appropriate continuous optimisation.

Within Chapter 2, the ground structure approach arises as a suitable option to extract feasible ST models from solid structures. The inconveniences of the ground structure lie in the fact that a low populated ground structure itself needs to be proposed based on experience leading again to the need of highly skilled structural engineers. Another possibility is to initially propose high populated ground structures and introduce powerful optimisation algorithms.

Chapter 3 proposes an alternative algorithm able to automatically propose and design ground structures from the results of bi- or three-dimensional linear elastic analysis.

- **Strut pattern search.** The fashion developed to construct the initial strut pattern structures was directly inspired from the recommendations made by Schlaich and also the thumb rules found principally in the Eurocodes and the ACI. This aspect allowed to keep the methodology as close as possible to the manual approach. The division of the geometry based on the Voronoi tessellation, as well as the application of the *loess* regression over the direction of the stress fields, are original ideas developed during this work.
- **Construction of ground structures.** Even though the use of ground structures has been applied before to find ST models, the definition of such structures is predefined by the user and automatically developed as in the approach proposed.
- **Optimised ST models.** The selected optimisation scheme is presented as an advantageous tool for weight (cost) reduction in the engineering domain. Despite of the benefits that the inclusion of optimisation techniques may have in the industrial field, its application remain mostly for research purposes. This project examines the application of this type of techniques to cases commonly encountered in the building industry.

- **Capabilities in 2D and 3D.** The advantages of having computer aided ST approaches become clearer when facing three-dimensional problems. For some cases, the distribution of stress in volume structures may not always be evident and at first glance a ST model may appear to be nearly impossible. Computer aided approaches tend to reduce the complexity of the problem by predefining whether load-transfer mechanisms, element distributions, nodal positions, cross sections or, as in this case, a suitable ST model. This capability opens the door for the analysis and reinforcement of complex three-dimensional problems and places it beyond surface-like FE models.

Referring to the objectives, this work attained to merge the rational approach known as Strut-and-Tie with an automatic optimisation. The central hypothesis was confirmed given that the proposed methodology and the implemented algorithm allow to obtain suitable ground structures based on the direction fields of principal stresses. The results show that it is also plausible to automatically obtain an optimum ST pattern from the proposed ground structure.

Future work

This work represents a first stage of a potential future project that intends to develop an open-source analysis tool.

Given the results attained within these three years, the author presents the tasks where, according to the experience, future work should focus.

- **Numerical computing environment and programming language.** In the author's experience, MATLAB is an excellent numerical computing environment and programming language adapted to the research and the development of prototype tools. Besides owning a wide range of specific libraries, MATLAB is intuitive and easy to learn. However, licensing for industry may be seen as a significant inconvenience (specially small companies or free-lancers). Free open-source alternatives such as C++, Java or even Python are available and some of them are potentially considerably more powerful than MATLAB for general programming purposes. These programming languages are arguably better suited to development of full-scale systems.
- **3D cases.** As it was stated, the algorithmic advances attained in this work are perfectible and can be optimised to reduce the manual intervention. Even if the procedure can lead to ST models, for three-dimensional cases, the implemented algorithm presents minor drawbacks that were not encountered for bi-dimensional structures.
- **Optimisation procedure.** Given the vast quantity of optimisation procedures, it would be impossible to test all of them. As it was mentioned before, the selection of the used optimisation scheme was based on literature review. It would be worthy to design a campaign of numerical tests to select a more appropriated procedure, single or a combination.
- **Non-linear capabilities.** One of the main practical issues in the practice of RC is that almost any methodology present is that the design is performed on two steps:

the computation of the internal forces developed on an idealised linear-elastic homogeneous material and, 2) the equilibrium of such forces through the inclusion a tensile resistant material. Within the real element, the inclusion of reinforcement bars could deviate the stress distribution for which it was designed.

A non-linear revision of the final ST model could help to validate the models by glimpse the strut formation and the developpement of the inner elements.

- **Application in practice.** Being based on a full stress design, the proposed algorithm suits a serviceability limit state. Further modifications may have be done in order to be used for ultimate limit state.

Projected trends

In recent years it can be observed a trend to develop ST models for steel concrete. From the point of view of the mechanics, a truss-like reinforcement would be preferred over the traditional grids. For decades the use of steel reinforcement has been aligned to principal constructive axis mainly due to technical (economical) constraints. With the development of industrial 3D printings this may change. Potential advantages of this process include faster construction, lower labour costs and the production of less waste.

The reinforcement of real structures according to strut-and-tie models can represent an suitable alternative. Truss-like reinforcement following stress trajectories would help to reduce the existent gap between the linear-elastic models (commonly used for the design) and the real structures.

Closing notes

In summary, it has been shown that this research has satisfied the objective of reducing the evident gap between the rational approach known as Strut-and-Tie and automatic applied methodologies based on finite element analysis industrially applied.

The algorithm developed within this work can be seen as one more alternatives that the structural engineer has to safely design specific zones of the reinforced concrete structures.

Even if some algorithmic challenges, specially in terms of process optimisation, are still to be addressed, the proposed methodology could guide the structural engineer through the design of D-regions using strut-and-tie models.

Bibliography

- [Aashto L.R.F.D., 1998] Aashto L.R.F.D. (1998). Bridge design specifications.
- [Achtziger, 1996] Achtziger, W. (1996). Truss topology optimization including bar properties different for tension and compression. *Structural and Multidisciplinary Optimization*, 12(1):63–74.
- [Achtziger, 2007] Achtziger, W. (2007). On simultaneous optimization of truss geometry and topology. *Structural and Multidisciplinary Optimization*, 33(4-5):285–304.
- [ACI-318, 2008] ACI-318 (2008). Building code requirements for structural concrete : (aci 318-95) ; and commentary (aci 318r-95). American Concrete Institute.
- [Adeli, 2002] Adeli, H. (2002). *Advances in design optimization*. CRC Press.
- [Adeli and Kamal, 1986] Adeli, H. and Kamal, O. (1986). Efficient optimization of space trusses. *Computers & structures*, 24(3):501–511.
- [Aguilar et al., 2002] Aguilar, G., Matamoros, A. B., Parra-Montesinos, G. J., Ramírez, J. A., and Wight, J. K. (2002). Experimental evaluation of design procedures for shear strength of deep reinforced concrete beams.
- [Almeida et al., 2013] Almeida, V. S., Simonetti, H. L., and Neto, L. O. (2013). Comparative analysis of strut-and-tie models using smooth evolutionary structural optimization. *Engineering Structures*, 56:1665–1675.
- [Alshegeir and Ramirez, 1992] Alshegeir, A. and Ramirez, J. (1992). Computer graphics in detailing strut-tie models. *Journal of computing in civil engineering*, 6(2):220–232.
- [Armer et al., 1968] Armer, G., Mills, H., and Wood, R. (1968). Reinforcement of slabs in accordance with a pre-determined field of moments. *Concrete*, 2(8):319.
- [Arora, 2004] Arora, J. (2004). *Introduction to optimum design*. Academic Press.
- [Arora and Haug, 1976] Arora, J. and Haug, E. (1976). Efficient optimal design of structures by generalized steepest descent programming. *International Journal for Numerical Methods in Engineering*, 10(4):747–766.
- [Aruoba and Fernández-Villaverde, 2015] Aruoba, S. B. and Fernández-Villaverde, J. (2015). A comparison of programming languages in macroeconomics. *Journal of Economic Dynamics and Control*, 58:265–273.

-
- [Baldock and Shea, 2006] Baldock, R. and Shea, K. (2006). Structural topology optimization of braced steel frameworks using genetic programming. In *Intelligent Computing in Engineering and Architecture*, pages 54–61. Springer.
- [Barton et al., 1991] Barton, D., Anderson, R., Bouadi, A., Jirsa, J., and Breen, J. (1991). An investigation of strut-and-tie models for dapped beam details.
- [Bathe, 2006] Bathe, K.-J. (2006). *Finite element procedures*. Klaus-Jurgen Bathe.
- [Bazaraa et al., 2013] Bazaraa, M. S., Sherali, H. D., and Shetty, C. M. (2013). *Nonlinear programming: theory and algorithms*. John Wiley & Sons.
- [Bekdaş et al., 2017] Bekdaş, G., Nigdeli, S. M., and Türkakin, O. H. (2017). Non-linear programming for sizing optimization of truss structures.
- [Bendsøe et al., 1994] Bendsøe, M. P., Ben-Tal, A., and Zowe, J. (1994). Optimization methods for truss geometry and topology design. *Structural optimization*, 7(3):141–159.
- [Bendsøe and Kikuchi, 1988] Bendsøe, M. P. and Kikuchi, N. (1988). Generating optimal topologies in structural design using a homogenization method. *Computer methods in applied mechanics and engineering*, 71(2):197–224.
- [Bendsøe and Sigmund, 2003] Bendsøe, M. P. and Sigmund, O. (2003). *Topology optimization: theory, methods and applications. 2003*. Springer.
- [Birrcher et al., 2009] Birrcher, D., Tuchscherer, R., Huizinga, M., Bayrak, O., Wood, S. L., and Jirsa, J. O. (2009). Strength and serviceability design of reinforced concrete deep beams. Technical report.
- [Bisch, 2013] Bisch, P. (2013). *Mécanique des coques: théorie et applications*. Presses des Ponts.
- [Blaauwendraad and Hoogenboom, 2002] Blaauwendraad, J. and Hoogenboom, P. C. (2002). Design instrument spancad for shear walls and d-regions. In *FIB Congress*, volume 1, page 2002.
- [Boissonnat and Cazals, 2000] Boissonnat, J.-D. and Cazals, F. (2000). *Natural neighbour coordinates of points on a surface*. PhD thesis, INRIA.
- [British Standards Institution, 2005] British Standards Institution (2005). Eurocode 8: Design of structures for earthquake resistance-.
- [Capra and Maury, 1978] Capra, A. and Maury, J. (1978). Calcul automatique du ferrailage optimal des plaques ou coques en béton armé. *Annales de l'insitut technique du bâtiment et des travaux publics*, 367.
- [Chae and Yun, 2016] Chae, H.-S. and Yun, Y. M. (2016). Strut-tie models and load distribution ratios for reinforced concrete beams with shear span-to-effective depth ratio of less than 3 (ii) validity evaluation. *Journal of the Korea Concrete Institute*, 28(3):267–278.

-
- [Cherkaev, 2012] Cherkaev, A. (2012). *Variational methods for structural optimization*, volume 140. Springer Science & Business Media.
- [Christensen and Klarbring, 2008] Christensen, P. W. and Klarbring, A. (2008). *An introduction to structural optimization*, volume 153. Springer Science & Business Media.
- [Clarke and Cope, 1984] Clarke, L. and Cope, R. (1984). *Concrete slabs: analysis and design*. CRC Press.
- [Cleveland and Devlin, 1988] Cleveland, W. S. and Devlin, S. J. (1988). Locally weighted regression: an approach to regression analysis by local fitting. *Journal of the American statistical association*, 83(403):596–610.
- [Collins and Mitchell, 1980] Collins, M. P. and Mitchell, D. (1980). Shear and torsion design of prestressed and non-prestressed concrete beams. *PCI journal*, 25(5):32–100.
- [Cuevas and Villegas, 2006] Cuevas, O. M. G. and Villegas, F. R. F. (2006). *Aspectos fundamentales del concreto reforzado*. Limusa Noriega.
- [Dammika and Anwar, 2013] Dammika, A. and Anwar, N. (2013). Extraction of strut and tie model from 3d solid element mesh analysis.
- [Dantzig, 2016] Dantzig, G. (2016). *Linear programming and extensions*. Princeton university press.
- [Davidovici et al., 2013] Davidovici, V. et al. (2013). *Pratique du calcul sismique: guide d'application de l'Eurocode 8*. Editions Eyrolles.
- [Delmas, 2011] Delmas, J. (2011). *Calculation algorithm of the densities of reinforcement*. Code_ Aster.
- [Devadas, 2003] Devadas, M. (2003). *Reinforced concrete design*. Tata McGraw-Hill Education.
- [Dorn, 1964] Dorn, W. S. (1964). Automatic design of optimal structures. *Journal de mecanique*, 3:25–52.
- [Edelsbrunner et al., 1983] Edelsbrunner, H., Kirkpatrick, D., and Seidel, R. (1983). On the shape of a set of points in the plane. *IEEE Transactions on information theory*, 29(4):551–559.
- [El-Metwally and Chen, 2017] El-Metwally, S. and Chen, W.-F. (2017). *Structural Concrete: Strut-and-Tie Models for Unified Design*. CRC Press.
- [Eschenauer and Olhoff, 2001] Eschenauer, H. A. and Olhoff, N. (2001). Topology optimization of continuum structures: a review. *Applied Mechanics Reviews*, 54(4):331–390.
- [Eurocode2, 2008] Eurocode2 (2008). Design of concrete structures.
- [Farshi and Alinia-Ziazi, 2010] Farshi, B. and Alinia-Ziazi, A. (2010). Sizing optimization of truss structures by method of centers and force formulation. *international Journal of Solids and Structures*, 47(18):2508–2524.

-
- [Fisher, 1995] Fisher, N. I. (1995). *Statistical analysis of circular data*. Cambridge University Press.
- [Fleury, 1979] Fleury, C. (1979). A unified approach to structural weight minimization. *Computer Methods in Applied Mechanics and Engineering*, 20(1):17–38.
- [for Structural Concrete, 2008] for Structural Concrete, I. F. (2008). Practitioners’ guide to finite element modelling of reinforced concrete structures. *State-of-Art Report*.
- [Foster et al., 2003] Foster, S. J., Marti, P., and Mojsilovic, N. (2003). Design of reinforced concrete solids using stress analysis. *Structural Journal*, 100(6):758–764.
- [Foulds, 2012] Foulds, L. R. (2012). *Optimization techniques: an introduction*. Springer Science & Business Media.
- [Fraternali et al., 2011] Fraternali, F., Marino, A., Sayed, T. E., and Cioppa, A. D. (2011). On the structural shape optimization through variational methods and evolutionary algorithms. *Mechanics of Advanced Materials and Structures*, 18(4):225–243.
- [Ganzreli, 2013] Ganzreli, S. (2013). Direct fully stressed design for displacement constraints. In *10th World Congress on Structural and Multidisciplinary Optimization*, pages 19–24.
- [Gaynor et al., 2012] Gaynor, A. T., Guest, J. K., and Moen, C. D. (2012). Reinforced concrete force visualization and design using bilinear truss-continuum topology optimization. *Journal of Structural Engineering*, 139(4):607–618.
- [Gil and Andreu, 2001] Gil, L. and Andreu, A. (2001). Shape and cross-section optimisation of a truss structure. *Computers & Structures*, 79(7):681–689.
- [Gordon, 2009] Gordon, J. E. (2009). *Structures: or why things don’t fall down*. Da Capo Press.
- [Grandić et al., 2015] Grandić, D., Šćulac, P., and Grandić, I. Š. (2015). Shear resistance of reinforced concrete beams in dependence on concrete strength in compressive struts. *Technical Gazette*, 22(4):925–934.
- [Greene, 2003] Greene, W. H. (2003). *Econometric analysis*. Pearson Education India.
- [Griffith and Stewart, 1961] Griffith, R. E. and Stewart, R. (1961). A nonlinear programming technique for the optimization of continuous processing systems. *Management science*, 7(4):379–392.
- [Haftka and Gürdal, 2012] Haftka, R. T. and Gürdal, Z. (2012). *Elements of structural optimization*, volume 11. Springer Science & Business Media.
- [Hancock, 1917] Hancock, H. (1917). *Theory of maxima and minima*.
- [Hernández, 1993] Hernández, S. (1993). Del diseño convencional al diseño óptimo. posibilidades y variantes. parte i. análisis de sensibilidad y optimización local y global.

-
- [Herve et al., 2014] Herve, G., Cloitre, L., El Kadiri, S., Secourgeon, E, Mennela, D., and Carême, C. (2014). Comparative study of shell element and brick element models for npp structures. In *Proceedings of TINCE 2014 Conference*, pages –.
- [Hillier, 2012] Hillier, F. S. (2012). *Introduction to operations research*. Tata McGraw-Hill Education.
- [Hofer and McCabe, 1998] Hofer, A. A. and McCabe, S. L. (1998). Comparison of shear capacity of t-beams using strut and tie analysis. Technical report, University of Kansas Center for Research, Inc.
- [Hoogenboom and De Boer, 2010] Hoogenboom, P. and De Boer, A. (2010). Computation of optimal concrete reinforcement in three dimensions. In *Proceedings of EURO-C*, pages 639–646.
- [Hrennikoff, 1941] Hrennikoff, A. (1941). Solution of problems of elasticity by the framework method. *J. appl. Mech.*
- [Hsu, 1992] Hsu, T. T. (1992). *Unified theory of concrete concrete*, volume 5. CRC press.
- [Johansen, 1962] Johansen, K. W. (1962). *Yield-line theory*. Cement and Concrete Association.
- [Johnson, 1986] Johnson, D. (1986). *Advanced structural mechanics: an introduction to continuum mechanics and structural dynamics*. Collins.
- [Karmarkar, 1984] Karmarkar, N. (1984). A new polynomial-time algorithm for linear programming. In *Proceedings of the sixteenth annual ACM symposium on Theory of computing*, pages 302–311. ACM.
- [Kennedy and Goodchild, 2004] Kennedy, G. and Goodchild, C. (2004). Practical yield line design. *The concrete centre, Riverside house*, 4.
- [Khot and B., 1979] Khot, N. S., B. L. and B., V. V. (1979). Comparison of optimality criteria algorithms for minimum weight design of structures. *AIAA Journal*, 17(2):182–190.
- [Kirsch, 1989] Kirsch, U. (1989). Optimal topologies of truss structures. *Computer Methods in Applied Mechanics and Engineering*, 72(1):15–28.
- [Kirsch, 2012] Kirsch, U. (2012). *Structural optimization: fundamentals and applications*. Springer Science & Business Media.
- [Klee and Minty, 1970] Klee, V. and Minty, G. J. (1970). How good is the simplex algorithm. Technical report, WASHINGTON UNIV SEATTLE DEPT OF MATHEMATICS.
- [Kuchma and Tjhin, 2001] Kuchma, D. A. and Tjhin, T. N. (2001). Cast (computer aided strut-and-tie) design tool. In *Structures 2001: A Structural Engineering Odyssey*, pages 1–7.

-
- [Kvasnica et al., 2004] Kvasnica, M., Grieder, P., Baotic, M., and Morari, M. (2004). Multi-parametric toolbox (mpt). In *HSCC*, pages 448–462. Springer.
- [Lamberti and Pappalettere, 2000] Lamberti, L. and Pappalettere, C. (2000). Comparison of the numerical efficiency of different sequential linear programming based algorithms for structural optimisation problems. *Computers & Structures*, 76(6):713–728.
- [Ledoux and Gold, 2005] Ledoux, H. and Gold, C. (2005). An efficient natural neighbour interpolation algorithm for geoscientific modelling. *Developments in spatial data handling*, pages 97–108.
- [Levy, 2010] Levy, D. (2010). Introduction to numerical analysis. *Department of Mathematics and Center for Scientific Computation and Mathematical Modeling (CSCAMM) University of Maryland*, pages 2–2.
- [Lew and Narov, 1983] Lew, I. P. and Narov, F. (1983). Three-dimensional equivalent frame analysis of shearwalls. *Concrete International*, 5(10):25–30.
- [Li, 1990] Li, X. (1990). Truss structure optimum design and its engineering application. *Computers & Structures*, 36(3):567–573.
- [MacGregor, 1992] MacGregor, J. G. (1992). *Reinforced concrete: Mechanics and design*.
- [Marti, 1978] Marti, P. (1978). *Plastic analysis of reinforced concrete shear walls*. Birkhäuser.
- [Marti, 1985] Marti, P. (1985). Basic tools of reinforced concrete beam design. In *Journal Proceedings*, volume 82, pages 46–56.
- [Marti, 1990] Marti, P. (1990). Design of concrete slabs for transverse shear. *Structural Journal*, 87(2):180–190.
- [Marti et al., 1987] Marti, P., Leesti, P., and Khalifa, W. U. (1987). Torsion tests on reinforced concrete slab elements. *Journal of Structural Engineering*, 113(5):994–1010.
- [Mattock et al., 1976] Mattock, A. H., Chen, K., and Soongswang, K. (1976). The behavior of reinforced concrete corbels. *PCI Journal*, 21(2):52–77.
- [May and Ganaba, 1988] May, I. and Ganaba, T. (1988). A full range analysis of reinforced concrete slabs using finite elements. *International Journal for Numerical Methods in Engineering*, 26(4):973–985.
- [May and Lodi, 2005] May, I. and Lodi, S. H. (2005). Deficiencies of the normal moment yield criterion for rc slabs. *Proceedings of the Institution of Civil Engineers-Structures and Buildings*, 158(6):371–380.
- [Mehrotra, 1992] Mehrotra, S. (1992). On the implementation of a primal-dual interior point method. *SIAM Journal on optimization*, 2(4):575–601.
- [Moaveni, 2011] Moaveni, S. (2011). *Finite element analysis theory and application with ANSYS, 3/e*. Pearson Education India.

-
- [Mörsch, 1902] Mörsch, E. (1902). Der eisenbetonbau, seine anwendung und theorie. *Wayss and Freytag, AG, Im selbstverlag der Firma, Neustadt ad Haardt, May*.
- [Mueller and Burns, 2001] Mueller, K. M. and Burns, S. A. (2001). Fully stressed frame structures unobtainable by conventional design methodology. *International Journal for Numerical Methods in Engineering*, 52(12):1397–1409.
- [Muttoni et al., 2015] Muttoni, A., Ruiz, M. F., and Niketic, F. (2015). Design versus assessment of concrete structures using stress fields and strut-and-tie models. *ACI Structural Journal*, 112(5):605.
- [Nagarajan et al., 2010] Nagarajan, P., Jayadeep, U., and Pillai, T. M. (2010). Application of micro truss and strut and tie model for analysis and design of reinforced concrete structural elements. *Sonklanakarın Journal of Science and Technology*, 31(6):647.
- [Nawy, 2000] Nawy, E. (2000). *Reinforced concrete: A fundamental approach*.
- [Nielsen, 1964] Nielsen, M. P. (1964). *Limit analysis of reinforced concrete slabs*. Danish Acad. of Technical Sciences.
- [Nilson, 1997] Nilson, A. (1997). *Design of concrete structures*. Number 12th Edition.
- [Ohsaki and Swan, 2002] Ohsaki, M. and Swan, C. (2002). Topology and geometry optimization of trusses and frames. *Recent advances in optimal structural design*, 46.
- [Papalambros and Wilde, 2000] Papalambros, P. Y. and Wilde, D. J. (2000). *Principles of optimal design: modeling and computation*. Cambridge university press.
- [Park and Gamble, 2000] Park, R. and Gamble, W. L. (2000). *Reinforced concrete slabs*. John Wiley & Sons.
- [Park et al., 2006] Park, S. W., Linsen, L., Kreylos, O., Owens, J. D., and Hamann, B. (2006). Discrete sibson interpolation. *IEEE Transactions on Visualization and Computer Graphics*, 12(2):243–253.
- [Przemieniecki, 1985] Przemieniecki, J. S. (1985). *Theory of matrix structural analysis*. Courier Corporation.
- [Pyzara et al., 2011] Pyzara, A., Bylina, B., and Bylina, J. (2011). The influence of a matrix condition number on iterative methods’ convergence. In *Computer Science and Information Systems (FedCSIS), 2011 Federated Conference on*, pages 459–464. IEEE.
- [Ramirez and Breen, 1991] Ramirez, J. A. and Breen, J. E. (1991). Evaluation of a modified truss-model approach for beams in shear. *Structural Journal*, 88(5):562–572.
- [Rao et al., 2007] Rao, G. A., Kunal, K., and Eligehausen, R. (2007). Shear strength of rc deep beams. In *Proceedings of the 6th International Conference on Fracture Mechanics of Concrete and Concrete Structures*, volume 2, pages 693–699.
- [Razani, 1965] Razani, R. (1965). Behavior of fully stressed design of structures and its relationship to minimum-weight design. *AIAA Journal*, 3(12):2262–2268.

-
- [Ringertz, 1985] Ringertz, U. T. (1985). On topology optimization of trusses. *Engineering optimization*, 9(3):209–218.
- [Ritter, 1899] Ritter, W. (1899). Die bauweise hennebique (the hennebique construction method). *Die Bauweise Hennebique, Schweizerische Bauzeitung*, 33(7):41–61.
- [RoboBat, 2002] RoboBat (2002). *Manuel d'utilisation Robot Béton Armé*.
- [Saniee, 2008] Saniee, K. (2008). A simple expression for multivariate lagrange interpolation.
- [Schittkowski et al., 1994] Schittkowski, K., Zillober, C., and Zotemantel, R. (1994). Numerical comparison of nonlinear programming algorithms for structural optimization. *Structural and Multidisciplinary Optimization*, 7(1):1–19.
- [Schlaich et al., 1987] Schlaich, J., Schäfer, K., and Jennewein, M. (1987). Toward a consistent design of structural concrete. *PCI journal*, 32(3):74–150.
- [Schmith and Fox, 1965] Schmith, L. and Fox, R. (1965). An integrated approach to structural synthesis and analysis. *AIAA JOURNAL*, 3(6).
- [Sedaghati and Esmailzadeh, 2003] Sedaghati, R. and Esmailzadeh, E. (2003). Optimum design of structures with stress and displacement constraints using the force method. *International journal of mechanical sciences*, 45(8):1369–1389.
- [Shah et al., 2011] Shah, A., Haq, E., and Khan, S. (2011). Analysis and design of disturbed regions in concrete structures. *Procedia Engineering*, 14:3317–3324.
- [Shobeiri, 2016] Shobeiri, V. (2016). Topology optimization using bi-directional evolutionary structural optimization based on the element-free galerkin method. *Engineering Optimization*, 48(3):380–396.
- [Sibson, 1981] Sibson, R. (1981). A brief description of natural neighbor interpolation. *Interpreting multivariate data*, pages 21–36.
- [Singh et al., 2018] Singh, B., Vimal, A., and Gaurav, G. (2018). Whither transverse reinforcement in bottle-shaped struts? In *Structures*. Elsevier.
- [Soltani and Corotis, 1988] Soltani, M. and Corotis, R. B. (1988). Failure cost design of structural systems. *Structural safety*, 5(4):239–252.
- [Starčev-Ćurčin et al., 2013] Starčev-Ćurčin, A., Rašeta, A., and Brujić, Z. (2013). Automatic generation of planar rc strut-and-tie models. *Facta universitatis-series: Architecture and Civil Engineering*, 11(1):1–12.
- [Svanberg, 1981] Svanberg, K. (1981). On local and global minima in structural optimization. Technical report, ROYAL INST OF TECH STOCKHOLM (SWEDEN).
- [Swan et al., 1999] Swan, C. C., Arora, J. S., and Kocer, F. Y. (1999). Continuum and ground structure topology methods for concept design of structures. In *1999 New Orleans Structures Congress*.

-
- [Thompson, 2002] Thompson, K. (2002). *The anchorage behavior of headed reinforcement in CCT nodes and lap splices*. PhD thesis.
- [Topkis and Veinott, 1967] Topkis, D. M. and Veinott, Jr, A. F. (1967). On the convergence of some feasible direction algorithms for nonlinear programming. *SIAM Journal on Control*, 5(2):268–279.
- [Turmo et al., 2009] Turmo, J., Ramos, G., and Aparicio, A. (2009). Shear truss analogy for concrete members of solid and hollow circular cross section. *Engineering Structures*, 31(2):455–465.
- [Unnikrishna and Devdas, 2003] Unnikrishna, P. and Devdas, M. (2003). Reinforced concrete design.
- [Van Kreveld et al., 2011] Van Kreveld, M., Van Lankveld, T., and Veltkamp, R. C. (2011). On the shape of a set of points and lines in the plane. In *Computer Graphics Forum*, volume 30, pages 1553–1562. Wiley Online Library.
- [Vanderplaats, 1984a] Vanderplaats, G. N. (1984a). An efficient feasible directions algorithm for design synthesis. *AIAA Journal(ISSN 0001-1452)*, 22:1633–1640.
- [Vanderplaats, 1984b] Vanderplaats, G. N. (1984b). *Numerical optimization techniques for engineering design: with applications*, volume 1. McGraw-Hill New York.
- [Vanderplaats and Moses, 1973] Vanderplaats, G. N. and Moses, F. (1973). Structural optimization by methods of feasible directions. *Computers & Structures*, 3(4):739–755.
- [Vecchio and Selby, 1991] Vecchio, F. and Selby, R. (1991). Toward compression-field analysis of reinforced concrete solids. *Journal of Structural Engineering*, 117(6):1740–1758.
- [Vecchio and Collins, 1986] Vecchio, F. J. and Collins, M. P. (1986). The modified compression-field theory for reinforced concrete elements subjected to shear. In *Journal Proceedings*, volume 83, pages 219–231.
- [Venkayya, 1971] Venkayya, V. (1971). Design of optimum structures. *Computers & Structures*, 1(1-2):265–309.
- [Venkayya, 1978] Venkayya, V. B. (1978). Structural optimization: a review and some recommendations. *International Journal for Numerical Methods in Engineering*, 13(2):203–228.
- [Wahlgren and Bailleul, 2016] Wahlgren, M. and Bailleul, N. (2016). Experimental analysis of limitations in the strut-and-tie method.
- [Williams et al., 2012] Williams, C., Deschenes, D., and Bayrak, O. (2012). Strut-and-tie model design examples for bridges: Final report. *Center for Transportation Research, Report No. FHWA/TX-12/5-5253-01-1, Austin, Texas*.
- [Winston and Goldberg, 2004] Winston, W. L. and Goldberg, J. B. (2004). *Operations research: applications and algorithms*, volume 3. Thomson Brooks/Cole Belmont.

-
- [Wood, 1968] Wood, R. (1968). Reinforcement of slabs in accordance with a pre-determined field of moments. *Concrete*, 2(2):69.
- [Wood, 1961] Wood, R. H. (1961). *Plastic and elastic design of slabs and plates: with particular reference to reinforced concrete floor slabs*. Thames and Hudson.
- [Wright and Nocedal, 1999] Wright, S. J. and Nocedal, J. (1999). Numerical optimization. *Springer Science*, 35(67-68):7.
- [Yun and Lee, 2005] Yun, Y. and Lee, W. (2005). Nonlinear strut-tie model analysis of pre-tensioned concrete deep beams. *Advances in Structural Engineering*, 8(1):85–98.
- [Zechmann and Matamoros, 2002] Zechmann, R. and Matamoros, A. B. (2002). Use of strut-and-tie models to calculate the strength of deep beams with openings. Technical report, University of Kansas Center for Research, Inc.
- [Zhong et al., 2016] Zhong, J., Wang, L., Li, Y., and Zhou, M. (2016). A practical approach for generating the strut-and-tie models of anchorage zones. *Journal of Bridge Engineering*, 22(4):04016134.
- [Zoutendijk, 1960] Zoutendijk, G. (1960). *Methods of feasible directions: a study in linear and non-linear programming*. Elsevier.

List of Figures

1.1	Assumed material stress-strain relationships according to Eurocode2.	14
1.2	Simplified strain and stress distribution in a plane section [EC2].	15
1.3	Failure patterns as a function of beam slenderness [Nawy, 2000].	16
1.4	Ritter’s truss analogy.	17
1.5	Example of output from a membrane’s FE modelling	19
1.6	Concrete and steel reinforcement stress components	20
1.7	Mohr’s circle for reinforcing steel placed solely in the Y-direction	20
1.8	Mohr’s circles for isotropically reinforced pannels	21
1.9	Simply supported two-way slab with the bottom steel having yielded along the yield lines	23
1.10	Normal yield criterion.	24
1.11	Sandwich model.	25
1.12	Reinforced plate moments	27
1.13	Orthogonal reinforcement	27
1.14	Reinforced shell element	29
1.15	Validity domain (adapted from [Capra and Maury, 1978]).	31
1.16	General validity domain for different values of Θ [Capra and Maury, 1978].	31
1.17	Typical nuclear island structural outline adapted from [Herve et al., 2014] .	32
1.18	Thermal load case modelling of a thick raft with engineering practices [Herve et al., 2014]	33
1.19	Compression field for 3-dimensional stresses	34
1.20	Idealised 3-dimensional reinforcement	34
1.21	Flowchart design procedure using STM	38
1.22	Local zone of a beam with sudden thickness change	39
1.23	Different ST models developed under different loading systems.	39
1.24	Nodal proportioning techniques - hydrostatic versus non-hydrostatic nodes [Birrcher et al., 2009]	41
1.25	Representative node types [Birrcher et al., 2009]	41
1.26	Bottle-shaped strut (adapted from [Singh et al., 2018]).	42
1.27	Parameters for the determination of transverse tensile forces in a compression field with smeared reinforcement [Eurocode2, 2008].	43
2.1	Three categories of structural optimisation.	50
2.2	Shape of feasible region (adapted from [Adeli, 2002]).	52
2.3	Graphical explanation of KKT conditions as seen in [Kirsch, 2012]	56
2.4	Improving feasible directions (modified from [Bazaraa et al., 2013]).	59
2.5	Conceptual processes of optimisation of continuum structures (as seen in [Eschenauer and Olhoff, 2001])	64

2.6	Three possible ground structures for a 4x6 grid ($n = 35$)	64
2.7	Flowchart design procedure using FSD (inspired from [Li, 1990]).	67
2.8	ST models obtained from 3 different ground structures [Gaynor et al., 2012].	68
2.9	Piece-wise linear stress-strain relations (modified from [Achtziger, 1996]) .	69
3.1	Flowchart showing proposed the design procedure	73
3.2	Polynomial interpolation over 8 random XYZ triplets.	75
3.3	Grid based numerical differentiation	76
3.4	Flowchart of the proposed truss optimisation	81
3.5	Element suppression flowchart	84
3.6	Hydrostatic nodes	86
3.7	Schematic representation of element's length reduction and space verification	87
3.8	Anchorage zone models [Zhong et al., 2016]	89
3.9	Schematic representation of the needed: mesh and principal stress direction fields	90
3.10	Schematic representation of the needed data: principal stress fields	90
3.11	Strut path generation: (a) Computed Voronoi seeds, (b) Clipped Voronoi division, (c) Associated direction strut direction and (c) Initial strut path .	91
3.12	Ground structure development: (a) merged strut path and (b) proposed ground structure ($m=447$).	92
3.13	Anchorage Strut-and-Tie models obtained from a fine mesh	92
3.14	Anchorage Strut-and-Tie models obtained from a coarse mesh	93
3.15	Anchorage Strut-and-Tie models obtained from a locally refined mesh . . .	94
3.16	Different Strut-and-Tie model propositions	95
3.17	Comparison of different Strut-and-Tie model propositions(anchorage $e=0.75m$)	96
4.1	Planar corbel initial model	100
4.2	Schematic representation of the needed data	101
4.3	Strut generation subroutines	102
4.4	Ground structure	103
4.5	Different ST models for the corbel case. Figure (a) depicts the ties in red and the struts in blue; figure (b) is presented with shifted colours	103
4.6	Nodal geometry	104
4.7	Optimisation evolution	107
4.8	Coarse mesh	108
4.9	Free mesh	108
4.10	Computed components of reinforcement given in local coordinates	110
4.11	Views of model representation in Code_Aster software	110
4.12	Capra-Maury computed required steel reinforcement (Coarse mesh).	111
4.13	ST model found through Bi-directional Evolutionary Structural Optimisa- tion [Shobeiri, 2016]	114
4.14	Three-dimensional model representation	114
4.15	Caption	115
4.16	(a) directions associated to the Voronoi zones, (b) initial strut path, (c) merged strut path and (d) ground structure ($m = 1919$)	115
4.17	Filtered Strut and tie model resultant of a size-topology scheme ($m = 88$) .	116

4.18	Strut-and-tie model resultant of size-topology-geometry optimisation scheme ($m = 247$)	116
4.19	Manually modified Strut and tie model resultant from a size-topology-geometry scheme ($m = 86$)	117
A.1	Trimmed wall: design domain	138
A.2	Optimisation process	139
A.3	Different strut and tie models	139
A.4	Trimmed square (dimensions in meters)	140
A.5	Steep of ST model	141
A.6	(a) Cracking pattern, (b) ST model [Muttoni et al., 2015], and (c) proposed model (only Topology and Size optimisation scheme)	141
B.1	Second load case: $e = 0.75$ m	142
B.2	Schematic representation of the needed: mesh and principal stress direction fields	143
B.3	Schematic representation of the needed data: principal stress fields	143
B.4	Strut path generation: (a) Computed Voronoi seeds, (b) clipped Voronoi division, (c) associated direction strut direction and (c) Initial strut path	144
B.5	Ground structure development: (a) merged strut path and (b) proposed ground structure ($m=325$).	144
B.6	Anchorage Strut-and-Tie models obtained from a fine mesh	145
B.7	Comparison of different Strut-and-Tie model propositions	146
C.1	Manually modified Strut and tie model resultant from a size-topology-geometry scheme ($m = 86$)	147

List of Tables

- 1.1 ACI and Eurocode values for nodal zones resistance 41
- 1.2 ACI and Eurocode values for strut resistance 43

- 4.1 Considered materials 100
- 4.2 Steel reinforcement for the ST model 105
- 4.3 Steel reinforcement for the planar ST model: projection over the X and Y axis [cm³] 106
- 4.4 Steel reinforcement for the planar ST model: need of steel reinforcement per zone [cm³] 107
- 4.5 Computed need of steel reinforced per zone (coarse model) [cm³] 112
- 4.6 Computed need of steel reinforced per zone (3D ST) [cm³] 117
- 4.7 Comparative table of need of steel reinforcement per zone [cm³] 118
- 4.8 Comparative table of need of steel reinforcement per zone. kg of steel per cubic meter of concrete 118

- C.1 3D corbel ST nodal list 148
- C.2 3D corbel ST tie table 149

Appendix A

Other examples

A.1 Trimmed deep wall

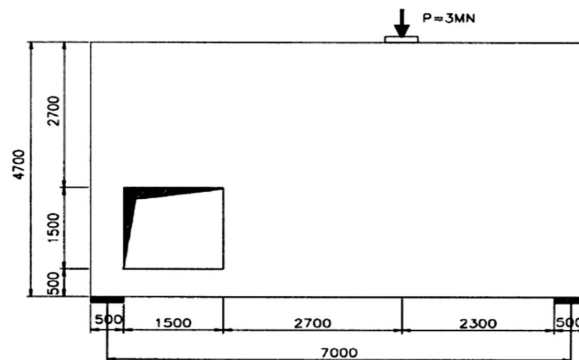


Figure A.1: Trimmed wall: design domain

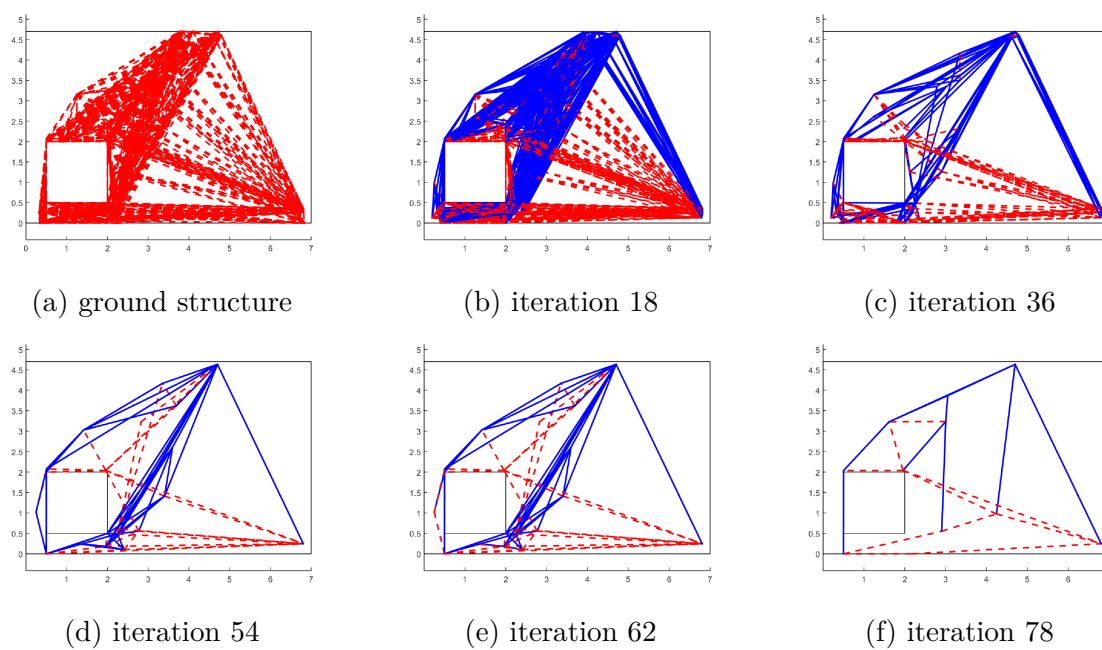


Figure A.2: Optimisation process

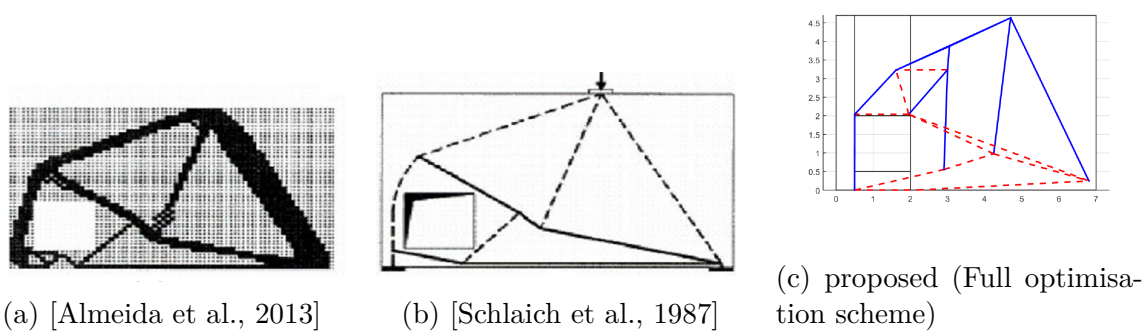


Figure A.3: Different strut and tie models

A.2 Trimmed square

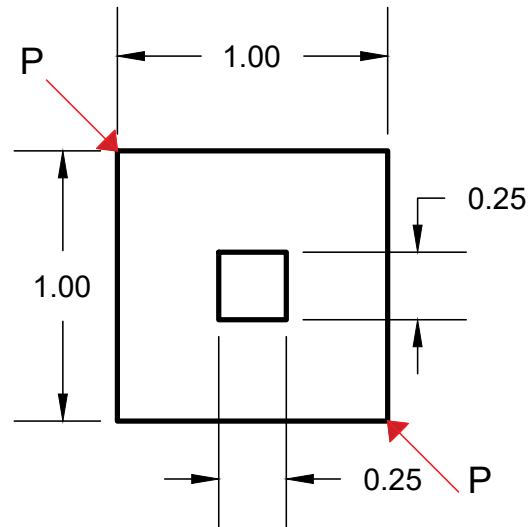


Figure A.4: Trimmed square (dimensions in meters)

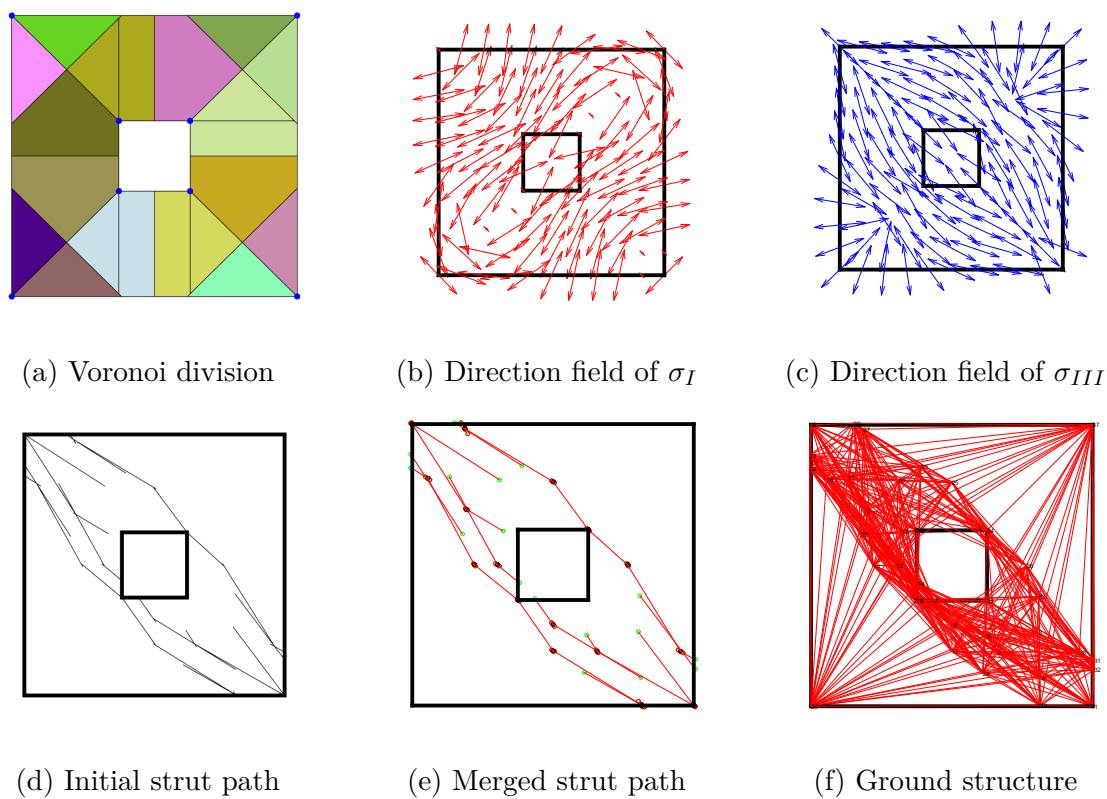


Figure A.5: Step of ST model

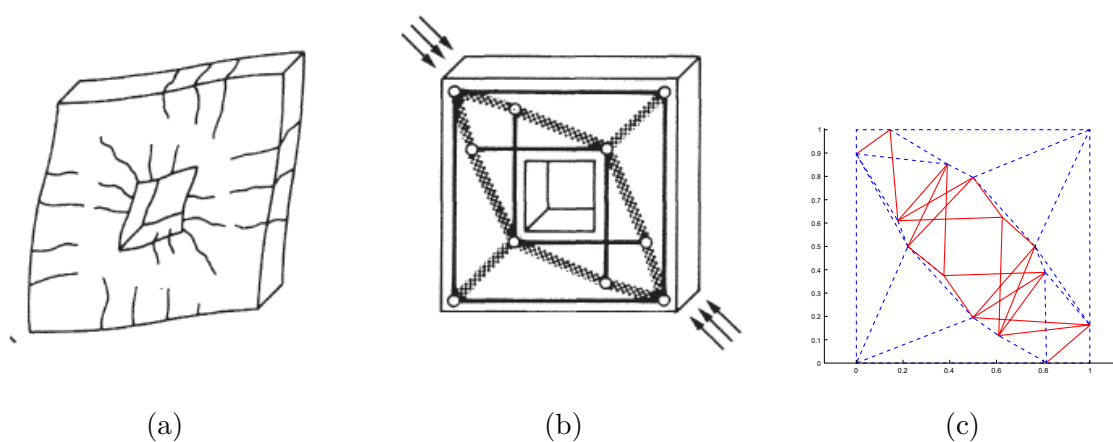


Figure A.6: (a) Cracking pattern, (b) ST model [Muttoni et al., 2015], and (c) proposed model (only Topology and Size optimisation scheme)

Appendix B

Anchorage: different load cases

B.1 Load eccentricity of 0.75 meters

The case herein presented corresponds to a small variation in the load position of the example presented in section 3.2. The length of the structures is $L = 6\text{m}$, the width is $b = 3\text{m}$ and the considered thickness of the elements is $t = 0.2\text{ m}$. The effect of the prestressing tendons has been simplified into one concentrated load $F = 5\text{ KN}$. The considered eccentricity, e is 0.75. The model is considered fixed at the opposite side of the force. Regarding the material, the Young's modulus, E , and the Poisson's ratio, ν , were specified according to a concrete of $f_{ck} = 35\text{MPa}$: $E = 34.5 \times 10^4\text{GPa}$ and $\nu = 0.3$.

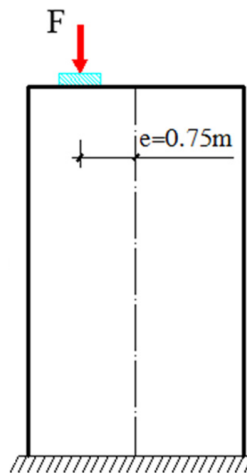


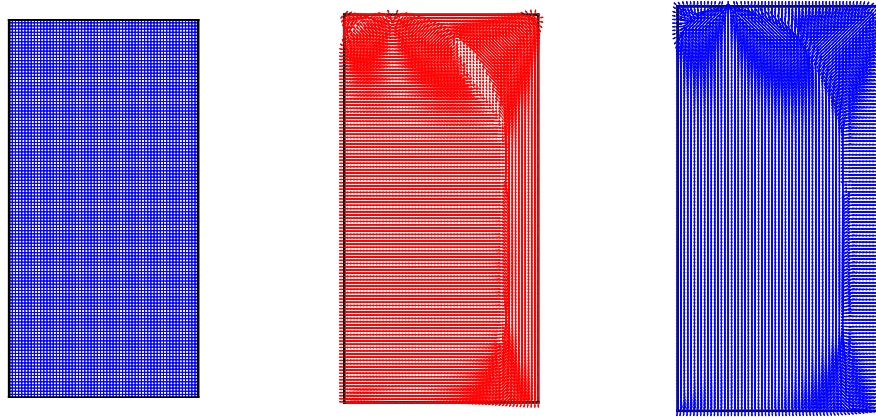
Figure B.1: Second load case: $e = 0.75\text{ m}$

A planar representation of the structure was built up using a regular mesh consisting in 1800 4-node plane stress elements (figure B.2a). The load was represented by a unique punctual force. Concerning the support, all degrees of freedom were suppressed for the nodes at the base zone. Plane strain hypothesis were considered during the procedure.

B.1.1 Input

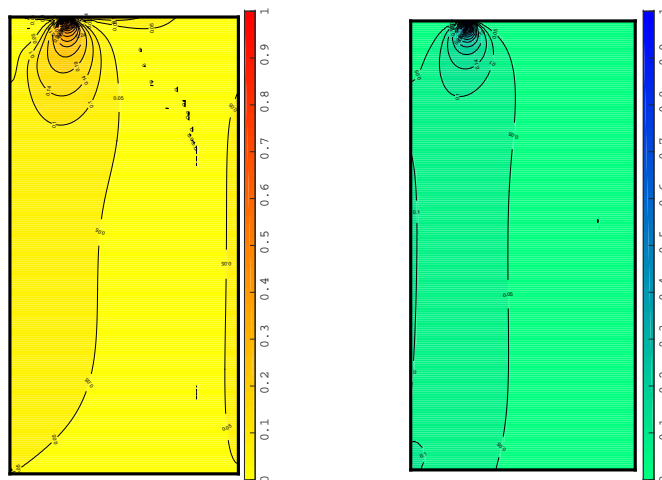
After having imposed the respective boundary conditions and solving some results were extracted. The information extracted from ANSYS software was the nodal list (NLIST in

ANSYS environment), the connectivity matrix (ELIST), the principal stresses computed at the Gauss points and also smoothed at the nodes (PRESOL and PRNSOL respectively) and the direction field of the principal stresses (PVSOL). This information, schematised in figures B.2 and B.3, is the starting point to develop the ground structure.



(a) Mesh (b) σ_I direction field (c) σ_{III} direction field

Figure B.2: Schematic representation of the needed: mesh and principal stress direction fields



(a) Normed σ_I contours (b) Normed σ_{III} contours

Figure B.3: Schematic representation of the needed data: principal stress fields

B.1.2 Ground structure

Figure B.4 shows the principal stress fields all over the structural element developed under the specified boundary conditions and in subfigure B.4a the peaks and valleys detected by the code are also shown.

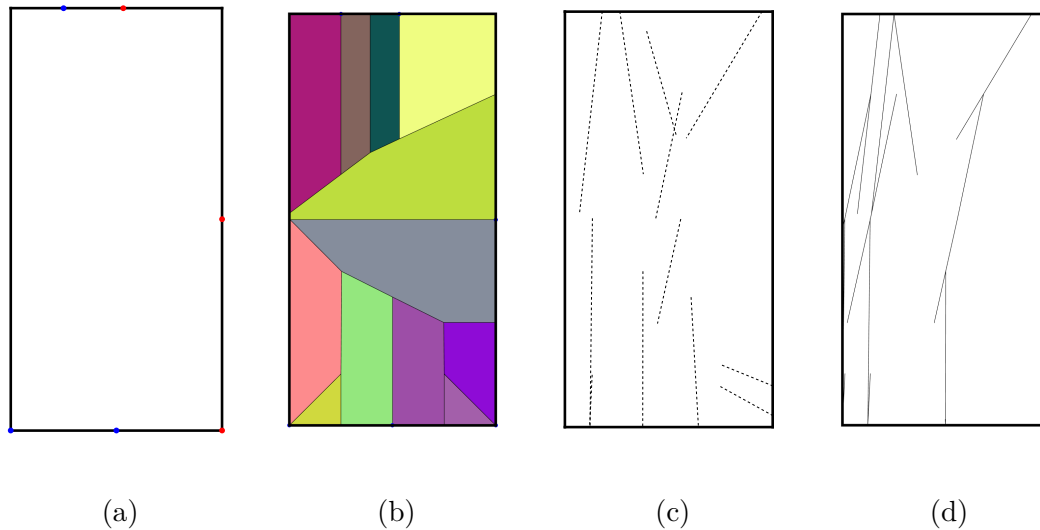


Figure B.4: Strut path generation: (a) Computed Voronoi seeds, (b) clipped Voronoi division, (c) associated direction strut direction and (d) Initial strut path

Taking the local maximum and minimum as seeds for the Voronoi division and the geometry as the feasible region, the division is performed. For this case, 20 cells were found during the performed division (refer to subfigure B.5a).

Following the presented methodology, the *loess* was applied at the centre of every cell. Considering the principal directions of all the elements found in the cell, the regression was applied and the results are schematised in figure B.5b.

The initial strut path (subfigure B.4d) was achieved through the sub routine described in the previous chapter. An initial node is selected (node containing a maximum of σ_{III}) and a straight line is developed until finding the limits of a cell).

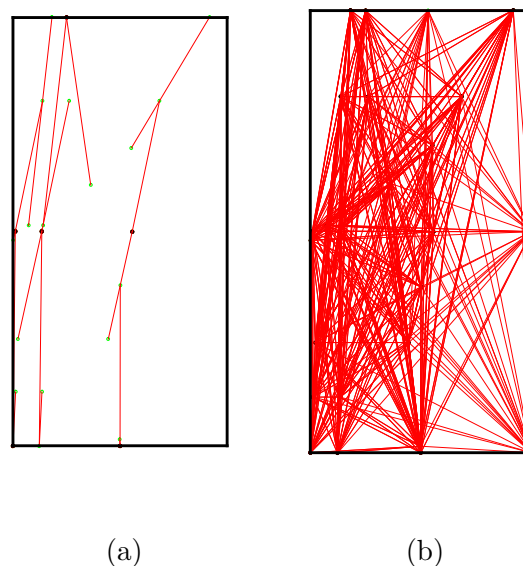


Figure B.5: Ground structure development: (a) merged strut path and (b) proposed ground structure ($m=325$).

B.1.3 Truss optimisation

Figure B.6 shows the results obtained through the application of 2 mixed schemes: sizing-topology and sizing-topology-geometric. As in previous tests, the main difference between the results obtained by the two different mixed schemes lies in the quantity of elements conforming the final Strut-and-Tie model.

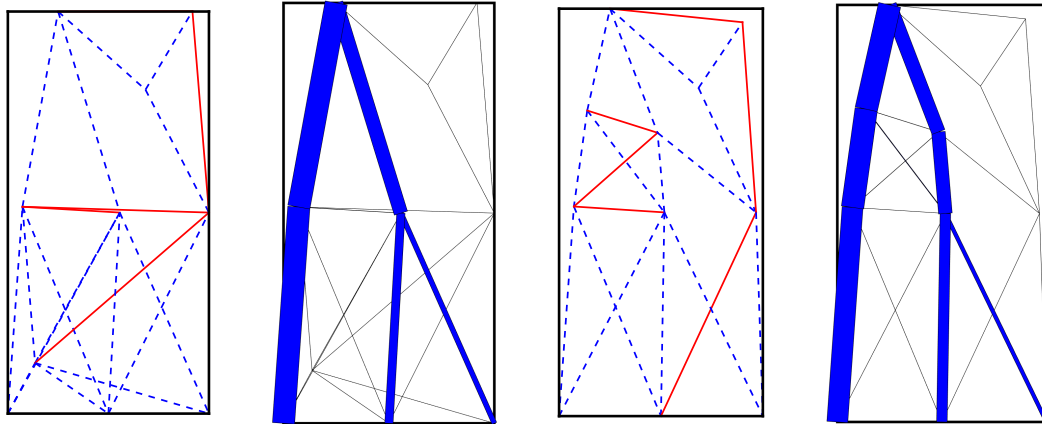
(a) $m=25$ $i=46$ (b) $m=25$, $i=46$ (c) $m=24$, $i=69$ (d) $m=24$, $i=69$

Figure B.6: Anchorage Strut-and-Tie models obtained from a fine mesh. Figure (a) shows the results obtained through an optimisation scheme considering only size and topology techniques; figure (c) shows the results obtained through an optimisation scheme considering size, topology, and geometric techniques. Figures (b) and (d) are graphical representations of the associated cross sections corresponding to (a) and (c) .

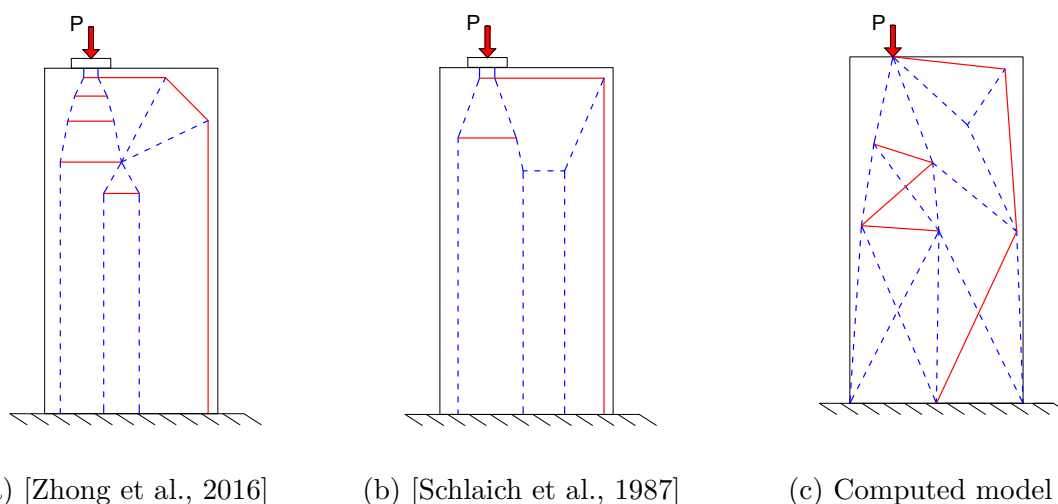


Figure B.7: Comparison of different Strut-and-Tie model propositions

B.1.4 Literature results

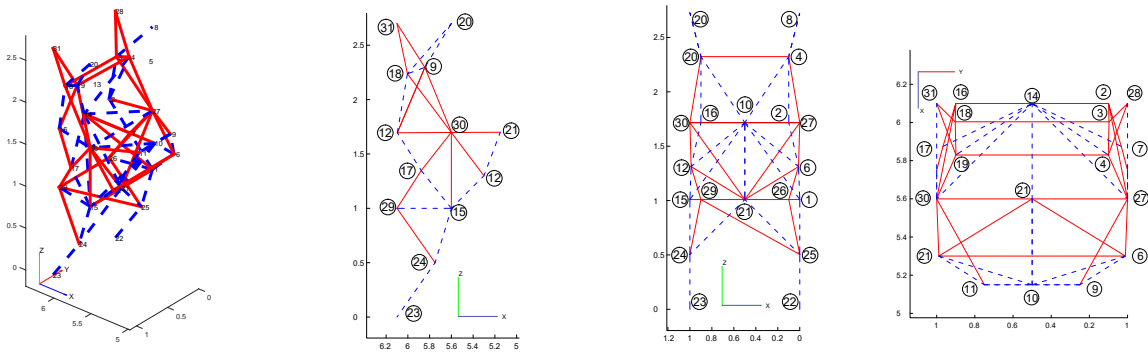
Figure B.7 shows the proposed Strut-and-Tie models. As in previous figures, the blue dashed lines represent members in compression and the continuous red lines represent elements in tension; the original figures were adapted to respect this colour pallet.

It can be observed that this is so far the model that differs the most from the literature examples. Even though the models present strong similarities in terms of load-transfer mechanisms, the mere existence of some elements in the proposed model brings effects of compression in a zone that do not consider struts in the other two models (right support in figures B.7).

The differences presented in this model come from the fact that, for this case, the obtained the automatically obtained Voronoi seeds did not allow a satisfactory geometry division (clipped Voronoi division) and some seeds were need to be added manually to the algorithm to continue the procedure. The present results permit to state that the present approach is highly sensitive to the number and position of the Voronoi seeds. In case of not being satisfied with the final results, it was decided to let the user the liberty to add, erase or modify the proposed Voronoi seed hence adapting a computer aided scheme over a fully automatic one.

Appendix C

3D strut-and-tie model corbel



(a) 3D view

(b) Side view

(c) Front view

(d) Top view

Figure C.1: Manually modified Strut and tie model resultant from a size-topology-geometry scheme ($m = 86$)

Table C.1: 3D corbel ST nodal list

id	X	Y	Z
1	5.6	0	1
2	6.1	0.1	1.7
3	6.004	0.0971	2.237
4	5.83	0.1009	2.301
5	5.595	0.093	2.335
6	5.3005	0.0114	1.2997
7	5.875	0.0329	1.3448
8	5.6	0	2.7
9	5.15	0.25	1.7
10	5.15	0.5	1.7
11	5.15	0.75	1.7
12	5.3002	0.9886	1.3
13	5.9798	0.5	2.105
14	6.1	0.5	1.695
15	5.6	1	1
16	6.1	0.9	1.7
17	5.8807	0.9724	1.3428
18	6.0082	0.9177	2.2505
19	5.85	0.9114	2.3115
20	5.6	1	2.7
21	5.6	0.5	1
22	6.1	0	0
23	6.1	1	0
24	5.75	1	0.5
25	5.75	0	0.5
26	6.1	0.1	1
27	5.6	0	1.7
28	6.1	0	2.7
29	6.1	0.9	1
30	5.6	1	1.7
31	6.1	1	2.7

Table C.2: 3D corbel ST tie table

Tie	i	j	length	force	area	volume
T1	1	14	99.15	2.27	0.05	5
T2	1	15	100	16.26	0.36	36.12
T3	1	21	50	7.2	0.16	8.01
T4	2	27	50.99	36.43	0.81	41.28
T5	3	4	18.54	8.77	0.19	3.61
T6	3	18	82.07	21.62	0.48	39.43
T7	3	27	67.9	84.71	1.88	127.81
T8	3	28	48.27	98.1	2.18	105.23
T9	4	19	81.08	39.95	0.89	71.97
T10	4	27	65.14	98.94	2.2	143.23
T11	4	28	49.22	74.3	1.65	81.26
T12	6	12	97.72	173.05	3.85	375.78
T13	6	21	64.67	11.45	0.25	16.45
T14	6	27	50.01	105.65	2.35	117.41
T15	7	14	62.57	6.01	0.13	8.36
T16	7	26	41.72	0.11	0	0.1
T17	7	27	45.04	4.64	0.1	4.65
T18	9	27	51.48	71.68	1.59	82
T19	10	14	95	79.71	1.77	168.28
T20	11	30	51.48	71.59	1.59	81.9
T21	12	30	50	102.39	2.28	113.77
T22	15	21	50	21.82	0.48	24.25
T23	15	30	70	13.05	0.29	20.3
T24	16	17	42.54	0.16	0	0.15
T25	16	19	66.07	0.19	0	0.27
T26	17	29	41.33	64.35	1.43	59.11
T27	17	30	45.51	62.76	1.39	63.47
T28	18	30	69.03	69.75	1.55	107
T29	18	31	46.61	69.15	1.54	71.63
T30	19	30	66.65	96.64	2.15	143.13
T31	19	31	47.04	103.42	2.3	108.1
T32	21	27	86.02	18.5	0.41	35.37
T33	21	30	86.02	0.09	0	0.17
T34	24	29	61.85	63.35	1.41	87.07
T35	25	26	61.85	68.61	1.52	94.3
T36	25	29	108.74	4.69	0.1	11.33
T37	26	27	86.6	68.51	1.52	131.85
T38	26	29	80	3.33	0.07	5.93
Total						2595.1